

DEVELOPMENT AND INVESTIGATIONS OF BIO-BASED COMPOSITE RIGID POLYURETHANE FOAM

A Thesis submitted in the partial fulfilment of the requirements for the award of the degree

of

DOCTOR OF PHILOSOPHY

by

ANUJA AGRAWAL

(2K16/PhD/AC/03)

Under the supervision of

DR. RAMINDER KAUR

Faculty of Polymer Science

& Chemical Technology

Department of Applied Chemistry

Delhi Technological University

Delhi-110042

PROF. R. S. WALIA

Department of Mechanical Engineering

Delhi Technological University

Delhi-110042



DEPARTMENT OF APPLIED CHEMISTRY

DELHI TECHNOLOGICAL UNIVERSITY

DELHI-110042

NOVEMBER-2019

© DELHI TECHNOLOGICAL UNIVERSITY- 2019
ALL RIGHTS RESERVED

DELHI TECHNOLOGICAL UNIVERSITY
Shahbad Daultpur, Bawana Road, Delhi-110042, India



DECLARATION

I hereby declare that the thesis entitled “**DEVELOPMENT AND INVESTIGATIONS OF BIO-BASED COMPOSITE RIGID POLYURETHANE FOAM**” is an original work carried out by me under the supervision of **Dr. Raminder Kaur**, Faculty of Polymer Science & Chemical Technology, Department of Applied Chemistry, Delhi Technological University, Delhi and **Prof. R.S. Walia**, Department of Mechanical Engineering, Delhi Technological University, Delhi. This thesis has been prepared in conformity with the rules and regulations of the Delhi Technological University, Delhi. The research work reported and results presented in the thesis have neither partially nor fully submitted to any other university or institute for the award of any other degree or diploma.

Place: Delhi

Date:

(Anuja Agrawal)

(Roll No: 2K16/PhD/AC/03)

Research Scholar

Department of Applied Chemistry

Delhi Technological University,

Delhi-110042

DELHI TECHNOLOGICAL UNIVERSITY

Shahbad Daultpur, Bawana Road, Delhi-110042, India



CERTIFICATE

This is to certify that the work embodied in the thesis entitled “**DEVELOPMENT AND INVESTIGATIONS OF BIO-BASED COMPOSITE RIGID POLYURETHANE FOAM**” by **Ms. Anuja Agrawal (Roll No: 2K16/PhD/AC/03)**, in the partial fulfilment of the requirements for the award of the degree of **Doctor of Philosophy**, is an authentic record of student’s own work carried out by her under the supervision of **Dr. Raminder Kaur**, Assistant Professor, Faculty of Polymer Science & Chemical Technology, Department of Applied Chemistry, Delhi Technological University, Delhi and **Prof. R.S. Walia**, Professor, Department of Mechanical Engineering, Delhi Technological University, Delhi.

This is also certified that this work has neither partially nor fully submitted to any other Institute or University for the award of any other diploma or degree.

DR. RAMINDER KAUR

Faculty of Polymer Science
& Chemical Technology
Department of Applied Chemistry
Delhi Technological University
Delhi-110042

PROF. R. S. WALIA

Department of Mechanical Engineering
Delhi Technological University
Delhi-110042

PROF. S. G. WARKAR

HOD, Department of Applied Chemistry
Delhi Technological University
Delhi-110042

ACKNOWLEDGEMENTS

It gives me immense pleasure to express my deep sense of gratitude to my supervisors **Dr. Raminder Kaur**, *Department of Applied Chemistry, Delhi Technological University, Delhi* and **Prof. R.S. Walia**, *Department of Mechanical Engineering, Delhi Technological University, Delhi* for assisting me in identifying and formulating the research problem. Despite their busy schedule, *Dr. Raminder Kaur* and *Prof. R.S. Walia* were always available for the advice and discussions. Their valuable comments and advice gave me the confidence to overcome the challenges in formulation of this Ph.D thesis work.

I owe my heartfelt gratitude to **Prof. Yogesh Singh**, *Hon'ble Vice-Chancellor, Delhi Technological University* for his kind permission and **Prof. S. G. Warkar**, *Head, Department of Applied Chemistry, DTU*, **Prof. Archana Rani**, *Chairperson DRC, Department of Applied Chemistry, DTU* for providing me the necessary facilities to carry out this research work. I wish to express my sincere thanks to the all faculty members of *Department of Applied Chemistry, DTU* for their help and support during this research work.

I would like to thank all technical and non-technical staff and my friends, seniors and fellow researchers: *Dr. Mukesh Kumar, Dr. Manjeet Malik, Ms. Monika Duhan, Mr. Surya Tanwar, Mr. Ankesh Kumar, Mr. Jawed Alam* who have supported me through their encouragement, support and friendship during this period of thesis research work. I would like to thank to all those who directly and indirectly supported me in carrying out this thesis work successfully. I wish to pay my sincere thanks to **Defence Research and Development Organization (DRDO)** for providing me financial support to carry out this research work.

Furthermore, I am indebted to **my parents** and my husband **Prof. Rajesh Kumar** for their endless inspiration, moral support and guidance throughout my whole life, *daughter Nitya* and *son Darsh* for their selfless love and support, that has always been a driving force for the completion of my research work.

Above all, I owe to **Almighty God** for granting me wisdom, health and strength to accept the challenges of the life.

Place: Delhi

Date:

(Anuja Agrawal)

ABSTRACT

Polymeric foams are used extensively in a wide range of applications such as disposable packaging, cushioning, thermal insulation and construction. Foams derived from renewable sources are a requirement of the modern world due to the increasing concern about the environment and various issues related to petroleum based foams. Much research has been conducted recently to produce foams using renewable sources; however, low mechanical strength, high flammability and low thermal stability are the matters of concern when using these foams on a commercial scale. Various approaches have been used in past to overcome these problems; including the modification of raw material or the incorporation of property-enhancing fillers, with or without a surface treatment. In this research, different fillers (carbon fibre powder, zirconia powder, alumina powder, feldspar, kaolinite clay, copper powder and calcium carbonate nanoparticles) have been used as reinforcement to enhance the mechanical, thermal and flame retardant properties of the bio-based rigid polyurethane foams.

It was observed that the addition of ceramic filler showed the improved mechanical and thermal properties. The best properties were shown by 6% zirconia with a compressive strength of 6.61 MPa and the flexural strength of 5.72 MPa. Zirconia also demonstrated an increase in $T_{5\%}$ up to 260°C. It is also revealed that the foams with 8% carbon fibre concentration showed up to 288% increase in compressive strength. Furthermore, up to 28% decrease in the peak of heat release rate (PHRR) was observed on the incorporation of carbon fibre powder. The foams with 8% and 10% carbon fibre concentration show conductivity of 1.9×10^{-4} and 7.1×10^{-4} S/m respectively. Also, the foams incorporated with mineral filler demonstrated up to 182% increase in compressive strength and 351% increase in flexural strength. Thermal stability of these composite foams was also found to be enhanced on the incorporation of kaolinite clay filler, with an increase in 5% weight loss temperature ($T_{5\%}$) from 192°C to 260°C.

Furthermore, the total heat release (THR), the smoke production rate (SPR) and the total smoke release (TSR) were also found to decreased remarkably on the incorporation of different fillers used in this study. Present study also investigated the impact of drilling on the residual compressive strength of bio-based rigid polyurethane foam (RPUF) composites. RPUFs have been prepared by the incorporation of copper powder in castor oil-based foams. The formulation of the samples employed for the drilling experiments was optimized by performing compressive strength, thermo-gravimetric analysis (TGA) and flammability experiments. The effect of various drilling parameters (density, feed rate, spindle speed and drill diameter) on the thrust force, delamination and, residual compressive strength has been investigated. The polynomial mathematical model reliant on the Response Surface Method (RSM) employing central composite design has been developed. It was concluded that the density is the most influential factor for maximizing the residual compressive strength, Additionally, the enhancement in residual compressive strength was observed on increasing the spindle speed, while, the feed rate shows a negligible effect on the residual compressive strength. The optimized process parameters for maximizing residual compressive strength were attained as high spindle speed and low feed rate. Furthermore, the equations designated as the coded factors are also presented to identify the relative impact of the various drilling parameters.

TABLE OF CONTENTS

<u>Contents</u>	<u>Page no.</u>
Declaration	
Certificate	
Acknowledgements	i
Abstract	ii
Table of Content	iv
List of Figures	viii
List of Tables	xii
List of Abbreviations	xiv
CHAPTER 1:	
INTRODUCTION AND LITERATURE REVIEW	1-40
1.1 Polyurethane Derived from Renewable Sources	2
1.1.1 Renewable Sources with Lower Number of Hydroxyl Groups	2
1.1.2 Renewable Sources with Higher Numbers of Hydroxyl Groups	9
1.2 Non-Isocyanate Polyurethane (NIPU)	10
1.3 Fillers to Enhance the Mechanical Strength of PU Foams	12
1.3.1 Fibres	12
1.3.1.1 Synthetic Fibres	12
1.3.1.2 Natural Fibres	14
1.3.2 Nanofillers	15
1.3.3 Particulate Fillers	16
1.4 Surface Treatment of Fillers	21
1.4.1 Treatment with Silanes	23
1.4.2 Treatment with Other Coupling Agents	24
1.5 Enhancement of Thermal Insulation and Flame Retardancy of PU Foams	25
1.5.1 Incorporation of Flame Retardant Groups	25
1.5.2 Addition of Flame Retardants	27
1.5.3 Addition of Aerogels	30
1.5.4 Addition of Phase Change Materials	33

<u>Contents</u>	<u>Page no.</u>
1.6 Analysis for Machining Performance of Polymers	34
1.7 Significant Findings from Literature	37
1.8 Research Gaps	37
1.9 Research Objectives	38
1.10 Overview of the Thesis	39
CHAPTER 2:	
MATERIALS AND METHODS	41-54
2.1 Raw Materials/Chemicals	41
2.1.1 Specification and Sources of Raw Materials/Chemicals	42
2.1.2 Purity of Raw Materials/ Chemicals	44
2.2 Research Methodology	45
2.2.1 Physicochemical Characterization of Raw Materials	45
2.2.1.1 Determination of Acid Value of the Oil used	45
2.2.1.2 Determination of the Hydroxyl Value of the Oil and Modified Polyol	46
2.2.1.3 Determination of the Viscosity of the Oil	46
2.2.1.4 Determination of the Percentage NCO Content	46
2.2.1.5 FTIR and ¹ H NMR analysis	46
2.2.2 Modification of the Vegetable Oil	47
2.2.3 Preparation of the Calcium Carbonate Nanoparticles	47
2.2.4 Synthesis of Rigid Polyurethane Foam Composite	48
2.2.5 Characterization of Synthesized RPUF Composite	49
2.2.5.1 Mechanical Testing	49
2.2.5.2 Thermo-Gravimetric Analysis (TGA)	50
2.2.5.3 Cone Calorimeter Testing	52
2.2.5.4 Scanning Electron Microscopy	52
2.2.5.5 Conductivity Measurement	52
2.2.6 Optimization of mechanical, Thermal and Flame Retardant Properties of RPUF	53
2.2.7 Drilling Performance Test of the RPUF Composite	53

<u>Contents</u>	<u>Page no.</u>
CHAPTER 3:	
INVESTIGATIONS ON CASTOR OIL-BASED RPUF REINFORCED WITH CERAMIC FILLERS	55-71
3.1 Introduction	55
3.2 Results and Discussion	58
3.2.1 FTIR and IH NMR Analysis	59
3.2.2 Mechanical Testing	60
3.2.3 Scanning Electron Microscopy	63
3.2.4 Thermo-Gravimetric Analysis (TGA)	64
3.2.5 Cone Calorimeter Testing	66
3.3 Significant Findings	70
CHAPTER 4:	
DEVELOPMENT OF CONDUCTING RPUF USING CARBON FIBRE REINFORCEMENT	72-82
4.1 Introduction	72
4.2 Results and Discussion	75
4.2.1 Mechanical Properties	76
4.2.2 Thermo-Gravimetric analysis (TGA)	77
4.2.3 Cone Calorimeter Testing	79
4.2.4 Conductivity Measurement	80
4.3 Significant Findings	81
CHAPTER 5:	
STUDIES ON THE MINERAL FILLER REINFORCED RPUF	83-103
5.1 Introduction	83
5.2 Results and Discussion	86
5.2.1 Mechanical properties	86
5.2.2 Scanning Electron Microscopy (SEM)	88
5.2.3 Thermo-Gravimetric Analysis (TGA)	89
5.2.4 Cone Calorimeter Testing	92
5.3 RPUF Incorporated with Calcium Carbonate Nanoparticles	96
5.3.1 FTIR Analysis	96
5.3.2 Transmission Electron Microscopy	97
5.3.3 XRD Analysis	98

<u>Contents</u>	<u>Page no.</u>
5.3.4 Scanning Electron Microscopy (SEM)	99
5.3.5 Thermo-Gravimetric Analysis (TGA)	99
5.3.6 Cone Calorimeter Testing	100
5.4 Significant Findings	102
CHAPTER 6:	
DEVELOPMENT OF THE METALLIC FILLER REINFORCED RPUF AND OPTIMIZATION OF THE REINFORCING FILLER COMPOSITION	104-110
6.1 Introduction	104
6.2 Results and Discussion	104
6.2.1 Compressive Strength Measurement	104
6.2.2 Thermo-Gravimetric Analysis (TGA)	106
6.2.3 Cone Calorimeter Testing	107
6.2.4 Optimization of the Filler Concentration	110
6.3 Significant Findings	110
CHAPTER 7:	
RESPONSE SURFACE METHOD FOR THE EVALUATION AND OPTIMIZATION OF THE DRILLING PARAMETERS FOR THE BIO-BASED RPUF COMPOSITES	111-127
7.1 Introduction	111
7.2 Results and Discussion	112
7.2.1 Thrust Force Analysis	115
7.2.2 Delamination Analysis	119
7.2.3 Residual Compressive Strength Analysis	122
7.2.4 Optimization Employing Desirability Function	125
7.3 Significant Findings	126
CHAPTER 8:	
CONCLUSIONS AND FUTURE PROSPECTS	128-130
8.1 Conclusions	128
8.2 Future Prospects	130
REFERENCES	131
LIST OF PUBLICATIONS	151
APPENDIX-I	153
BRIEF BIO-DATA OF THE AUTHOR	155

LIST OF FIGURES

Figure No.	Title	Page No.
1.1	Schematic Representation of (a) Epoxidation Followed by Ring Opening, (b) Hydroformylation Followed by Hydrogenation, (c) Ozonolysis Followed by Hydrogenation, (d) Ozonolysis with the Addition of Ethylene Glycol, (e) Thiol-ene Coupling, (f) Transesterification and (g) Amidation.	4
1.2	Structure of Polyfunctional Alcohols (a) Diethanolamine, (b) Triethanolamine, (c) Glycerol, (d) Trimethylol Propane and (e) Pentaerythritol.	5
1.3	Structure of polyols (a) Soybean oil-based polyol modified with TEA, (b) Castor oil-based polyol modified with TEA, (c) Castor oil-based polyol modified with glycerol (d) Rosin-based polyol and (e) Castor oil-based polyol modified with different glycols.	8
1.4.	Some Routes to Synthesize (a) NIPU from Dicyclocarbonate and Diamines, (b) NIPU from Terpene Derivatives, (c) Urethane Linkage from Cyclocarbonate	11
1.5	Plots of Percentage Change in Specific Compressive Strength vs. Percentage Filler Content (for foams with high filler content)	17
1.6.	Plots of Percentage Change in Specific Compressive Strength vs. Percentage Filler Content (for foams with low filler content)	18
1.7	Schematic Diagram for the Preparation of COFPL	26
1.8.	Structure of Different Flame Retardants (a) COFPL, (b) DOPO-BA, (c) HPHPCP	27
1.9.	Flow Chart for Aerogel Preparation	31
1.10	Plots of Percentage LOI vs. Percentage Filler Content Incorporated in Different PU Foam Matrices	33
2.1	FTIR (Nicolet 380) Spectrometer	46
2.2	NMR (Bruker Avance II-400) Spectrophotometer	47
2.3	Reaction scheme of Transesterification of Castor Oil and Polyurethane Formation	48

Figure No.	Title	Page No.
2.4	UTM used for Mechanical Testing of Foam Samples	50
2.5	Thermo-gravimetric Analyzer (Perkin Elmer 4000)	51
2.6	Cone Calorimeter	51
2.7	Scanning Electron Microscope (Hitachi S-3700N)	52
2.8	Four Probe Digital Conductivity Meter	53
2.9	Computer numerical control (CNC) vertical machining center (VMC)	54
3.1	¹ H NMR of (a) Modified Polyol and (b) Castor Oil	59
3.2	FTIR of Castor Oil and Modified Polyol	60
3.3	Plots of (a) Compressive Strength vs. Filler Percentage, (b) Flexural Strength vs. Filler Percentage, (c) Specific Compressive Strength vs. Filler Percentage and (d) Specific Flexural Strength vs. Filler Percentage	61
3.4	Variation in Density with Increase in the Concentration of Ceramic Fillers	62
3.5	Scheme for Surface Treatment and Adhesion of Filler with Polyol	63
3.6	SEM Images of RPUF with (a) 0% Filler, (b) 6% Zirconia and (c) 8% Alumina	64
3.7	(a) TGA Curve of RPUF Incorporated with Alumina Powder, (b) DTG Curve of RPUF Reinforced with Alumina Powder, (c) TGA Curve of RPUF Incorporated with Zirconia Powder, (d) DTG Curve of RPUF Reinforced with Zirconia Powder	66
3.8	(a) HRR (Heat Release Rate), (b) THR (Total Heat Release), (c) SPR (Smoke Production Rate) and (d) TSR (Total Smoke Release) of RPUFs Incorporated with Alumina Powder	67
3.9	(a) HRR (Heat Release Rate), (b) THR (Total Heat Release), (c) SPR (Smoke Production Rate) and (d) TSR (Total Smoke Release) of RPUFs Incorporated with Zirconia Powder	68

Figure No.	Title	Page No.
4.1	Plots of (a) Mechanical Strength vs. Filler Concentration, (b) Density vs. Filler Concentration, (c) Specific Strength vs. Filler Concentration	75
4.2	SEM Micrographs of RPUF with (a) 0% and (b) 8% Concentration of Carbon Fibre Powder	76
4.3	(a)TGA Plots, (b) DTG Plots, (c) HRR (Heat Release Rate), (d) THR (Total Heat Release), (e) SPR (Smoke Production Rate) and (f) TSR (Total Smoke Release) of RPUFs Incorporated with Carbon Fibre	78
4.4	Plots of Electrical Conductivity of Carbon Fibre Reinforced RPUF (S/m) vs. Percentage of Filler	81
5.1	Variation in (a) Compressive Strength, (b) Flexural Strength, (c) Specific Compressive Strength, (d) Specific Flexural Strength with Increase in Concentration of the Fillers	87
5.2	Variation in Density of the RPUF with Increase in the Concentration of the Mineral Fillers	87
5.3	SEM Micrographs of Foam Reinforced with (a) 0% Filler, (b) 8% Feldspar and (c) 6% Kaolinite Clay	89
5.4	(a) TGA Curve of RPUF Incorporated with Feldspar, (b) DTG Curve of RPUF Reinforced with Feldspar, (c) TGA Curve of RPUF Incorporated with Kaolinite Clay and (d) DTG Curve of RPUF Reinforced with Kaolinite Clay	90
5.5	(a) HRR (Heat Release Rate), (b) THR (Total Heat Release), (c) SPR (Smoke Production Rate) and (d) TSR (Total Smoke Release) of RPUFs Incorporated with Kaolinite Clay	94
5.6	(a) HRR (Heat Release Rate), (b) THR (Total Heat Release), (c) SPR (Smoke Production Rate) and (d) TSR (Total Smoke Release) of RPUFs Incorporated with Feldspar	95
5.7	FTIR Spectra of the Prepared Calcium Carbonate Nanoparticles	97

Figure No.	Title	Page No.
5.8	TEM Analysis of the Calcium Carbonate Nanoparticles	98
5.9	XRD Pattern of the Calcium Carbonate Nanoparticles	98
5.10	SEM Micrographs of the RPUF with (i) 0%, (ii) 2%, (iii) 4%, (iv) 6%, (v) 8% and (vi) 10% Concentration of the CaCO ₃ Nanoparticles.	99
5.11	TGA Plots of the RPUF Incorporated with CaCO ₃ Nanoparticles	100
5.12	(a) HRR (Heat Release Rate), (b) THR (Total Heat Release), (c) SPR (Smoke Production Rate) and (d) TSR (Total Smoke Release) of RPUFs Incorporated with CaCO ₃ Nanoparticles	101
6.1	Plots of (a) Compressive Strength vs. Concentration of Copper Filler, (b) Specific Compressive Strength vs. Concentration of Copper Filler and (c) Density vs. Concentration of Copper Filler	105
6.2	TGA Curves of the Neat and the Copper Powder Reinforced RPUF	107
6.3	(a) HRR (Heat Release Rate), (b) THR (Total Heat Release), (c) SPR (Smoke Production Rate) and (d) TSR (Total Smoke Release) of RPUFs Incorporated with Copper Powder	108
7.1	Samples Used For Drilling Test	111
7.2	Drilled Holes after Performing Drilling Test at Various Factor Levels	112
7.3	Predicted vs Actual Plot for Thrust Force on RPUF Composite	117
7.4	Predicted vs Actual Plot for Delamination of RPUF Composite	117
7.5	Predicted vs Actual Plot for Residual Compressive Strength of RPUF Composite	118
7.6	Response Surface for the Effect of Drilling on Thrust Force for RPUF Composite	119
7.7	Response Surfaces for the Effect of Drilling on Delamination of RPUF Composite	121
7.8	Response Surface for the Effect of Drilling on Residual Compressive Strength of RPUF Composite	124

LIST OF TABLES

Table No.	Title	Page No.
1.1	The Renewable Sources used to Develop the Polyols	3
1.2.	Different Modification Methods for the Development of Polyols from the Vegetable Oils	6
1.3	Effect of Different Fillers on Mechanical Properties of PU Composite Foams	19
1.4	Different Surface Treatment Methods Used to Modify the Filler Surface	22
1.5	Different Types of Flame Retardants	29
1.6.	Effect of Different Additives on the Thermal Properties of PU Foams	32
2.1	Specification and Sources of Raw Materials/Chemicals	42
2.2	Purity of Raw Materials/ Chemicals	44
2.3	Foaming Formulation of Castor Oil-Based RPUF	49
2.4	Factor Levels for Performing Drilling Test	54
3.1	Thermal Characteristics of the RPUF Incorporated with Ceramic Fillers	65
3.2	Fire Characteristics of the RPUF Incorporated with Ceramic Fillers	69
4.1	Cone Calorimeter Data of the RPUF Incorporated with Carbon Fibre	80
5.1	Thermal Characteristics of RPUF Incorporated with Different Mineral Fillers	91
5.2	Flammability Characteristics of the RPUF Incorporated with Mineral Fillers	93
5.3	Cone Calorimeter Data of the RPUFs Incorporated with the Calcium Carbonate Nanoparticles	102
6.1	Thermal Characteristics of the RPUF Incorporated with the Metallic Fillers	106
6.2	Cone Calorimeter Data of the RPUF Incorporated with the Metallic Fillers	109
6.3	Data for Optimization of the Filler Concentration	109
7.1	Experimental Results for Drilling of RPUF Composites	113

7.2	ANOVA and Fit Statistics for Thrust Force on RPUF Composite	116
7.3	ANOVA and Fit Statistics for Delamination of RPUF Composite	120
7.4	ANOVA and Fit Statistics for Residual Compressive Strength of RPUF Composite	123
7.5	Optimized Values of Factors and Responses after Numerical Optimization	125

LIST OF ABBREVIATIONS

ANOVA	Analysis of Variance
APP	Ammonium Polyphosphate
APTES	3-Aminopropyl)triethoxysilane
ATH	Aluminium Tri-Hydroxide
BDE	Polybrominated Diphenyl Ether
CFRP	Carbon Fibre Reinforced Polymer
CNC	Cellulose Nanocrystals, Computer Numerical Controlled
CNSL	Cashew Nut Shell Liquid
CNT	Carbon Nanotubes
COFPL	Castor Oil Phosphate Flame-Retarded Polyol
CTF	Critical Thrust Force
C.V.	Coefficient of Variance
DAP-MMT	Diaminopropane Montmorillonite
DMMP	Dimethyl Methylphosphonate
DMSO	Dimethyl Sulphoxide
DOPO-BA	Condensation Product of Benzaldehyde, Aniline and 9,10-Dihydro-9-Oxa-10-Phosphaphenanthrene-10-Oxide (DOPO)
DTG	Derivative Thermo-Gravimetry
EG	Expandable Graphite
EMI	Electromagnetic Interference
ES	Egg Shell
FRC	Fibre Reinforced Composites
FTIR	Fourier Transform Infrared
GCO	Glycerolysed Castor Oil
GRA	Grey Relational Analysis
HBCD	Hexabromocyclododecane
HMDA	Hexamethylenediamine

HPHPCP	Hexa- (Phosphite-Hydroxyl-Methyl-Phenoxy)-Cyclotriphosphazene
HRR	Heat Release Rate
HSS	High Speed Steel
IPDA	Isophoronediamine
LOI	Limiting Oxygen Index
LRPF	Lignin based Rigid Polyurethane Foams
MAPP	Maleated Polypropylene
MFI	Melt Flow Index
MH	Magnesium Di-Hydroxide
MWCNT	Multi-walled Carbon Nanotubes
NIPU	Non Isocyanate Polyurethane
NMR	Nuclear Magnetic Resonance
OMMT	Organically Modified Montmorillonite
PBT	Polybutylene Terephthalate
PCM	Phase Change Material
PEG	Polyethylene Glycol
PHHR	Peak of Heat Release Rate
PMDI	Polymeric Methylene Diphenylenediisocyanate
PMMA	Poly (methyl methacrylate)
PP	Polypropylene
PS	Polystyrene
PU	Polyurethane
rGO	Reduced Graphene Oxide
RHA	Rice Husk Ash
RPUF	Rigid Polyurethane Foam
RSM	Response Surface Method
SEBS-MA	Maleated Styrene-Ethylene/Butylene-Styrene
SEM	Scanning Electron Microscope
SiC	Silicon Carbide
SMA	Styrene-Maleic Anhydride
SPR	Smoke Production Rate
T _{5%}	5% Weight Loss Temperature

TBAB	Tetrabutylammonium Bromide
TBBPA	TetrabromoBisphenol A
TBC	Thermal Barrier Coating
TBD/LiOTf	Triazabicyclodecene/Lithium Triflate
TEA	Triethylene Amine
TEM	Transmission Electron Microscopy
TEP	Triethyl Phosphate
T _g	Glass Transition Temperature
TGA	Thermo-Gravimetric Analysis
THR	Total Heat Release
T _{init}	Initial Degradation Temperature, corresponding to 5% weight loss
T _{Max1}	Temperature at First Peak of Maximum Weight Loss
T _{Max2}	Temperature at Second Peak of Maximum Weight Loss
TNAP	Tri(N, N-bis- (2-hydroxy-ethyl) acyloxyethyl) phosphate
TPP	Triphenyl Phosphate
TPU	Thermoplastic Polyurethane
TSR	Total Smoke Release
TTI	Time to Ignition
UTM	Universal Testing Machine
VMC	Vertical Machining Center
WSi	Whisker Silicon
XRD	X-Ray Diffraction

CHAPTER 1

INTRODUCTION AND LITERATURE REVIEW

The polymeric foams such as polyurethane, polystyrene, phenolics and polyvinyl chloride are extensively used in wide range of applications; from disposable packaging and cushioning to insulation and construction. Their properties such as low density and low thermal conductivity establish them as a good material for insulation, while the flexibility and the softness make them a promising material for human comfort [1]. Of these polymeric foams, polyurethane (PU) is widely used for the industrial and household purposes. The total production of PU products in the Asia Pacific region was approximately 11.5 million tonnes in 2014 and it is estimated to be over 15.5 million tonnes by 2019 with a 6.2% annual average growth rate [2]. As the market of PU foams is increasing day-by-day, the waste generated during production and from the post-consumer products is also increasing at an alarming rate [3]. Therefore, a proper disposal of waste PU products is a major concern for the environmental protection [4]. The need of the hour is to develop a more eco-friendly version of PU from renewable sources that poses less threat to the environment.

Polyurethane (PU) foams are derived from the polyols and the polyisocyanate as raw materials. Commercially, these raw materials of PU foam are derived from petroleum, but due to its status as a limited resource and various environmental concerns, the biodegradable and renewable source-based raw materials are gaining popularity [5–7]. The most widely used renewable source to produce raw material for PU products is vegetable oil, which is available in abundance [8–16]. Several researchers have prepared polyols by using different vegetable oils, such as soybean oil [10, 17–21], castor oil [22–24], rapeseed oil [25–28], palm oil [29, 30], sunflower oil [31], tung oil [32, 33] and canola oil [34] etc. to develop polyurethane. Polyols have also been derived from other renewable sources such as corn starch [35], wood

[36], lignin [37–39], sugar cane bagasse [40], polyglycerol [41, 42], and others. Polyester polyols have also been reported to be produced commercially by using dicarboxylic acids, diols, triols and polyol derived from renewable sources [43]. Although polyols have been successfully derived from these renewable sources, the studies reveal that the properties of these renewable source-based foams are inferior to the foam derived from petroleum-based raw materials. Numerous studies have been conducted seeking to improve the mechanical, thermal and anti-flammable properties of these foams by incorporating different fillers and anti-flaming agents. The focus of this literature review is to discuss the methods used by different researchers for the structural modification of polyols and to select the potential fillers to enhance the desired properties of PU foams. The main emphasis has been given to the enhancement of mechanical, thermal and flame retardant properties of PU foams.

1.1 POLYURETHANE DERIVED FROM RENEWABLE SOURCES

Owing to increasing environmental concerns and decreasing petroleum resources, many renewable sources are being used for the development of PU foams and other PU products. Polyols, a raw material of PU foam, have been derived from different renewable sources such as vegetable oils, sugarcane bagasse, and pine wood to produce environmentally friendly PU products, as shown in Table 1.1.

Depending upon the number of hydroxyl groups present, the renewable sources for polyols formation can be classified into two broad categories: 1) the sources with a lower number of hydroxyl groups, and 2) the sources with a higher number of hydroxyl groups.

1.1.1 Renewable Sources with Lower Number of Hydroxyl Groups

Various types of vegetable oils are available, but the absence of hydroxyl groups (except castor oil, which naturally contains an average of 2.7 hydroxyl groups per triglyceride)

makes them unacceptable for the preparation of PU foam. It is therefore desirable to introduce some hydroxyl groups into their molecular chains to prepare polyols.

Table 1.1: The Renewable Sources used to Develop the Polyols

S. No.	Renewable Sources	Method Used to Develop Polyol	Reference(s)
1.	Soybean Oil	Epoxidation followed by ring opening with lactic acid	[17]
2.	Castor Oil	Transesterification using glycerol or used as supplied	[22, 23]
3.	Rapeseed Oil	Epoxidation followed by ring opening	[27]
4.	Palm Oil	Polycondensation of glycerol monostearate and glutaric acid	[30]
5.	Sunflower Oil	Reaction with glycerol in the presence of calcium oxide	[31]
6.	Tung Oil	Hydroformylation followed by transesterification	[32, 33]
7.	Pine Wood	Liquefaction using PEG 400/glycerin in the presence of sulfuric acid	[36]
8.	Eucalyptus	Liquefaction using PEG 400/glycerin in the presence of sulfuric acid	[36]
9.	Lignin	Liquefaction using PEG 400/glycerol or Extraction with mild alkaline solution	[37–39]
10.	Sugarcane Bagasse	Liquefaction in ethylene glycol/phthalic anhydride mixture catalysed by sulphuric acid	[40]
11.	Coffee Ground Waste	Acid liquefaction using polyhydric solvents (PEG 400/glycerol, 90/10 wt/wt) in the presence of sulfuric acid	[44]
12.	Soybean Straw	Liquefaction using crude glycerol and sulphuric acid	[45]

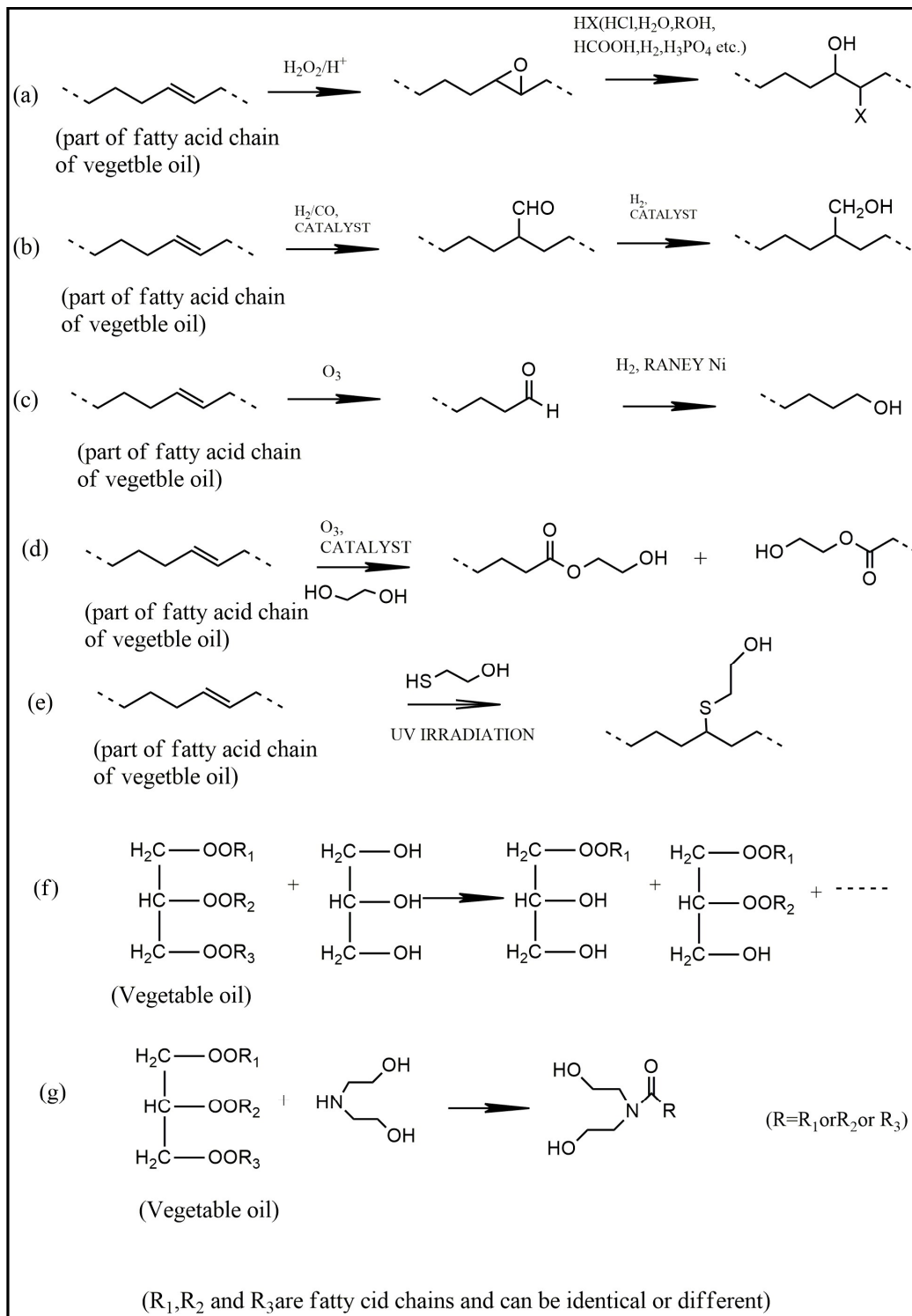


Figure 1.1: Schematic Representation of (a) Epoxidation Followed by Ring Opening, (b) Hydroformylation Followed by Hydrogenation, (c) Ozonolysis Followed by Hydrogenation, (d) Ozonolysis with the Addition of Ethylene Glycol, (e) Thiol-ene Coupling, (f) Transesterification and (g) Amidation [46].

In addition, the content of reactive hydroxyl groups in castor oil is not sufficient to produce a rigid PU foam, as the rigidity of the polymeric foams depends on the number of hydroxyl groups present in the polyol [46]. Therefore, some chemical modifications are required to increase the hydroxyl value of the polyols derived from renewable sources.

Table 1.2 presents different methods used by the researchers to modify the basic structure of the vegetable oils and thereby, increase their hydroxyl value. A schematic representation of different modification methods is shown in Figure 1.1. To enhance the hydroxyl value of castor oil-based polyols, two modification pathways have been widely used, namely: the transesterification of castor oil using its ester functional groups, and the alkoxylation of castor oil, using its hydroxyl moieties.

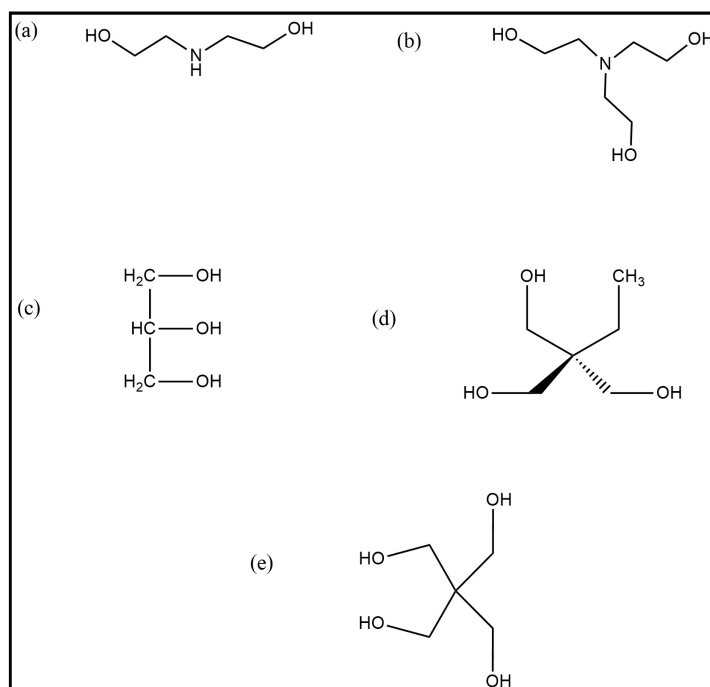


Figure 1.2: Structure of Polyfunctional Alcohols (a) Diethanolamine, (b) Triethanolamine, (c) Glycerol, (d) Trimethylol Propane and (e) Pentaerythritol.

Polyfunctional alcohols such as triethanolamine, glycerol, trimethylol propane and pentaerythritol may be used for the transesterification of castor oil, which results in the increase in hydroxyl value of the compound. Consequently, it provides hardness to the product, while

long chain fatty acids of triglycerides promote flexibility [47]. The structures of some polyfunctional alcohols are shown in Figure 1.2.

Table 1.2: Different Modification Methods for the Development of Polyols from the Vegetable Oils

Vegetable oil used	Modification Method	Reference(s)
Soybean Oil	Thiol-ene coupling	[11]
Vegetable Oil	Ozonolysis	[14]
Soybean Oil	Epoxidation followed by oxirane ring-opening	[17]
Dry Ricinoleic Acid	Transesterification with triethylene glycol or diethylene glycol or ethylene glycol	[22]
Sunflower Oil	Glycerol	[31]
Tung Oil	Reaction with hydrogen peroxide solution and formic acid followed by reaction with triethanolamine	[32]
Castor Oil	Amidation with diethanolamine or transesterification with triethanolamine or alkoxylation	[46]
Castor Oil	Alcoholysis with triethanolamine	[48]
Castor Oil	Transesterified by triethanolamine or glycerin	[49, 50]
Soybean Oil	Peracid method followed by transesterification	[49]
Vegetable Oil	Hydroformylation	[51]
Palm Oil	Tranesterification followed by epoxidation and ring opening	[52]
Epoxidized Soybean Oil	Oxirane ring opening by alcoholysis using methanol and ethylene glycol	[53]
Plant based Fatty acids	Thiol-ene/yne coupling	[54, 55]

By using alkoxylation, epoxide monomers such as ethylene oxide or propylene oxide may be introduced into triglycerides of castor oil to form the polyols. To enhance the hydroxyl value of castor oil, other modification methods such as amidation has also been used. Castor

oil-based polyols, prepared by the amidation of oil with diethanolamine and transesterification with triethanolamine, display hydroxyl values in the range of approximately 291-512 mg equivalent KOH/g and are suitable for the preparation of PU foams, adhesives, films or coatings. PU coatings prepared by using this polyol exhibit higher tensile strength and glass transition temperatures compared to the coatings based on unmodified castor oil [46]. Figure 1.3 shows the structure of various renewable source-based polyols that have been used to prepare environment friendly PU products. In the case of oils other than castor oil, e.g., rapeseed oil and soybean oil, epoxidation followed by transesterification is a widely used modification method to enhance the hydroxyl value of polyols [47].

Rigid PU foam with properties similar to the commercially used foams has been developed for the thermal insulation applications by using modified soybean oil and castor oil. The modification of soybean oil was conducted according to a peracid method using formic acid and hydrogen peroxide to prepare formiated soy polyol. Subsequently, transesterification was performed on this polyol using the polyfunctional alcohol triethanolamine (TEA) and glycerine to increase its hydroxyl value (Figure 1.3 (a)). Castor oil, which already possesses hydroxyl groups in its molecular structure, was modified by transesterification with TEA or glycerine (Figure 1.3 (b), (c)) [49]. Figure 1.3 (d) shows the structure of rosin based polyol, which has been used to prepare RPUF incorporated with phosphorus-nitrogen based flame retardant [56]. Polyols were also prepared by the dry ricinoleic acid formed after vacuum drying of castor oil. Different glycols (triethylene glycol, diethylene glycol and ethylene glycol) were taken in a 1:1 molar ratio of acid and glycol to prepare polyols with varied hydroxyl value (Figure 1.3 (e)) [22].

Flexible PU foams were synthesized by substituting some part of petroleum based polyol with soybean oil-based polyol, cross-linker polyol and styrene acrylonitrile copolymer-filled polyols. The resulting foams showed an increase in the compression modulus and the

best results were found in the 30% soybean oil-based polyol substituted foams. Styrene acrylonitrile-filled polyol reduced the foam cell size to a greater extent compared to soybean oil-based polyol and cross-linker polyol. An increase in the compression modulus of all substituted polyol-based foams was explained by the changes in phase morphology of the foams [17].

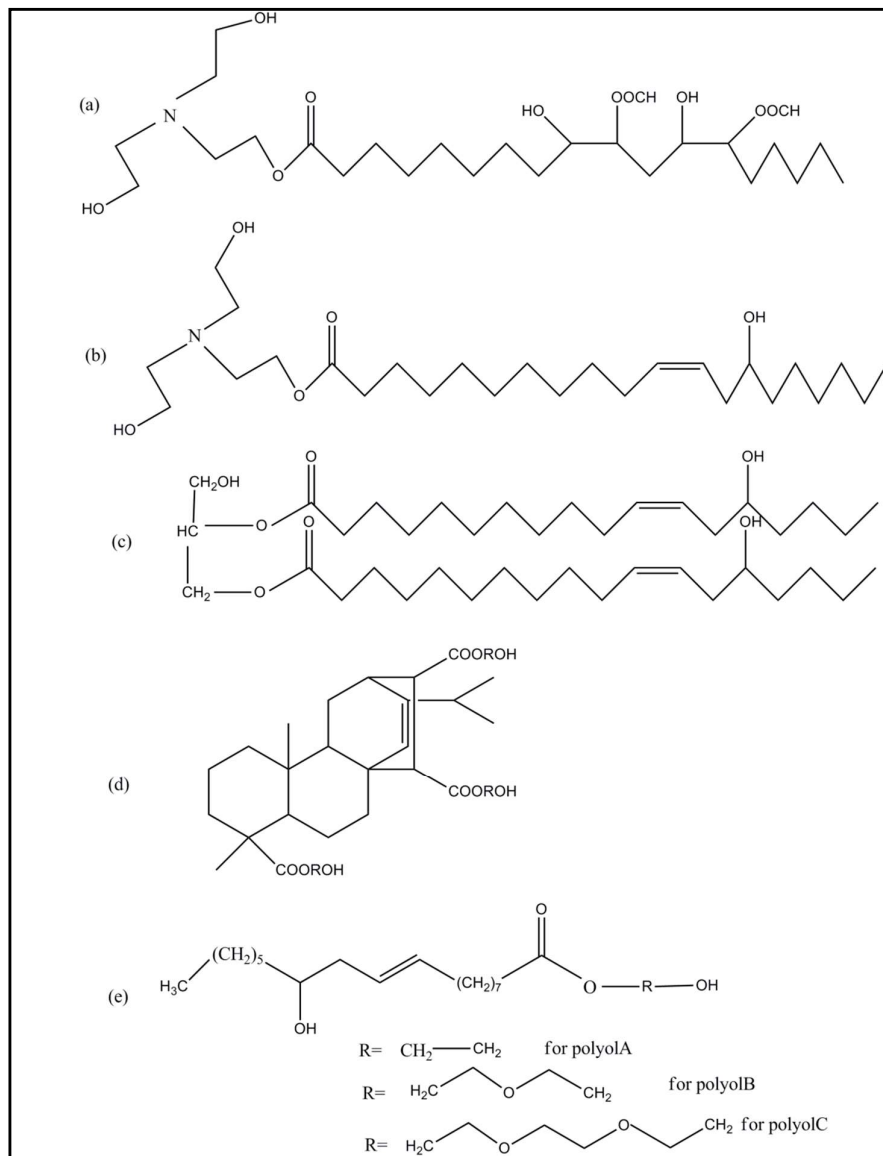


Figure 1.3: Structure of Polyols (a) Soybean Oil-Based Polyol Modified with TEA [49], (b) Castor Oil-Based Polyol Modified with TEA [49], (c) Castor Oil-Based Polyol Modified with Glycerol [49, 50] (d) Rosin-Based Polyol [56] and (e) Castor Oil-Based Polyol Modified with Different Glycols [22].

1.1.2 Renewable Sources with Higher Numbers of Hydroxyl Groups

Other renewable sources used for the production of polyols to develop environmentally friendly PU products are corncobs, pine wood and eucalyptus. These lignocellulosic materials are natural polymers and contain a large number of hydroxyl groups. Xue *et al.* [57] extracted lignin from corncob residue using a mild alkaline solution after the hydrolysis of hemicelluloses. Lignin-based rigid polyurethane foams (LRPF) were prepared by replacing petroleum based polyol with different amounts of lignin (8.33–37.19% w/w). Further, the foams with 37.19% lignin content were reinforced with the pulp fibre. These pulp fibre-reinforced foams had larger cell size and lower foam density due to the embedded pulp fibres in the foam structure, which provide better insulation and improve thermal stability. In another approach, the liquefaction of the eucalyptus and pine woods has been conducted using a mixture of polyethylene glycol PEG-400/glycerine at 140-160°C in the presence of sulphuric acid. Polyurethane-type rigid foams were prepared by the copolymerization reaction of this liquefied wood and polymeric methylene diphenylenediisocyanate (PMDI). The density, thermal conductivity, compressive strength and the modulus of elasticity of this foam were found to be almost comparable with other synthetic foams. Additionally, these biomass-based foams had better biodegradability compared to the synthetic foams [36, 58]. Polyols have also been obtained by acid liquefaction of waste coffee grounds to prepare PU foams. Thermogravimetric analysis (TGA) confirmed that these bio-based PU foams were thermally stable up to 190°C. Additionally, these foams regained their original shape even after 70% of creep compression, which shows their good elastic behaviour. Thus, these materials may prove to be a better option where damping properties are an additional requirement along with thermal insulation, such as aeronautics and acoustic insulation [44].

Thus, renewable sources may be considered as a promising raw material to produce polyurethane foams. For vegetable oils having lower numbers of hydroxyl groups, several

modification methods such as transesterification, epoxidation, hydroformylation, amidation, and thiol-ene coupling may be used to enhance the hydroxyl value, while for renewable sources with a higher number of hydroxyl groups, liquefaction may be used to produce polyols.

1.2 NON-ISOCYANATE POLYURETHANE (NIPU)

Polyisocyanates used to prepare PU foams are highly toxic in nature and may be harmful for mankind. Finding a green, sustainable route to produce PUs from renewable sources without using toxic raw materials is the prime requirement of the polyurethane industry. Therefore, recent efforts have been made to develop Non-isocyanate Polyurethane. NIPU has attracted the attention in both academia and applied research, as it has the potential to be used in the global PU market [59–61]. Various researchers have synthesized several cyclic carbonates to be used as a precursor to prepare isocyanate-free polyurethane [59, 62, 63]. In 1957, Groszos *et al.* patented a novel non-isocyanate methodology for the synthesis of polyurethane by aminolysis of dicyclic carbonate [64]. Figure 1.4 shows various routes adopted by different researchers to prepare NIPU. Recently, Sheng *et al.* [65] reported the synthesis of cyclic carbonate from glycol diglycidyl ether using an iron-based catalyst and tetrabutylammonium bromide (TBAB) to prepare NIPU and examined its thermal properties. These NIPUs showed an initial degradation temperature (T_{init} , corresponding to 5% weight loss) between 206°C and 266°C, while a maximum decomposition rate was observed between 241°C and 319°C. Epoxidized linseed oil and soybean oil were also converted into carbonated vegetable oil using TBAB and silica-supported 4-pyrrolidinopyridinium iodide catalyst for the production of vegetable oil-based NIPU. An increase in the stiffness and decrease in the water swelling was observed; in addition, the glass transition temperature of NIPU was found to increase from 17°C to 60°C [66].

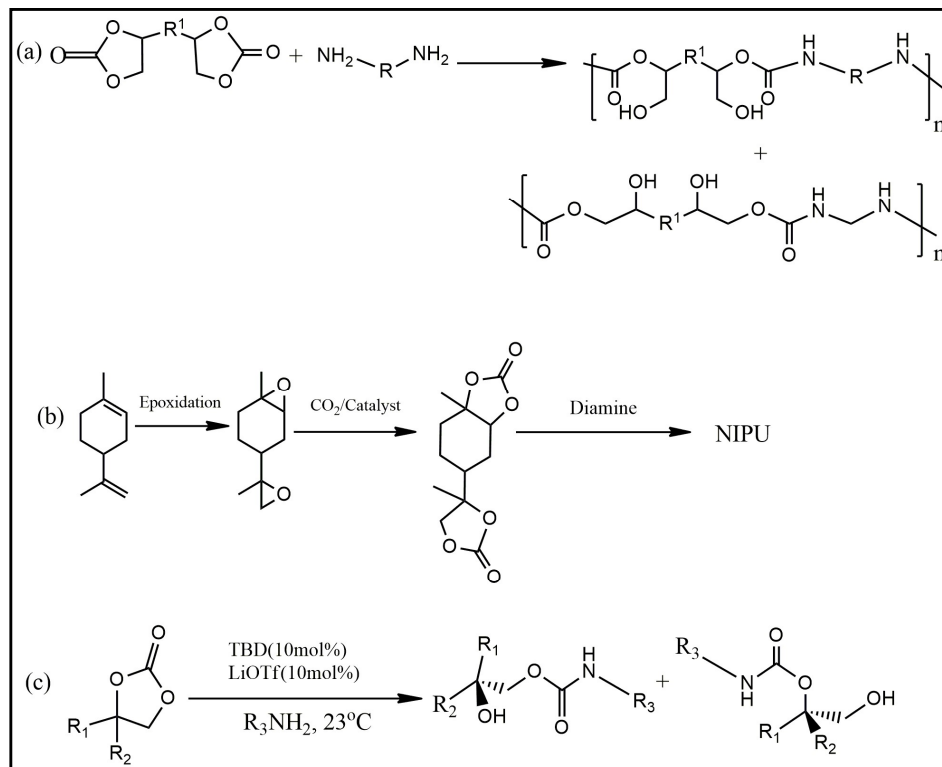


Figure 1.4: Some Routes to Synthesize (a) NIPU from Dicyclocarbonate and Diamines [64], (b) NIPU from Terpene Derivatives [67], (c) Urethane Linkage from Cyclocarbonate [68]

In another approach, limonene was used as a precursor to synthesize cyclic carbonate, which was further reacted with different amines to obtain linear NIPU. The results exhibited an increase in stiffness and glass transition temperature on increasing the amine functionality of the curing agent [67]. As the slow rate of aminolysis reaction is a major drawback while producing NIPU, Lombardo *et al.* [68] reported a new method to decrease the reaction time using triazabicyclodecene/lithium triflate (TBD/LiOTf) as catalyst for the synthesis of urethane and polyurethane. Cashew nut shell liquid (CNSL) and its derivatives have also been used as a raw material to prepare NIPU systems using different amine curing agents. It was observed that the mechanical and thermal properties of isophoronediamine (IPDA) cured NIPU was superior to hexamethylenediamine (HMDA) cured NIPU [69].

Renewable source-based polyols and cyclic carbonates may be a good option for the preparation of environmentally friendly PU products. The mechanical, thermal and flame retardant properties of these PU products, prepared by using these renewable materials, however, are not comparable to that of the products derived from the petroleum-based raw materials. Thus, different fillers or additives are used to enhance their properties

1.3 FILLERS TO ENHANCE THE MECHANICAL STRENGTH OF PU FOAMS

The main concern when using renewable source-based products as the raw material for the preparation of PU foams is their low mechanical strength. To enhance the mechanical strength of PU foams, the additives such as fibres, nanoparticles and particulate fillers have been used as reinforcement. Different researchers have worked on different types of fillers to enhance the mechanical strength of PU products. A brief overview of the literature employing these fillers to enhance the mechanical strength of the PU products is as follows.

1.3.1 Fibres

In 1960s, many researchers sought to prepare strong, stiff synthetic polymeric fibres and use them as reinforcements in various polymeric matrices [70]. To enhance the mechanical properties of PU foams and other composites, different types of fibres have been incorporated. Fibres, which have been commonly used as reinforcement, may be categorized as synthetic or natural fibres.

1.3.1.1 Synthetic Fibres – Synthetic fibres are man-made fibres with some advantageous properties such as high tensile strength and stiffness, which validate them as an excellent reinforcement material in the production of fibre-reinforced composites (FRC). Synthetic fibres are further classified as organic and inorganic fibres.

Organic Fibres- Synthetic organic fibres such as aramid, nylon, PE, and carbon fibre, have been widely used as a reinforcement in the FRCs. Of these, aramid fibres are high-performance

man-made fibres with certain exclusive properties such as good chemical resistance, good abrasion resistance, heat resistance, no melting up to decomposition, electrical non-conductivity and low flammability. Aramid fibres may therefore incorporate excellent performance characteristics in the reinforced composites. Proper safety measures must be taken while handling aramid fibres, however, as they may cause irritation to eyes and skin. In addition, the inhalation of chopped aramid fibres may be dangerous to human health [71]. In a study, nano-aramid fibre-reinforced PU foam was developed and exhibited enhanced mechanical properties without any deterioration in other properties such as density, thermal conductivity and processibility. These foams were reported to have a potential application as thermal insulation in crew exploration vehicles, crew launch vehicles, and lunar building blocks [72].

Inorganic Fibres- Glass fibre is the typical example of inorganic fibres. Glass fibres show desirable reinforcement properties for use in the PU matrix such as strength, stiffness, flexibility, chemical resistance, stability, and inertness. The mechanical and morphological properties of PU rigid foams are therefore reported to be altered by the incorporation of glass fibre as reinforcements [73, 74]. The influence of the incorporation of glass fibre on the mechanical properties of PU foams in terms of variations in fibre length and fibre mass content has been exclusively studied by many researchers. The variations in mass content of glass fibres have shown a greater influence on mechanical properties than the length of the fibre. As concluded from various studies, glass fibre reinforcement increases the mechanical properties of neat PU foam proportionally with the increase in the fibre mass content [75].

As glass fibres are inorganic fibres, their poor dispersion in polymer matrix is a drawback when using these fibres as a reinforcement with polymers. The treatment of glass fibres by using a coupling agent such as silanes before their incorporation in the polymer matrix

may improve their dispersion [70]. Different surface treatment methods used to modify the surface morphology of these reinforcing fillers are discussed in Section 1.4.

1.3.1.2 Natural Fibres - Natural fibres or bio-fibres such as jute, flex, betelnut fibre, banana fibre, and kenaf fibre may be a low cost substitute for high performance synthetic fibres [76–78]. A PU matrix loaded with kenaf fibres exhibited improvement in tensile strength and tensile modulus while the strain deteriorated with the increase of fibre content. Flexural strength, flexural modulus and hardness were also found to increase while a decline in impact strength, thermal stability and abrasion resistance of the composite was observed with the increase of fibre content [79]. Lignin-based rigid polyurethane foams (LRPF) were also prepared by reinforcing with different weight ratios of pulp fibre. It was noticed that the introduction of pulp fibre decreased the density without showing any effect on their compressive strength [57]. Nirmal *et al.* [80] compared the effect of incorporating betel nut fibres (natural fibre) and chopped strand mat glass fibre (synthetic fibre) in the polyester matrix. Betel nut fibre-filled composites showed competitive performance for compression, tensile and flexural tests with the glass fibre filled composites.

Natural fibres may be a better option for use as reinforcements due to their low cost and low density, but the major disadvantage of using these bio-fibres as reinforcement is the large variations in their mechanical properties under different weather conditions, methods of harvesting and technologies used for fibre separation [70]. The strong polar behaviour of natural fibres, which creates incompatibility while using them with most of the polymer matrices, is also a serious drawback. Natural fibres are lignocellulosic, so these fibres are hydrophilic in nature and absorb moisture from the environment, which causes deterioration in the mechanical properties of the fibre and composite [81]. To overcome this, some surface treatments are required prior to their incorporation in the polymer matrix, which are discussed in Section 1.4.

1.3.2 Nanofillers

Nanofiller is a nanoscale substance that has at least one of its dimensions less than 100 nm. Introducing nanofillers into polymeric foams creates a new class of materials that are lightweight and strong [82, 83]. Different types of nanofillers such as nanosilica [84], nanocalcium carbonate [85], and nanoclay [82] have been used to improve the properties of PU foams. Nanoclay adds some additional benefits by decreasing flammability and increasing thermal stability. When PU foams containing 15% soybean oil-based polyol were reinforced with glass microsphere and nanoclay, it was observed that on increasing the concentration of fillers, the density of the PU foam was reduced. The compressive strength of PU foams decreased when the content of the microsphere was raised from 1 to 3%, but it increased with a further increment of the microsphere load. When the microsphere content reached 7%, foams showed a compressive strength comparable to that of the foams made from 100% petroleum-based polyol [19]. When palm oil-based PU foam was incorporated with the modified diaminopropanemontmorillonite (DAP-MMT) nanoclay, it was observed that at a low concentration of nanoclay, the foams displayed exfoliated morphologies, while at an increasing concentration of nanoclay, the foams exhibited the intercalated structures. The cell size of the foam was observed to decrease upon increasing the concentration of DAP-MMT. Consequently, an increase in compressive strength and thermal stability was observed with the increase in DAP-MMT content up to 4%, while further increase in DAP-MMT concentration decreases the above said properties due to the agglomeration of nanoclay particles [86]. The cellular structure of the foams has also been altered by the incorporation of cellulose microfibrils and nanoclays. The compressive strength of foam was also found to be increased by using these fillers as reinforcement [18]. The addition of cellulose nanocrystals (CNC) in palm oil-based polyurethane foam showed a significant improvement in the compressive strength from 54 to 117 kPa and a decrease in the deformation resilience of the foam.

Furthermore, the increase in concentration of CNC increased the dimensional stability of foams in both freezing and heating conditions [29].

Carbon based nano-materials such as carbon nanotubes, carbon nanofibres, graphene and derivatives of graphene such as chemically modified graphene or functionalized graphene sheets have great potential to be used as reinforcing filler in rigid PU foam. Fire retardancy, strength, stiffness, electrical conductivity, piezoelectric and thermal properties of polymeric nanocomposites may be adjusted according to the requirement of the end product by incorporating carbon based nanomaterials [87, 88].

1.3.3 Particulate Fillers

Some of the approaches adopted simple particulate fillers to be used as low cost fillers to enhance the properties and decrease the cost of the final product. The properties of the rigid polyurethane foams may be enhanced by reinforcing these foams with different particulate fillers such as talc, calcium carbonate or dolomite [89, 90]. The effect of different concentrations of fillers (talc, chalk, aluminium hydroxide, borax and starch) on the properties of rigid polyurethane-polyisocyanurate foams has been analysed by Czuprynski *et al.* [91]. The addition of aluminium hydroxide and talc into the foam composition improved its functional properties such as compressive strength, closed cell content and apparent density, while the flammability and brittleness was found to be reduced. The introduction of talc into foam also increased the softening point, the starting temperatures of decomposition and the initial change in the mass of the foam.

Owing to high silica content of Rice Husk Ash (RHA), it has also been used as a reinforcing filler in rigid PU foam. Although RHA content did not affect the thermal stability, but significant changes were observed in thermal conductivity, foam morphology and density [32]. Due to the induction of some deleterious changes by RHA in the foam cellular structure, the compressive strength, compression modulus and storage modulus of the foam decreased

with the increase in rice husk ash concentration [33]. In a study, silkworm cocoons have been added as natural particulate filler in rigid polyurethane foams. Reinforcing the foam with different types of silkworm cocoons increased its density and compressive properties without affecting their dimensional and thermal stability [92].

In another approach, the flexible polyurethane (PU) foams were reinforced with coir fibres and tyre particles. The high decomposition temperature of coir and rubber make these fillers suitable for use as reinforcements in PU foams. Furthermore, it was also evident that these foam composites had a cellular structure with smaller cell sizes and higher cell density, which may provide better damping for energy absorption applications [93]. The introduction of egg shell (ES) waste into the foam composite as filler resulted in an increased apparent density, compressive strength and thermal stability. Additionally, these foams exhibited low water absorption and low friability, thus leading to an increase in the life span of the product, high dimensional stability in the aqueous media, no toxicity towards human skin cells and resistance towards bacterial adhesion [94].

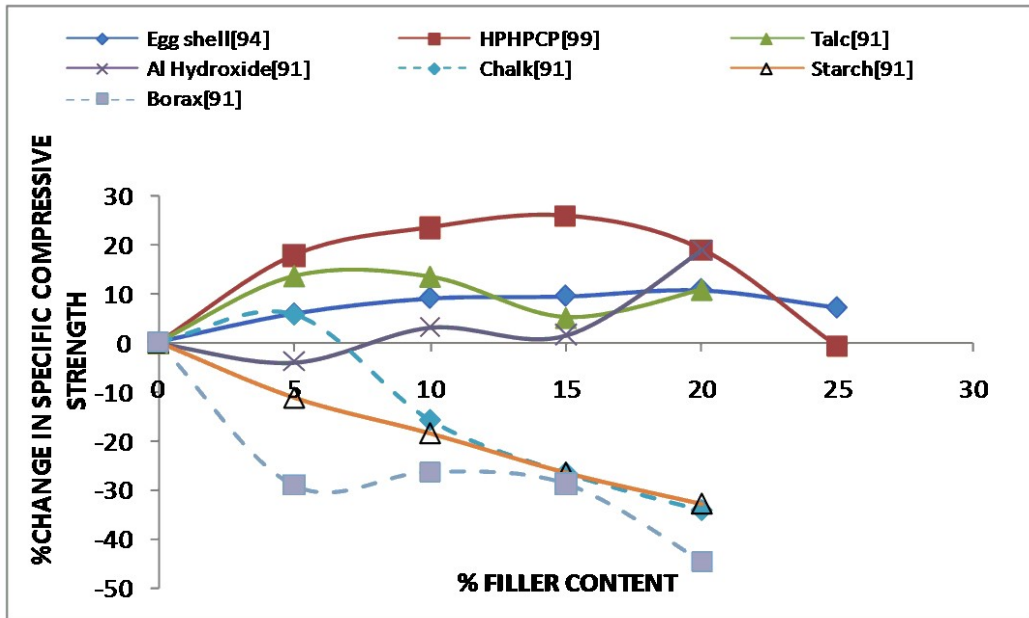


Figure 1.5: Plots of % Change in Specific Compressive Strength vs. % Filler Content (for foams with high filler content) [91,94,99]

The PU composite foam reinforced with SiO₂ and a fixed concentration of certain fibres (nylon, glass fibre and carbon fibre) showed an increase in tensile strength and hardness upon increasing the SiO₂ concentration up to 20%. On further increasing the SiO₂ concentration, the tensile strength decreases while the hardness remains nearly constant. Additionally, the impact strength decreases continuously with the increase in SiO₂ content. Water absorption also showed a maximum value at 10% SiO₂ concentration, then decreased as the SiO₂ concentration continued to increase [95]. Figures 1.5 and 1.6 show the effect of different fillers on the specific compressive strength (kPa/kg/m³) of PU foams.

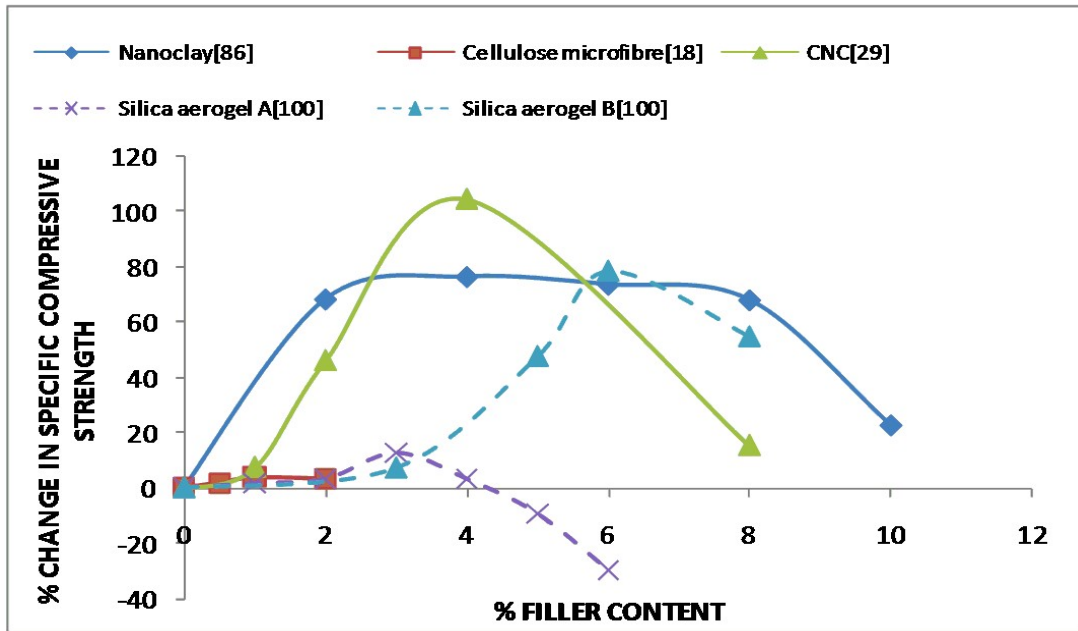


Figure 1.6: Plots of % Change in Specific Compressive Strength vs. % Filler Content (for foams with low filler content) [18,29,86,100]

The graphs show the percentage change in specific compressive strength (compressive strength/density) when considering the increasing concentration of filler. It is evident from the graphs that CNC, silica aerogel and nanoclay enhance the compressive strength at low filler concentrations, while chalk, borax and starch show a decrease in strength. Aluminium

hydroxide and talc also enhanced the strength slightly, while egg shell waste has not shown much effect on the specific compressive strength of PU foams.

Different synthetic or natural fibres such as glass fibre and pulp fibre may be used as reinforcing agents to enhance the mechanical strength of bio-based PU foams. Certain nanofillers such as nanosilica and nanoclay or particulate fillers such as egg shell waste and the ash of natural fibres may also be better options to improve the mechanical strength of PU foams. Table 1.3 summarizes the effect of different fillers on the mechanical properties of PU and other composite foams.

Table 1.3: Effect of Different Fillers on Mechanical Properties of PU Composite Foams

Filler Used	Percentage of Filler	Matrix Material	Results/Remarks	Ref.
Glass Fibre	0 – 20wt%	Polyurethane	Up to 121% increase in stiffness and 101% increase in strength	[75]
Nano-aramid Fibre	1wt%	Polyurethane	Tensile strength ~139% and compression results ~178% of the baseline	[72]
Kenaf bast Fibre	20–50wt%	Polyurethane	30% fibre loading exhibited the best tensile strength	[79]
SiO ₂ and Glass Fibre	SiO ₂ – 0 –30wt% glass fibre– 0 –12.5wt%	Polyurethane	Tensile strength is optimal at SiO ₂ 20% and glass fibre 7.8%	[95]
Glass Fibre	0 – 10wt%	Polyurethane	At 10%glass fibre, compressive strengths increased 35% and 54% at the room and cryogenic temperatures, respectively, while the tensile strengths increased 220% and 210%	[74]
Pulp Fibre	0 – 5wt%	Polyurethane	Compressive strength not influenced by pulp, but thermal stabilities were slightly improved.	[57]
Rice Husk Ash (RHA)	0 – 5wt%	Polyurethane	Compressive strength and storage modulus increase	[33]
Carbon Nanotubes and Graphite	0.01, 0.05 and 0.1 wt% of CNTs or 5	Polyurethane	CNTs (up to 0.05 wt.%) improve the mechanical strength by	[96]

	and 7 wt% of graphite		approximately 20%, while graphite decreases the mechanical strength	
Cellulose Microfibres and Nanoclays	Both 0 – 2wt%	Polyurethane	Compressive strength enhanced	[18]
Cellulose Nanocrystals (CNC)	1 – 8wt%	Polyurethane	CNC as an additive significantly improved the compressive strength from 54 to 117 kPa	[29]
Microsphere and Nanoclay	1 – 7%	Polyurethane	Foams containing 5 to 7% microspheres or 3 to 7% nanoclay had superior density-compressive strength	[19]
EG ¹	0 – 30wt%	Castor oil based polyol	Mechanical strength decreased	[47]
Silkworm Cocoon	60-90% by weight (40-70% by volume) of polymer matrix	Polyurethane	Increased density from 45 kg/m ³ to 60 kg/m ³ with domesticated cocoon and 120 kg/m ³ with wild cocoons	[92]
Coir Fibre, Tyre Particle	2.5 wt%	Polyurethane	Smaller cell size and higher cell density	[93]
Egg Shell Waste	20 wt%	Polyurethane	Increased density and compressive strength, low water absorption, low friability, high dimensional stability in aqueous media	[94]
EG, DMMP ² , TEA ³ ,	EG- 3-15wt%, TEA- 2-10wt%, DMMP -1-5wt%	Polyurethane	EG and TEA increase the compressive strength, DMMP achieved the maximum value of compressive strength at DMMP dosage of 4%.	[97]
EG or/and (WSi ⁴)	0 – 20 wt % EG 0 – 30 wt % WSi	Polyurethane	At 10% WSi maximum mechanical strength	[98]
DAP-MMT ⁵	0 – 10wt%	Polyurethane	Compressive strength increased with increasing DAP-MMT contents up to 4 wt%,	[86]
HPHPCP ⁶	0 – 25%	Polyurethane	At 15 wt% HPHPCP concentration, compressive strength reached to the maximum 328.1 kPa	[99]
DOPO-BA ⁷	0 – 20%	Polyurethane	Compressive strength containing 20 wt% DOPO-BA increased to 0.48 MPa	[56]

Granular Silica Aerogel	1 –8wt%	Polyisocyanate	At 6 wt.% silica aerogel, compressive strengths enhanced by 136%	[100]
Calcium Carbonate and Dolomite	5 – 30wt%	Polyether polyurethane	For calcite, all properties were maximized at 10% concentration except for tensile strength; for dolomite, all properties were maximized at 20% except for maximum strain	[89]
Talc	0 – 30wt%	Polyurethane	The use of talc as filler up to 20% is an advantage	[90]
Talc, Aluminium Hydroxide, Chalk, Starch and Borax	2.5 to 20wt%	Polyurethane	Foams with addition of talc and aluminium hydroxide have industrial applications	[91]
Wood Flour	0 – 15wt%	Polyurethane	Compression properties decrease, thermal conductivity and thermal stability increase	[48]

1: Expandable Graphite, 2: Dimethyl Methylphosphonate, 3: Triethylene Amine, 4: Whisker Silicon, 5: Modified DiaminopropaneMontmorillonite, 6:Hexa- (Phosphite-Hydroxyl-Methyl-Phenoxy)-Cyclotriphosphazene, 7: Condensation Product of Benzaldehyde, Aniline and 9,10-Dihydro-9-Oxa-10-Phosphaphenanthrene-10-Oxide (DOPO)

1.4 SURFACE TREATMENT OF FILLERS

Different types of fibres such as jute, flex, coir, sugarcane bagasse and rick husks are available for improving the properties of the polymeric composites. The hydrophilic nature of these fibres, however, is a major problem while using these fibres as reinforcement. Certain surface treatment methods have therefore, been adopted to make these fibres hydrophobic and improve their adhesion with the polymer matrix [81]. Additionally, different type of inorganic fillers such as glass fibres have also been used to enhance the properties of foam composites, but these inorganic fillers are incompatible with the organic polymer matrix and prior to addition, some surface treatments are required to enhance the adhesion of these fillers to the matrix. Table 1.4 summarizes the different surface treatment methods used to modify the surface properties of the fillers.

Table 1.4: Different Surface Treatment Methods Used to Modify the Filler Surface

S. No.	Surface Treatment Method	Commonly Used Coupling Agent	Mode of Functioning
1.	Alkali Treatment	NaOH	Works by disrupting hydrogen bonding of the network, consequently increasing surface roughness
2.	Silane Treatment	R-Si(OR') _n	Most widely used coupling agent, attaches through alkoxy or silanol group
3.	Acetylation	Acetic Anhydride	Introduces an acetyl functional group into an organic compound
4.	Benzoylation Treatment	Benzoyl Chloride	Benzoyl chloride contains a benzoyl group, which is responsible for the decrease in hydrophilicity of the fibre
5.	Maleated Coupling Agents	Maleic Anhydride	Activation of maleic anhydride grafted copolymer, then esterification of fibre
6.	Permanganate Treatment	Potassium Permanganate Solution in Acetone	Formation of radical through MnO ₃ ⁻ ion formation
7.	Acrylation	Acrylic Acid	Leads to strong covalent bond formation
8.	Acrylonitrile Grafting	Acrylonitrile	Graft copolymerization reaction occurs
9.	Peroxide Treatment	Dicumyl Peroxide or Benzoyl Peroxide	Peroxide decomposes easily to form free radicals, then reacts with hydrogen group of polymer and fibre
10.	Isocyanate Treatment	Isocyanates	Isocyanate group reacts readily with hydroxyl group of fibres
11.	Other Chemical Treatment Methods	For Stearic Acid dissolved in Ethyl Alcohol, Sodium Chlorite, Triazine derivatives	Used for the modification of natural fibres by reducing the number of cellulosic hydroxyl groups to render them more hydrophobic.

Different types of coupling agents are used for the surface treatment of the fillers. On the basis of their mode of functioning, coupling agents may be divided into different groups, namely compatibilizers, bonding agents and dispersing agents. Compatibilizers work through the reduction of the interfacial tension between fibres and the polymer matrix, which consequently increases compatibility between them. Generally, acetic anhydride and methyl isocyanate perform the function of compatibilizers by lowering the fibre surface energy,

thereby making it compatible with the polymer matrix. Bonding agents act as a bridge between fibres and the polymer matrix and join them together by polymer chain entanglement, covalent bonding or any strong secondary interactions. Some bonding agents, such as maleated polypropylene (MAPP), maleated styrene-ethylene/butylene-styrene (SEBS-MA) and styrene-maleic anhydride (SMA), also act as compatibilizers in wood fibre-reinforced polymer composites. Dispersing agents act by reducing the fibre-matrix interfacial energy for homogeneous dispersion of fibres without aggregation in the polymer matrix. Stearic acid and its metallic salts are used as dispersing agents to improve the uniform dispersion of the fibres in the polymer matrix [101].

Coupling agents may also be classified as inorganic, organic and organic-inorganic on the basis of their structure. Organic coupling agents comprise anhydrides, isocyanates, amides, acrylates, imides, epoxides, chlorotriazines, and organic acids. Inorganic coupling agents represent the smallest group of coupling agents and silicates are the members of this group. Organic-inorganic agents such as titanates and silanes are the most widely used coupling agents. Of these, silanes have shown better performance characteristics [84, 102, 103]. A brief overview of the literature about silanes and other coupling agents appears below.

1.4.1 Treatment with Silanes

Silanes are represented as $R-Si(OR')_n$, and may attach themselves to hydroxy groups of the fibres or fillers either by the alkoxy group (-OR') present or via its hydrolysed product silanol. Trialkoxysilanes are the most established silanes used for the surface treatment, which may have a non-reactive alkyl or reactive organic functional group. Silanols are formed by the hydrolysis of silane, which is then adsorbed and condensed on the surface of the fibre at a specific pH and temperature. The organic functional group of silane and the characteristics of the matrix material are the dominating factors, which explains the mode of interaction of the silane and the matrix. Silane coupling agents increase the weather resistance, reduce shrinkage

and lessen or even eliminate the surface or internal defects by providing a strong and stable bond between the filler and the resin [102]. Rostami *et al.* [84] investigated the effect of aminosilane treatment of nanosilica particles at varying pH on the properties of nanoparticle-reinforced polyurethane matrices. An improvement in the glass transition temperature (T_g) was observed, which consequently improved the mechanical performance of the PU matrix at higher temperatures.

The effect of silane surface treatments was also studied by Tayfun *et al.* [103] In this study, fullerene was incorporated in the polyurethane matrix and the effect of the surface treatment of fullerene on the mechanical, electrical and flow properties was investigated. The results showed higher MFI values as well as better tensile and electrical properties, which was attributed to the better dispersion of filler particles in PU matrix due to the surface treatment.

1.4.2 Treatment with Other Coupling Agents

After silanes, alkali is the other widely used coupling agent. It has been investigated in a few studies to enhance the surface properties of fillers with or without other treatments. In a study, Kenaf fibres treated with NaOH subjected to polyester, epoxy, and PU matrices exhibited excellent interfacial adhesion strength [104]. Tayfun *et al.* [105] applied alkali and isocyanate surface modifications to flax fibre and investigated its effect on the mechanical properties, modulus of elasticity, melt-flow, water uptake and morphological properties of thermoplastic polyurethane. The results from this study confirmed that the surface modifications lead to better mechanical properties in comparison with untreated flax fibres. Isocyanate treatments also reduced the melt flow rate due to the enhancements in the interfacial interactions between different phases. SEM micrographs showed that the dispersion of the surface treated fibres was more homogeneous in the TPU matrix. A reduction in the moisture absorption tendency and modification of the surface of coconut coir fibre has been observed with various treatments such as alkali, permanganate, acetylation, and heat [81]. During the

coupling treatment, different processing aids such as antioxidants, plasticizers, stabilizers, and flame retardants are also added to the mixture to improve the mechanical and physical properties of a composite.

1.5 ENHANCEMENT OF THERMAL INSULATION AND FLAME RETARDANCY OF PU FOAMS

Other requirements for developing pertinent rigid foam are good thermal insulation and anti-flammability. Since, blowing agents are required to develop porous foam with a closed cell structure, which enhances thermal insulation, but the widely used blowing agents (such as pentane) are flammable in nature. In addition, the existence of alkyl and ester groups also makes vegetable oil-based polyols highly flammable. Due to these concerns, it is imperative to decrease the flammability of renewable source-based RPUFs by adding suitable flame retardants or incorporating some flame retardant group in the foam structure, which may also improve their thermal insulation and thermal stability [106, 107]. Different approaches to enhance the thermal properties and the flame retardancy of PU foams are discussed in following subsections:

1.5.1 Incorporation of Flame Retardant Groups

Some studies have been carried out to decrease the flammability of the product by incorporating flame retardant groups in the structure of polyurethane. Phosphorylated polyols may be used to enhance the flame retardant properties of PU foams. In one of these studies, a novel castor oil-based flame-retarded polyurethane rigid foam was prepared using castor oil phosphate polyol (COFPL).

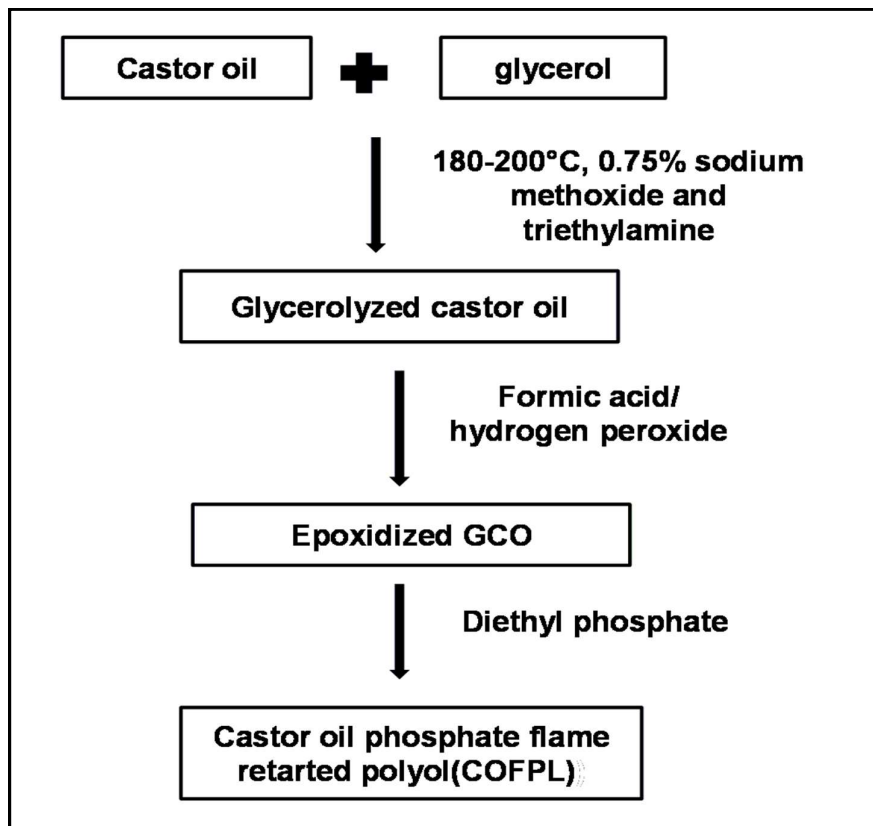


Figure 1.7: Schematic Diagram for the Preparation of COFPL [47]

Figure 1.7 shows the method adopted by Zhang *et al.* [47] for the preparation of COFPL, in which the phosphate group has been introduced in the polyol to generate flame retarded polyol. In this method, glycerolysed castor oil (GCO) is prepared by the reaction of castor oil with glycerol. Then, epoxidation of GCO is conducted and epoxidized GCO was formed, which was converted into COFPL by the reaction with diethyl phosphate. The structure of COFPL is as shown in Figure 1.8 (a) [47].

In an another approach, phosphorylated polyol was prepared by using soybean oil and the foams were prepared by using this phosphorylated polyol in combination with other polyols. The flame retardant properties of the resulting foam have been analysed by comparing the results with the foam samples prepared by incorporating the commercial flame retardants. The results showed that the foams prepared using phosphorylated polyols competed well with the foams incorporated with commercial flame retardants [108].

1.5.2 Addition of Flame Retardants

Flame retardants (FR) such as chlorinated FRs and different types of brominated FRs have been used earlier for their excellent performance. The frequent use of these halogenated flame retardants, however, raised many environmental issues, i.e., the depletion of the ozone layer, the generation of toxic gases on combustion, etc. Thus, in the recent studies, alternatives flame retardants such as phosphorus compounds, nitrogen compounds, metal hydroxide, boron compounds or nanomaterials [109–111] are being used and proved to be promising candidates to decrease the flammability.

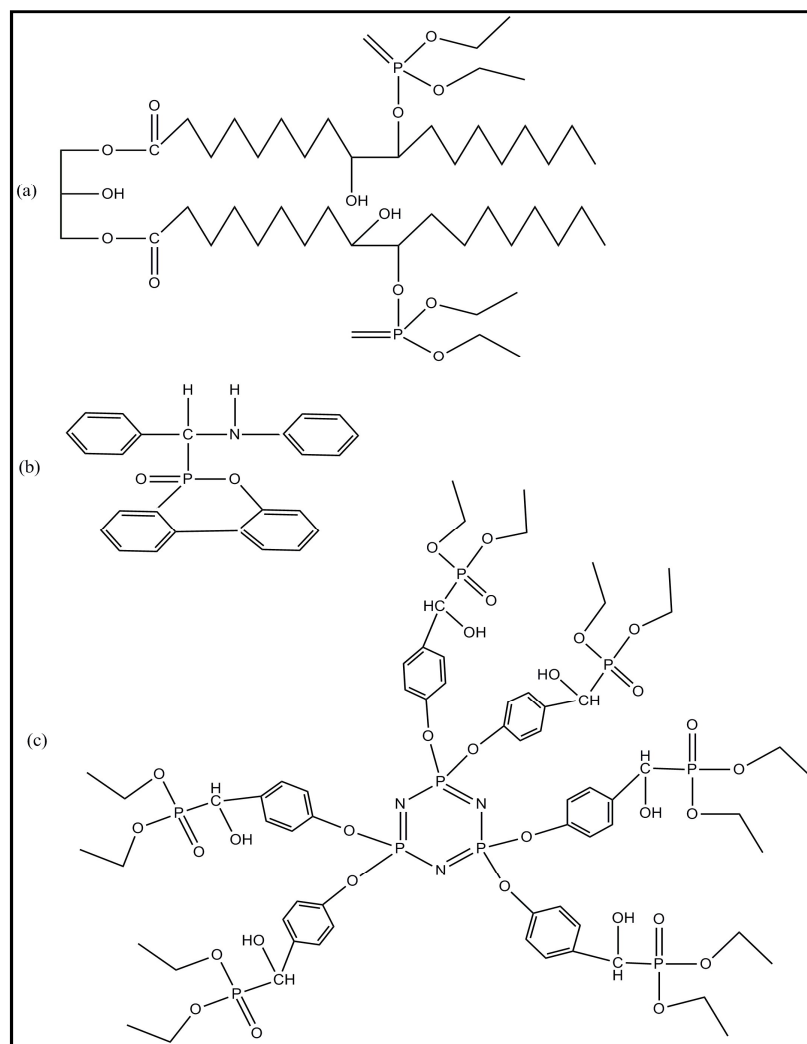


Figure 1.8: Structure of Different Flame Retardants (a) COFPL [47], (b)DOPO-BA [56], (c) HPHPCP [99]

Zheng *et al.* [112] introduced the phosphorus flame retardant using ammonium polyphosphate (APP) and triphenyl phosphate (TPP) in RPUF to promote the char-forming property of RPUF. It is evident from the results that the thermal stability and the char yield of RPUF have been improved by the addition of APP-TPP. Additionally, the organically modified montmorillonite (OMMT) was incorporated as an additional filler in the APP-TPP/ RPUF to further enhance the flame retardancy of RPUF. The resulting foams exhibited a significant increase in the combustion duration time and decrease in the heat release rate and total smoke production with the incorporation of phosphates and nanoclays. The extraordinary flame retardant performance of these foams is attributed to the synergy between the OMMT and APP-TPP system in forming a mass of integrated, stable and tight charred layers during the combustion of RPUF.

Hu *et al.* [97] studied the effect of incorporating the expandable graphite (EG) and dimethyl methyl phosphonate (DMMP) in PU foam as flame retardants. They reported that the expandable graphite increased the limiting oxygen index and decreased the closed cell content of RPUF, while the DMMP also showed a significant effect on the flame retardancy of RPUF. Percentage LOI was enhanced significantly by increasing the concentration of DMMP in the formulation. DMMP also reduced the cell size of the foam, accordingly showing an increase in the closed cell content. Whisker silicon (WSi) and expandable graphite (EG) have also been used by some researchers to enhance the anti-flammability characteristics of rigid polyurethane foam (RPUF) composites. The thermal stability as well as the glass transition temperature of the rigid polyurethane foam are reported to be enhanced by the addition of WSi and EG. On the other hand, increasing the EG concentration increased the percentage LOI, while increasing the WSi concentration did not show any significant effect on percentage LOI [98]. Descriptions of different types of flame retardants are summarized in Table 1.5.

Table 1.5: Different Types of Flame Retardants

S. No.	Flame retardant	Examples	Mode of Functioning	Ref.
1.	Halogenated Compounds	TBBPA ¹ , HBCD ² , penta-BDE ³ , octa-BDE and deca-BDE	Acts by chemical interference with the radical growth in the gas phase and removing the radicals formed during combustion	[107]
2.	Phosphorus Based Compounds	Elemental Phosphines, Red Phosphorus, Phosphonium Compounds, Phosphine Oxides, Phosphites, Phosphonates, Phosphates and Phosphinates	Acts by altering the pyrolytic path of the polymeric material in the condensed phase, consequently reducing the amount of gaseous combustibles	[47, 99, 107]
3.	Metal Hydroxides	ATH ⁴ and MH ⁵	Decomposes endothermically and release free water to cool the pyrolysis region	[107]
4.	Intumescent Agents	APP ⁶	Materials swell when exposed to fire or heat to form a porous foamed mass, usually carbonaceous, that acts as a barrier to heat, oxygen and other pyrolysis products	[107, 112]
5.	Boron-Based Flame Retardants	Hydrated Zinc Borates	Their endothermic decomposition liberates water	[107]
6.	Nitrogen-Based Flame Retardants	Guanidine, Triazine, Melamine, and Urea (Phosphate) Based Compounds	These compounds release low amounts of smoke during fire, are relatively less toxic and environmentally friendly	[56, 107]
7.	Nanofillers	Layered Silicates, Needle-like Sepiolite, Carbon Nanotubes, Graphite Oxide	Anti-flammability of carbon nanotube-reinforced foams increases due to the accumulation of a carbon layer on the polymer matrix surface	[96, 109–111]
8.	Other Flame Retardants	Aerogels, Phase Change Materials	Enhances thermal insulation and flame retardancy through their unique structure	[100, 113]

1: TetrabromoBisphenol A, 2: Hexabromocyclododecane, 3: PolybrominatedDiphenyl Ether, 4: Aluminium Tri-Hydroxide, 5: Magnesium Di-Hydroxide, 6: Ammonium Polyphosphate

Certain unique flame retardants have also been prepared by different researchers. A phosphorus and nitrogen-based flame retardant, DOPO-BA, has been synthesized by using 9,10-dihydro-9-oxa-10-phosphaphenanthrene-10-oxide (DOPO), aniline and benzaldehyde and incorporated in a polymer matrix to prepare rosin-based rigid polyurethane foams. Figure 1.8 (b) shows the structure of DOPO-BA. The physical properties, thermal stability and flame-retardancy of the RPUF was improved after the incorporation of DOPO-BA, while the closed cell content, cell size and thermal conductivity of rigid foam did not show any remarkable change [56]. Another flame retardant, hexa(phosphitehydroxymethylphenoxy) cyclotriphosphazene (HPHPCP), shown in Figure 1.8 (c), has also been synthesized using hexachlorocyclotriphosphazene, p-hydroxybenzaldehyde and diethyl phosphite. This flame retardant has been incorporated into rigid polyurethane foams prepared by using polyester polyol, polyether polyol and polymethylenepolyphenylisocyanate. HPHPCP contains multifunctional groups that introduced crosslinking into the foam structure, consequently improving its thermal stability, density and compressive strength. Additionally, the incorporation of HPHPCP into the rigid foam increased the percentage LOI while the values of the second peak of heat release rate, which relates with the surface pyrolysis of PU foam, were found to decrease gradually [99].

1.5.3 Addition of Aerogels

The thermal properties of PU foams may also be increased by the incorporation of unique materials such as aerogels, which provide thermal insulation and enhance the flame retardancy. Aerogels are highly porous materials with up to 99.98% porosity. These are ultra-lightweight materials developed from a gel after replacing the liquid part of the gel with a gas. Due to their highly porous structure, aerogels show extraordinarily low thermal conductivity and good acoustical properties for sound abatement. In addition, aerogels are non-combustible and show high optical transparency. These unique properties of the aerogels offer a wide range

of applications; from acoustic insulation and fire retardation board to improved energy savings in solar collector covers and window panes. Most importantly, they are user-friendly, recyclable and reusable materials [114].

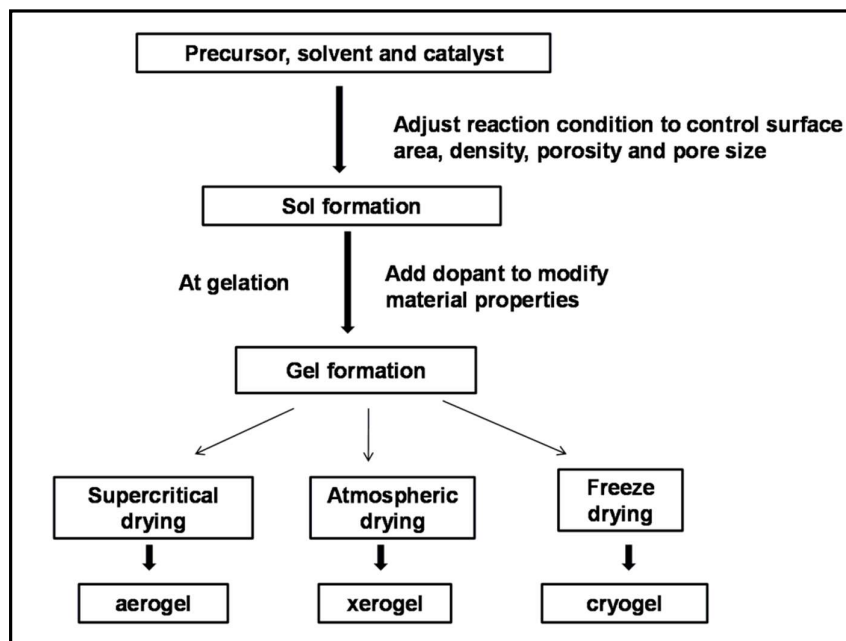


Figure 1.9: Flow Chart for Aerogel Preparation [115]

Due to these properties, aerogels may be used as filler in PU foams to enhance the thermal insulation and anti-flammability. Aerogels may be developed using a wide variety of substances such as silica, most metal oxides, carbon, organic polymers and biological polymers (cellulose, lignin, gelatin, pectin, etc.) as precursors. Figure 1.9 shows the method used for the preparation of aerogel. To prepare aerogels, precursors are mixed with a catalyst and solvent to prepare sol under predefined reaction conditions. At the gelation point, sol is converted into a gel and various dopants may also be added to enhance the material properties. When this gel is subjected to the supercritical drying, it converts into an aerogel with less than 15% shrinkage. Atmospheric drying and freeze drying of this gel results in xerogel and cryogel, respectively, and observes more than 90% shrinkage on drying, which results in a density higher than the aerogel.

Table 1.6: Effect of Different Additives on the Thermal Properties of PU Foams

Filler	Percentage of Filler	Matrix Material	Results	Ref.
TEP ¹ and EG ²	TEP -5 wt% EG -30 wt%	COFPL ¹⁵ Polyurethane	29.7% increase in LOI ¹²	[47]
APP ³ and TPP ⁴ , OMMT ⁵	APP-0-10wt% TPP-0-6wt% OMMT-0-7wt%	Polyester Polyol	Longest combustion duration time, slowest heat release rate and lowest smoke production	[112]
EG, DMMP ⁶ , TEA ⁷	EG- 3-15wt%, TEA-2-10wt%, DMMP -1-5wt%	Polyurethane	EG increased the LOI of RPUF, DMMP displayed the flame-retardation effects	[97]
EG or/and WSi ⁸	EG- 0-20wt% WSi- 0-30wt %	Polyurethane	At 10% WSi and increasing EG concentration, LOI increases	[98]
Kenaf Bast Fibre	20-50wt%	Polyurethane	Thermal stability decreases on fibre loading	[79]
DAP-MMT ⁹	0 – 10wt%	Polyurethane	Thermal stability increased upto DAP-MMT contents 4 wt. %	[86]
HPHPCP ¹⁰	0 – 25wt%	Polyurethane	The LOI value has been increased to 26%, TTI ¹³ value increased approximately 270%, much lower PHRR ¹⁴	[99]
DOPO-BA ¹¹	0 – 20wt%	Polyurethane	Containing 20 wt% DOPO-BA increased to 28.1%, increases TTI and decrease in PHHR	[56]
Carbon Nanotubes and Graphite	CNTs-0.01-0.1 wt.% graphite- 5 and 7 wt.%	Polyurethane	Carbon nanotubes improves the thermal stability by LOI 33.9% at expandable graphite 7%	[96]
Cellulose Microfibres and Nanoclays	Both upto 2wt%	Polyurethane	Microfibres delayed the onset of degradation temperature from 260 to 270°C, nanoclay did not affect thermal stability	[18]
Granular Silica Aerogel	1 -8 wt%	Polyisocyanurate	LOI 34.4% at 6 wt.% aerogel, thermal conductivity reduced by 30.2%	[100]

1: Triethyl Phosphate, 2: Expandable Graphite, 3: Ammonium Polyphosphate, 4: Triphenyl Phosphate, 5: Organically Modified Montmorillonite, 6: Dimethyl Methylphosphonate, 7: Triethylene Amine, 8: Whisker Silicon, 9: Modified Diaminopropane Montmorillonite, 10: Hexa- (Phosphite-Hydroxyl-Methyl-Phenoxy)-Cyclotriphosphazene, 11: Condensation Product of Benzaldehyde, Aniline and 9,10-Dihydro-9-Oxa-10-Phosphaphenanthrene-10-Oxide (DOPO), 12: Limiting Oxygen Index, 13: Time To Ignition, 14: Peak of Heat Release Rate, 15: Castor Oil Phosphate Flame-Retarded Polyol

Zhao *et al.* [100] incorporated granular silica aerogel in an organic/inorganic polyisocyanurate composite rigid foam to enhance its thermal insulation properties and flame

retardancy. The percentage LOI value of the composite foam was increased from 29.4% to 34.6% on increasing the concentration of aerogel from 0 to 8 wt. %, which indicates the significant improvement in anti-flammability of the foam. In addition, the reduction in thermal conductivity was also observed on increasing the aerogel concentration in the composite foam. Table 1.6 shows the effect of different additives on the anti-flammability, thermal insulation and thermal stability of PU foams.

Figure 1.10 shows the effect of different filler content on the percentage LOI of PU product formed. It shows that the percentage LOI value increases upon increasing the concentration of flame-retardant fillers.

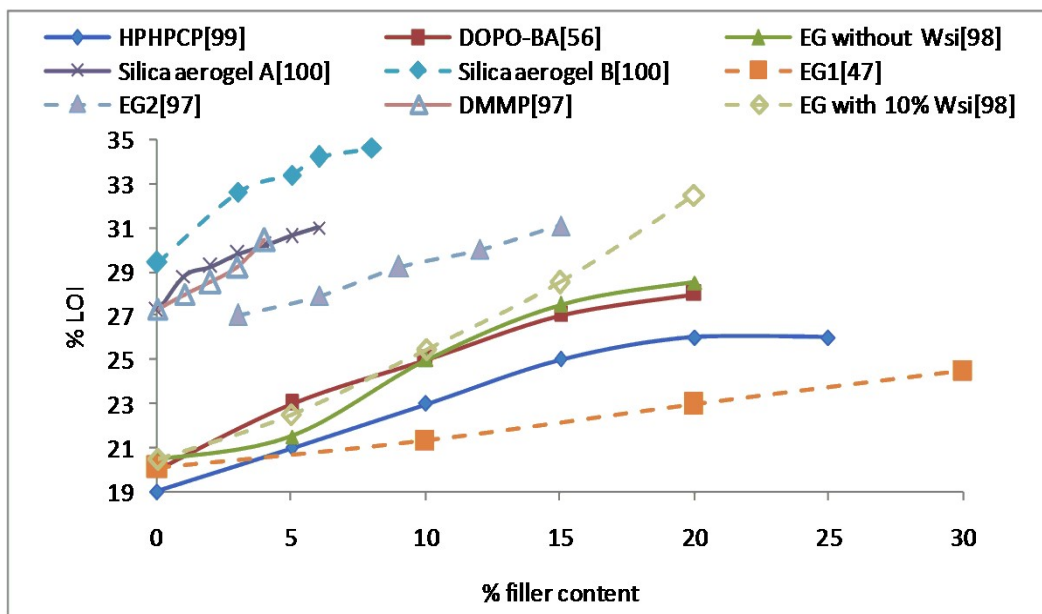


Figure 1.10: Plots of % LOI vs. % Filler Content Incorporated in Different PU Foam Matrices [47, 56, 97–100]

1.5.4 Addition of Phase Change Materials

Phase change materials (PCMs) have the ability to store or release a considerable amount of thermal energy during the phase change. Owing to the outstanding thermal energy storage capacity of PCMs, they may be employed to enhance the energy efficiency in buildings,

by incorporating these PCMs in rigid PU foams used in the building and construction industry. It is evident that with the addition of phase change materials in PU foam, the thermal energy storage capacity is enhanced considerably keeping the thermal conductivity nearly constant, but mechanical strength is decreased [113].

The flame retardancy of renewable source-based PU foams may be enhanced by using expandable graphite, aerogel or phosphorus based flame retardants as additives. In addition, the introduction of flame retardant group in polymer structure may also be a better option to decrease the flammability of bio-based PU foams.

1.6 ANALYSIS FOR MACHINING PERFORMANCE OF POLYMERS

For the commercialization of the RPUF, some machining operations such as milling, drilling, countersinking, grinding, boring and trimming are required for achieving desired geometrical shapes [116–118]. Of these, drilling is an important operation required for the fastening and riveting structural components in various applications such as aircraft and automobile [119–121]. The drilling of polymer composites is considerably different from that of metals & alloys and also require deliberations, owing to their unique characteristics of inherent inhomogeneity, anisotropy and abrasiveness [122–125]. The quality of drilled holes, specified by the dimensional tolerances, accuracy and precision, influences the load carrying capacity of the products prepared from the polymer composites, consequently ascertains the structural integrity, as well as, long term reliability of the product. Previous researches on drilling damages in composites have concluded that the peel-up and push-out are two distinguishable modes of delamination mechanisms, commencing when the thrust force surpasses the critical thrust force (CTF) [126]. Analytical studies reveal that cutting parameters such as feed rate, depth of cut, spindle speed and others control the thrust force, which is

required to be minimized to reduce the delamination. So, an optimized selection of these parameters administers the delamination-free drilling [127].

To correlate the thrust force and other drilling parameters in composite materials, a variety of empirical mathematical models have been established and it was concluded, that, the thrust force and the delamination increase with the feed rate while spindle speed showed specific behaviours for distinct materials [128–130]. The mechanical properties of polymer composites are also influenced by the delamination, so the impact of delamination on the residual mechanical strength also seeks attention. Several studies have been conducted to ascertain the effects of delamination on the residual mechanical strength [129, 131]. A. Diaz Alvarez *et al.* [132] studied the drilling-induced damages in aramid composites and analysed the influence of the drill geometry (Twist drill, Brad & Spur drill) on the torque, damage and thrust force. Some mechanistic models were developed to ascertain the relationship between process parameters and the quality of the final product. It was observed that the Twist drill showed better performance with high feed rate and cutting speeds, while with the Brad & Spur drills, higher speed and lower feed rate provides better results in terms of delamination.

N. Zarif Karimi *et al.* [131] investigated the effect of drilling-induced delamination on the compressive strength of epoxy composites reinforced with woven glass fiber. The feed rate and spindle speed were considered as process parameters to optimize the delamination and residual compressive strength. It was observed that the extent of damage due to delamination or interlaminar cracking is governed by the cutting forces. Results showed that the feed rate was the most influential factor to optimize the residual compressive strength and the optimized value of the residual compressive strength was attained at spindle speed of 1000 rpm and the feed rate of 31.5 mm/min.

Xu *et al.* [133] studied the severity of drilling-induced damage such as burrs, tearing and delamination in CFRP composites using three different types of specialized drill bits (twist

drill, brad spur drill and dagger drill). The ultrasonic C-scan showed that initially the delamination takes place inside the composite layer, and then transmits through plies on increasing the drill thrust load. The feed rate was identified as the most significant factor to generate defects during drilling of composite. It was concluded from the damage analysis that the brad spur drill provides the least damage in the course of the drilling of CFRP.

Heidary *et al.* [129] investigated the drilling performance of epoxy composites reinforced with E-glass fiber and multi-walled carbon nanotubes (MWCNT), and analysed the effect of drilling induced damage on the residual flexural strength. Feed rate (0.04-0.1 mm/rev), drill diameter (4 and 5 mm), spindle speed (315 and 630 rpm), and the weight % of carbon nanotubes (0-1%) were considered as process parameters. Taguchi method, in association with grey relational analysis (GRA), was employed for the multi-objective optimization of the drilling process. Results showed that the feed rate was the most influential factor for the optimization of the delamination and the thrust force, followed by spindle speed, while, the residual flexural strength was greatly affected by the concentration of the MWCNT, followed by feed rate. It was also reported that the feed rate of 0.04 mm/rev, the MWCNT concentration of 0.5%, a drill diameter of 4mm and spindle speed of 630 rpm are the optimized values of the process parameters. Silva *et al.* [134] studied the effect of tool geometry (twist, brad, step), feed rates (0.12 and 0.30 mm/rev) and cutting speeds (1120 and 1800 rpm) on the bearing load and fractal dimension of the carbon fibre reinforced epoxy composite plates. According to their results, better bearing load was achieved by using step geometry bit with higher cutting speed and lower feed rate. It was also observed that higher feed rate provides lower bearing load, higher delamination and higher fractal dimension.

Numerous research work has been conducted on the machinability of glass fibre reinforced epoxy composites, but, the polyurethane foam, which is being used in variety of structural applications, has not been explored yet, and, necessitates investigation of all operational

aspects. In addition, the compressive strength is crucial for RPUF, as the applications of RPUF require good compressive strength., but it is evident from the literature that there are immense possibilities of delamination growth under compressive loading [131].

1.7 SIGNIFICANT FINDINGS FROM LITERATURE

Accounting for the scarcity of the petroleum products and the raising awareness about the environment, among researchers, different plant-based materials such as vegetable oils, starch, wood, and lignin have been used as an alternative for polyols in PU production. Several modification methods such as transesterification, epoxidation, hydroformylation, ozonolysis, amidation, and thiol-ene coupling have been reported to increase the hydroxyl values of these bio-based materials. To incorporate the better mechanical strength and other desirable properties in these bio-based materials, different types of natural or synthetic fibres, nano fillers and particulate fillers are commonly used. Due to the incompatibility between the filler and the matrix, different surface treatments on the fillers are employed, resulting in the enhancement of the filler-matrix interaction. Devising methods to provide products that have desirable properties, as well as, enhancing the human safety are the vital demands in the modern world. Using these methods, the properties of the renewable material-based products may be enhanced, so that, these environmentally friendly products can acquire properties comparable to that of petroleum-based products and may be further used on commercial scale, as a substitute for petroleum-based PU foams.

1.8 RESEARCH GAPS

Polymeric foams derived from renewable sources are a requirement of the modern world due to the increasing concern about the environment and various issues related to petroleum based foams. Much research has been conducted recently to produce polyurethane foams using

renewable sources. Products formed by using renewable sources are biodegradable in nature, additionally they do not pose much hazard to the environment. So, these modified vegetable oils and other renewable sources based polyols are very good candidates for the preparation of environmental friendly PU products. But, it has been observed that the properties of these products are not as good as that of the foams derived from the petroleum based raw materials and generally a compromise has to be made in terms of mechanical, thermal and flame retardant properties of these products. Additionally, for the commercialization of the RPUF, some machining operations are required, for obtaining the desired geometrical shapes. Of these, drilling is an important operation required for the fastening and riveting the structural components. The drilling of the polymer composites is considerably different from that of metals & alloys and requires deliberations owing to their unique characteristics of inherent inhomogeneity, anisotropy and abrasiveness. So, an optimized selection of the drilling parameters administers the delamination-free drilling.

1.9 RESEARCH OBJECTIVES

The aim of this research work was **To Synthesize Castor Oil Based Rigid Polyurethane Foam With Enhanced Mechanical, Thermal And Flame Retardant Properties**. In addition, the samples with best combination of mechanical, thermal and flame retardant properties were optimized for the machining parameters to explore its application in practical fields. The detailed objectives of the present study were as follows:

- Development of castor oil based rigid polyurethane foam with enhanced mechanical properties by the addition of different reinforcing material.
- Characterization of these rigid polyurethane foams incorporated with reinforcing materials for the mechanical, thermal and flame retardant properties.

- Optimization of reinforcing material composition to get best combination of mechanical, thermal and flame retardant properties.
- Optimization of the machining parameters of the Rigid Polyurethane Foam.

1.10 OVERVIEW OF THE THESIS

The objective of this thesis is the development of vegetable oil based rigid polyurethane foam composites with enhanced mechanical, thermal and flame retardant properties. The whole thesis is organized in EIGHT chapters. **Chapter 1** of the thesis presents the overview of bio-based rigid polyurethane foam followed by the research work conducted by different researchers to enhance the properties of rigid polyurethane foam. Gaps in available literature and latest trend in the field are also covered in this chapter. **Chapter 2** deals with the experimental part which includes the materials and methods employed to develop the composite rigid polyurethane foam. Various characterization techniques used to analyse the mechanical, thermal and flame retardant properties of the synthesized rigid polyurethane composite foams have also been discussed in this chapter. In **Chapter 3**, studies on the incorporation of ceramic fillers zirconia and alumina powder in the rigid polyurethane foams, derived from the modified castor oil, and their impact on the mechanical, thermal and fire performance of composite foams have been analysed. **Chapter 4** highlights the influence of the carbon fibre powder, as reinforcement, on the enhancement of the electrical conductivity of bio-based rigid polyurethane foam. The mechanical, thermal and flame retardant properties of these foam shields have also been studied. **Chapter 5** investigates the incorporation of castor oil based rigid polyurethane foam with mineral fillers like feldspar, kaolinite clay and calcium carbonate nanoparticles and their subsequent effect on the foam properties. **Chapter 6** investigates the effect of metallic filler on the properties of RPUF. Additionally, the results obtained after incorporating all the filler have been compared to get the material with best

properties. The same formulation was used further, for studying the drilling experiments to ascertain the machining ability of the foam in **Chapter 7**. This chapter includes the influence of drilling parameters (feed rate, drill diameter, spindle speed and density of RPUF) on the residual compressive strength, thrust force and delamination of the copper powder reinforced RPUF. Response surface method based approach has been employed and reported to accomplish the optimized parameters for drilling of RPUF. In the last chapter, **Chapter 8** of the thesis, the overall conclusions of the results obtained in the above study are reported. In addition, some applications and future prospects of the developed material have also been presented. This chapter is further, followed by **References**.

CHAPTER 2

MATERIALS AND METHODS

2.1 RAW MATERIALS/CHEMICALS

In this study, following raw materials/ chemicals were used for the preparation and reinforcement of RPUFs:

1. Castor Oil
2. Diphenylmethane diisocyanate (PMDI)
3. n-Pentane
4. Silicon Oil
5. Glycerol
6. Catalyst Dabco[®] 33-LV (1,4-Diazabicyclo[2.2.2]octane solution)
7. Kaolinite Clay
8. Feldspar
9. Carbon Fibre
10. Alumina
11. Zirconia Powder
12. Copper Powder
13. (3-Aminopropyl) triethoxysilane (APTES)
14. Calcium Nitrate
15. Sodium Nitrate
16. Sodium Carbonate
17. Sodium Hydroxide
18. Acetic Anhydride
19. Pyridine

20. Ethanol
21. Potassium Hydroxide
22. Oxalic Acid
23. Phenolphthalein Indicator
24. Hydrochloric Acid
25. Di-n-butylamine
26. Bromophenol Blue Indicator
27. Methanol
28. Toluene

2.1.1 Specification and Sources of Raw Materials/Chemicals

Specification and sources of the raw materials and chemicals used to prepare RPUF and their characterization is given in Table 2.1.

Table 2.1: Specification and Sources of Raw Materials/Chemicals

S. No.	Chemical/Raw Material	Sources	Specification
1.	Castor Oil	Thomas Baker Chemicals (Pvt) Ltd, Mumbai	Analytical Reagent Grade
2.	Diphenylmethane diisocyanate (PMDI)	Krishna Enterprises, Delhi	30-32 wt% NCO
3.	n-Pentane	Central Drug House (P) Ltd, Delhi	Analytical Reagent Grade
4.	Silicon Oil	Central Drug House (P) Ltd, Delhi	Analytical Reagent Grade
5.	Glycerol	Thermo Fischer Scientific India Pvt. Ltd, Mumbai	Analytical Reagent Grade
6.	Catalyst Dabco [®] 33-LV (1,4-Diazabicyclo [2.2.2] octane solution)	Sigma-Aldrich Inc., USA	Analytical Reagent Grade
7.	Kaolinite Clay	Zirox technologies, Bewar, Rajasthan	particle size 100-500 nm
8.	Feldspar	Zirox technologies, Bewar, Rajasthan	particle size nano to submicron range and maximum particle size 3-4 micron

9.	Carbon Fibre	CFW Enterprises, Delhi	tensile strength ≥ 3500 GPa, density 1.65-1.75 g/cm ³ . electrical resistivity 1.5×10^{-33} Ω /cm and mesh size 50-1000
10.	Alumina	Thermo Fischer Scientific India Pvt. Ltd, Mumbai	50-200 μ m
11.	Zirconia Powder	Zirox technologies, Bewar, Rajasthan	Particle size in the range of 3 μ m
12.	Copper Powder	Central Drug House (P) Ltd, Delhi	Mesh size 325, electrolytic grade
13.	(3-Aminopropyl) triethoxysilane (APTES)	Alfa Aesar, Thermo Fischer Scientific India Pvt. Ltd, Mumbai	Analytical Reagent Grade
14.	Calcium Nitrate	Central Drug House (P) Ltd, Delhi	Analytical Reagent Grade
15.	Sodium Nitrate	Thermo Fischer Scientific India Pvt. Ltd, Mumbai	Analytical Reagent Grade
16.	Sodium Carbonate	Thermo Fischer Scientific India Pvt. Ltd, Mumbai	Analytical Reagent Grade
17.	Sodium Hydroxide	Central Drug House (P) Ltd, Delhi	Analytical Reagent Grade
18.	Acetic Anhydride	Thermo Fischer Scientific India Pvt. Ltd, Mumbai	Analytical Reagent Grade
19.	Pyridine	HiMedia Laboratories, Mumbai	Analytical Reagent Grade
20.	Ethanol	Chang Yu Hi-Tech Chemicals, China	Analytical Reagent Grade
21.	Potassium Hydroxide	Thermo Fischer Scientific India Pvt. Ltd, Mumbai	Analytical Reagent Grade
22.	Oxalic Acid	Thermo Fischer Scientific India Pvt. Ltd, Mumbai	Analytical Reagent Grade
23.	Phenolphthalein Indicator	Central Drug House (P) Ltd, Delhi	1% (w/v)
24.	Hydrochloric Acid	Thermo Fischer Scientific India Pvt. Ltd, Mumbai	36.5-38% (w/w)
25.	Di-n-butylamine	Sigma-Aldrich Inc., USA	Analytical Reagent Grade
26.	Bromophenol Blue Indicator	HiMedia Laboratories, Mumbai	0.1% (w/v)
27.	Methanol	Finar ISO 9001:2008 certified, Ahmedabad	Analytical Reagent Grade
28.	Toluene	HiMedia Laboratories, Mumbai	Analytical Reagent Grade

2.1.2 Purity of Raw Materials/ Chemicals

As the accuracy of results depends not only on the accuracy of the instrument used or experiment performed but also on the purity of the raw material used. So, the percentage purity of the raw materials/ chemicals is given in the Table 2.2.

Table 2.2: Purity of Raw Materials/ Chemicals

S. No.	Raw Material/Chemical	Percentage Purity
1.	Castor Oil	$\geq 99.9\%$
2.	Diphenylmethane diisocyanate (PMDI)	$\geq 99\%$
3.	n-Pentane	$\geq 99\%$
4.	Silicon Oil	$\geq 98\%$
5.	Glycerol	$\geq 99\%$
6.	Catalyst Dabco [®] 33-LV (1,4-Diazabicyclo[2.2.2]octane solution	31-35% Triethylenediamine
7.	Kaolinite Clay	above 98% kaolin contents
8.	Feldspar	Aluminosilicate with $\approx 70\%$ SiO ₂ , $\approx 17\%$ Al ₂ O ₃
9.	Carbon Fibre	Carbon content $\geq 98\%$,
10.	Alumina	$\geq 99\%$
11.	Zirconia Powder	ZrO ₂ : $\geq 98\%$
12.	Copper Powder	$\geq 99.5\%$
13.	(3-Aminopropyl)triethoxysilane (APTES)	$\geq 98\%$
14.	Calcium Nitrate	$\geq 99\%$
15.	Sodium Nitrate	$\geq 99\%$
16.	Sodium Carbonate	$\geq 99.5\%$
17.	Sodium Hydroxide	$\geq 98\%$
18.	Acetic Anhydride	$\geq 99\%$
19.	Pyridine	$\geq 99.5\%$
20.	Ethanol	$\geq 99.9\%$
21.	Potassium Hydroxide	$\geq 85\%$
22.	Oxalic Acid	$\geq 99\%$

23.	Phenolphthalein Indicator	1% (w/v)
24.	Hydrochloric Acid	36.5-38% (w/w)
25.	Di-n-butyl amine	≥ 99.5%
26.	Bromophenol Blue Indicator	0.1% (w/v)
27.	Methanol	≥ 99%
28.	Toluene	≥ 99.5%

2.2 RESEARCH METHODOLOGY

The methodology employed to achieve the objectives of the research is divided onto the following sections:

- ✓ Physicochemical characterization of the raw materials
- ✓ Modification of the vegetable oil
- ✓ Preparation of calcium carbonate nanoparticles
- ✓ Synthesis of rigid polyurethane foam composite incorporated with different fillers
- ✓ Characterization of synthesized RPUF composite
- ✓ Optimization of mechanical, thermal and flame retardant properties of the prepared RPUF
- ✓ Drilling performance test of the RPUF composite with optimized properties

2.2.1 Physicochemical Characterization of Raw Materials

The properties of the final product depend on the properties of the raw materials used. So, the study of the physicochemical properties of the raw materials is an important part of the research. Various physicochemical properties studied during this research are as follows:

2.2.1.1 *Determination of the Acid Value of the Oil used*

The Acid value of the oil provides the information about the free fatty acid present in the oil. It is measured according to the standard procedure, as reported in Appendix – I.

2.2.1.2 Determination of the Hydroxyl Value of the Oil and Modified Polyol

The hydroxyl value provides the information about the reactive hydroxyl group present in the given amount of the polyol. Hydroxyl value of the castor oil and the modified polyol was determined according to the standard procedure, as reported in Appendix - I.

2.2.1.3 Determination of the Viscosity of the Oil

The viscosity of the castor oil and the modified polyol was measured using Brookfield viscometer (Model- DV-II +Pro).

2.2.1.4 Determination of the Percentage NCO Content

The percentage NCO content provides the idea about the percentage of reactive isocyanate groups present in a fixed amount of isocyanate. Percentage NCO was determined according to the standard procedure, as reported in Appendix-I.



Figure 2.1: FTIR (Nicolet 380) Spectrometer

2.2.1.5 FTIR and ¹H NMR Analysis

The chemical structure of the transesterified castor oil was determined using FTIR spectroscopy on Nicolet 380 by preparing KBr pallets. The spectra were observed in the 450 – 4000 cm⁻¹ range. ¹H NMR of the modified and the virgin castor oil was also conducted (Bruker

Avance II-400) at SAIF, Punjab University, Chandigarh, using dimethyl sulphoxide (DMSO) as a solvent.



Figure 2.2: NMR (Bruker Avance II-400) Spectrophotometer

2.2.2 Modification of the Vegetable Oil

The transesterification of the castor oil was conducted to enhance its hydroxyl value and to produce modified polyol. The modification of the castor oil was performed under the inert atmosphere of nitrogen using 2:1 ratio of the castor oil to the glycerol at the temperature 180-200°C for 4-5 hours.

2.2.3 Preparation of the Calcium Carbonate Nanoparticles

0.1M Sodium Carbonate, 0.2 M Sodium Hydroxide and 0.18M Sodium Nitrate aqueous solutions were prepared respectively and added together to form Solution 1. The Solution 1 was stirred manually for 1 minute to ensure homogeneity. The Calcium Nitrate was dissolved in distilled water to give a 0.1M aqueous solution, and was named as Solution 2. The Solution 1 was placed on the magnetic stirrer and the Solution 2 was added to it dropwise at 700 rpm.

The Calcium Carbonate nanoparticles were obtained by filtering the above mixture (Solution 1 + Solution 2) and drying for 24 hours at 60°C.

2.2.4 Synthesis of Rigid Polyurethane Foam Composites

To synthesize the RPUF composites the predetermined quantity of the filler was added to the modified polyol of hydroxyl value 400 ± 30 mg KOH/g, taken in a paper cup. Prior to addition, the fillers were surface treated with 1 % solution of 3-aminopropyl triethoxysilane (APTES) in acetone/water; 50/50 by volume, using the method described in literature [101], to enhance the adhesion between matrix and filler.

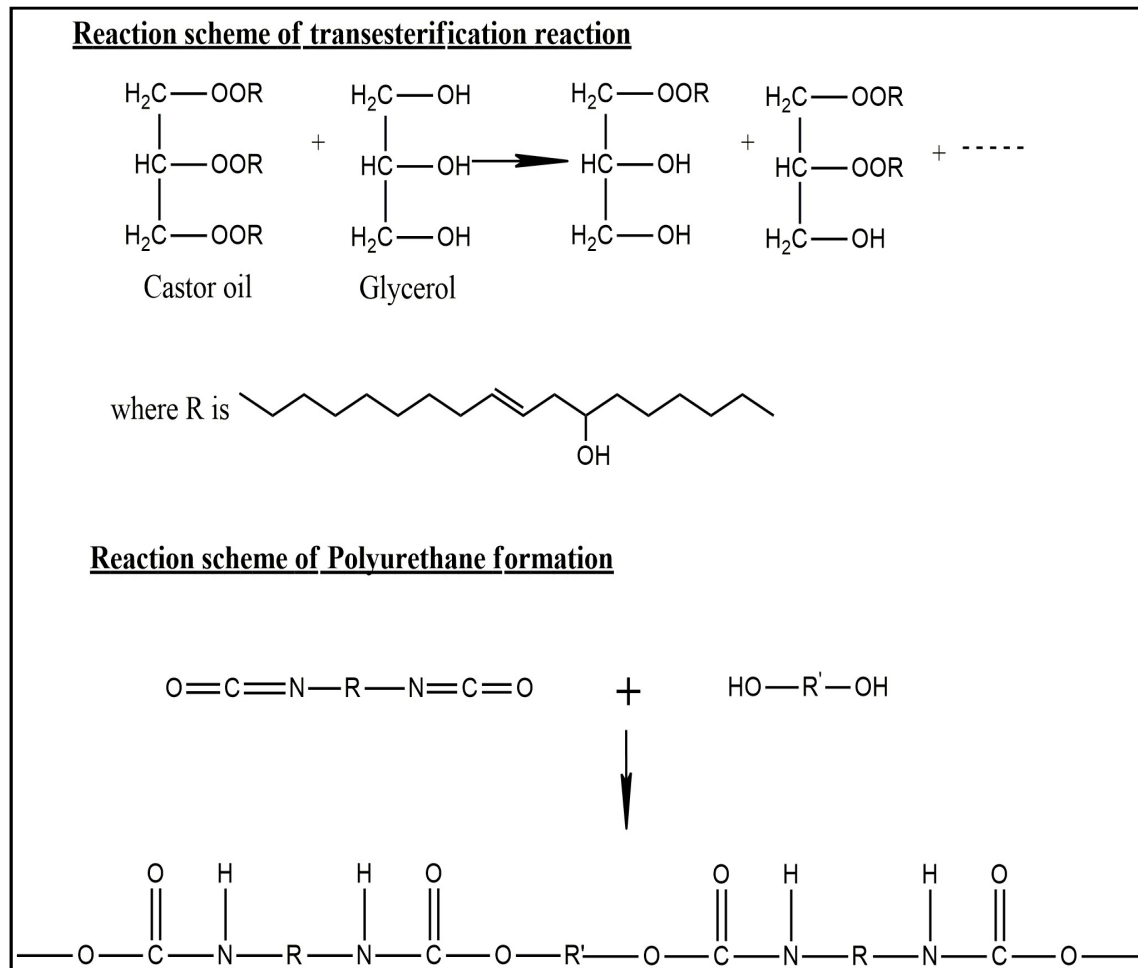


Figure 2.3: Reaction Scheme of Transesterification of Castor Oil and Polyurethane Formation

Then calculated amount of other ingredients, such as, catalyst (Dabco 33-LV), surfactant (Silicon Oil), blowing agent (*n*-Pentane) was added to the contents of the paper cup and thoroughly mixed at 1500 rpm by mechanical stirrer for 2 minutes, under controlled temperature conditions at $35\pm 2^{\circ}\text{C}$ to form polyol-premix. A calculated amount of PMDI was then added to the paper cup, and mixed at 2000 rpm for 10 seconds. Then, the prepared reaction mixture was poured into a metal mould (100mm x100mm x25 mm) coated with a releasing agent (silicon oil) and a free rise foam was prepared.

To ensure the complete curing, the moulds were left at room temperature for 72 hours. Different concentrations of the selected fillers were used to analyze the influence of these filler on the properties of RPUFs. Figure 2.3 shows the reaction scheme for polyurethane foam synthesis and modification of the castor oil. Rigid polyurethane foam prepared without adding fillers has been considered as reference sample. Table 2.3 shows the formulation of castor oil-based rigid polyurethane foams modified with different concentration of fillers.

Table 2.3: Foaming Formulation of Castor Oil based RPUF

Material	Amount (pbw)
Modified Polyol	100
DABCO 33 LV	3
n-Pentane (blowing agent)	10-15
Silicone oil (surfactant)	3
Filler	2-10
PMDI	125

Pbw = parts by weight of Polyol

2.2.5 Characterization of Synthesized RPUF Composites

2.2.5.1 Mechanical Testing: The mechanical properties of the castor oil based rigid polyurethane samples were determined according to the standard procedures. At least three specimens of each concentration were tested and the average value was reported. The

compressive and flexural properties of the foam specimen were measured at room temperature using Instron (model No. 3369) universal testing machine (UTM). The compression tests were performed according to the ASTM D-1621. The specimens of dimensions 25mm x 25mm x 25mm were cut from the foam in the in-plane direction and tested for 10% compression. The compressive strength was measured along parallel foam rise direction. The flexural tests were performed according to the ASTM D-790. The specimens of dimensions 80mm x 10mm x 4mm were cut from the foam, perpendicular to foam rise direction, and loaded under three-point bending, along parallel foam rise direction. The rate of crosshead movement was fixed at 5 mm/min for each sample.

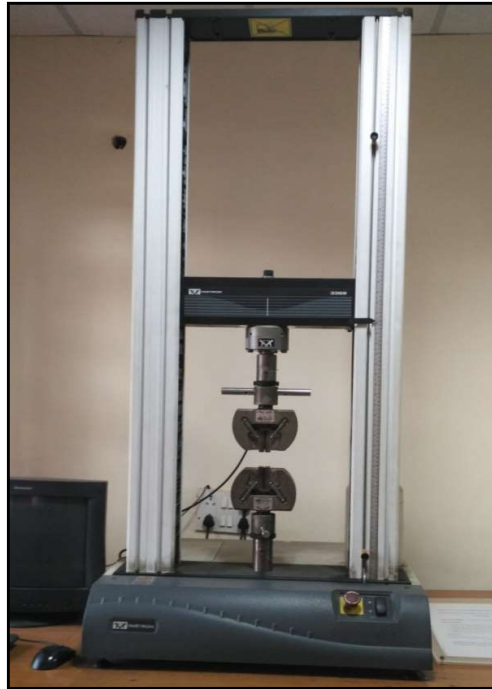


Figure 2.4: UTM used for Mechanical Testing of Foam Samples

2.2.5.2 Thermogravimetric Analysis (TGA): Thermogravimetric analysis (TGA) was performed on foam samples utilizing a thermogravimetric analyzer (Perkin Elmer 4000) in nitrogen atmosphere. The heating rate was 10°C/min with temperature ranging from 30°C to 700°C. All the samples were run in triplicate and the average value is reported.

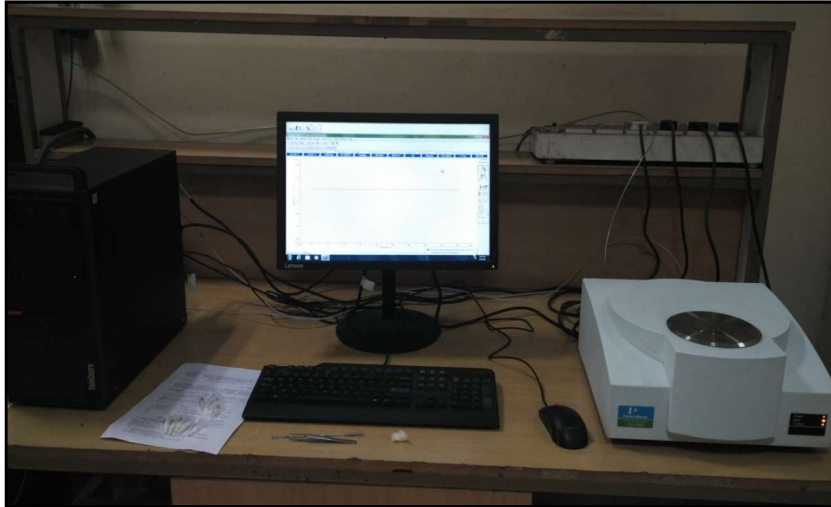


Figure 2.5: Thermo-gravimetric Analyzer (Perkin Elmer 4000)



Figure 2.6: Cone Calorimeter

2.2.5.3 Cone Calorimeter Testing: The response to fire, of RPUF samples, was examined with a Cone Calorimeter (Jupiter Electronics, India) according to ISO 5660-1 standard, at an incident heat flux of 35kW/m^2 . The size of the samples was taken as $100\text{mm} \times 100\text{mm} \times 20\text{mm}$. This instrument is capable of recording the time to ignition (TTI), total heat release (THR), heat release rate (HRR), smoke production rate (SPR) and total smoke release (TSR) etc. All the samples were tested in duplicate and the average values are reported.

2.2.5.4 Scanning Electron Microscopy: The cell structure of the samples was characterized with a Hitachi S3700 SEM (Scanning Electron Microscope). The samples were gold-sputter coated to render them electrically conductive and then scanned at an accelerating voltage of 15 kV. Image processing was conducted by using in-built software SEM data manager of Hitachi PC-SEMs.

2.2.5.5 Conductivity Measurement: The conductivity of the prepared rigid foam samples was measured by using four probe set-up (SES Instruments Pvt. Ltd., Roorkee).



Figure 2.7: Scanning Electron Microscope (Hitachi S-3700N)



Figure 2.8: Four Probe Digital Conductivity Meter

2.2.6 Optimization of Mechanical, Thermal and Flame Retardant Properties of RPUF

Optimization of the mechanical, thermal and flame retardant properties of the prepared RPUF composites was performed by the analysis of the results obtained after the characterization of their properties and comparing the data with that of the RPUF available commercially.

2.2.7 Drilling Performance Test of the RPUF Composite

In the present study, Response Surface Method (RSM) is used to establish the mathematical relation between the responses and the drilling parameters, using Central Composite Design. Design matrix was created by the employment of statistical analysis software, Design Expert. Foam density, feed rate, diameter of drill bit and the spindle speed, at five levels were selected as input parameters, and the delamination, thrust force and the residual specific compressive strength were considered as the responses. The input parameters and their levels were selected on the basis of the intensive literature survey. The drilling test parameters are summarised in Table 2.4. Computer numerical control (CNC) vertical machining center

(VMC) employed with standard high speed steel (HSS) twist drills was used to perform drilling experiments and each experiment was replicated in thrice. The consequences of drilling-induced delamination on the residual compressive strength were determined by performing compression tests in accordance with ASTM D-1621.

Table 2.4: Factor Levels for Performing Drilling Test

Symbol	Control Factor	Unit	Level 1	Level 2	Level 3	Level 4	Level 5
<i>P</i>	Density	kg/m ³	260	302.5	345	387.5	430
<i>F</i>	Feed Rate	mm/rev	0.12	0.34	0.56	0.78	1
<i>V</i>	Spindle Speed	rpm	56	342	628	914	1200
<i>D</i>	Drill Diameter	mm	4	6	8	10	12

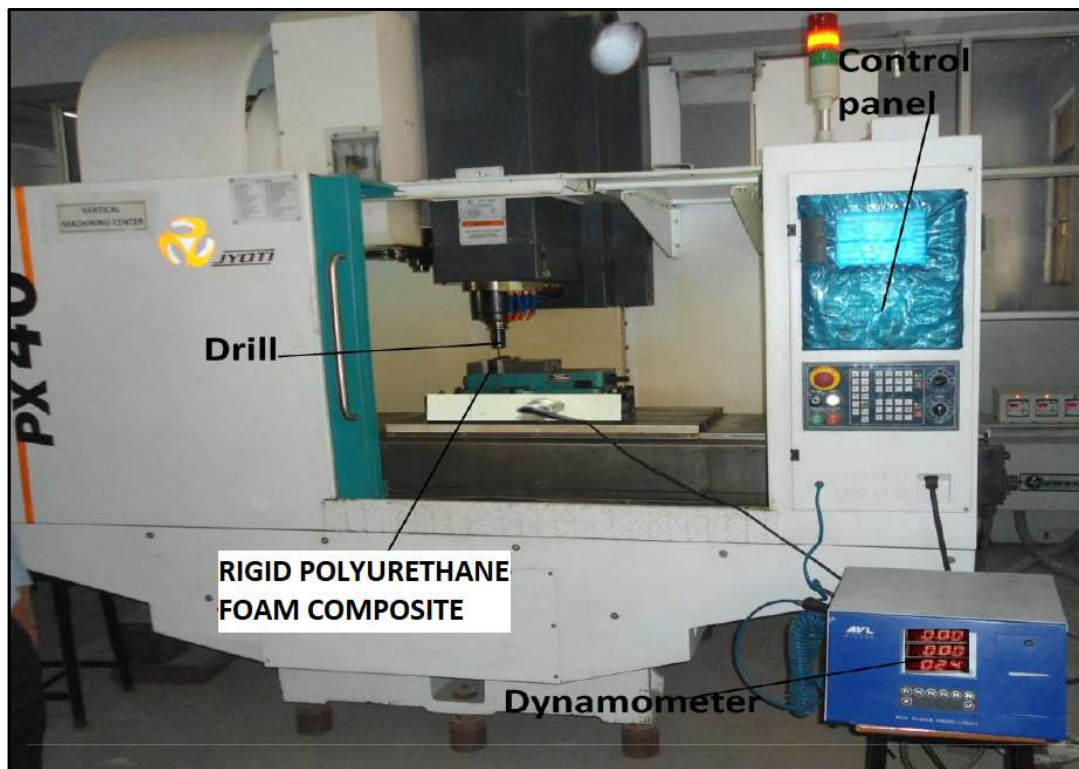


Figure 2.9: Computer Numerical Control (CNC) Vertical Machining Center (VMC)

CHAPTER 3

INVESTIGATIONS ON CASTOR OIL-BASED RPUF REINFORCED WITH CERAMIC FILLERS

3.1 INTRODUCTION

Rigid polyurethane foam (RPUF) has a wide range of applications in disposable packaging, thermal insulation, construction & refrigeration industry, prototypes and industrial patterns due to its unique properties such as low density, thermal conductivity, water absorption and comparatively high compressive strength [1]. The basic unit of polyurethane structure, urethane linkage is generated by the reaction of polyols with the polyisocyanate. Both polyols and polyisocyanates are obtained from the petroleum-based raw materials. In the recent years, due to diminishing resources, researchers are keenly oriented to replace the petroleum-based polyols with the renewable sources-based raw materials [8, 48, 57]. The utilization of renewable sources in place of petroleum-based raw material and the incorporation of blowing agent makes them more flammable [70]. Several studies have been conducted for abating the flammability of RPUFs for the application purposes, by introducing some flame retardant groups in the foam structure or by incorporating some unique flame retardants [107, 108, 135].

Zhang *et al.*[47] prepared a flame retarded polyol Castor Oil Phosphate Polyol (COFPL) by the introduction of the phosphate group in the polyol derived from castor oil and developed flame-retarded RPUF. In addition, different type of flame retardants such as chlorinated flame retardants, brominated flame retardants, phosphorus-based compounds, metal hydroxide, nitrogen-based compounds, nanomaterials or boron compounds are found to be promising candidates to reduce the flammability of polyurethanes. Char-forming property of rigid polyurethane foam was also enhanced by the incorporation of phosphorus flame retardant in the foam [112]. Different studies have revealed that the char yield and the thermal stability of

foams were improved by the incorporation of the flame retardant. Furthermore, an additional nanoclay filler, organically-modified montmorillonite (OMMT), was employed to further enhance the fire properties of foams. The resulted foams exhibited a reduction in the heat release rate and the total smoke production, while the duration time of combustion was increased.

Hu *et al.* [97] analyzed the effect of the incorporation of dimethyl methyl phosphonate (DMMP) and expandable graphite (EG) in PU foams as flame retardants. A significant improvement in the flame retardancy of RPUF was observed on the incorporation of DMMP, as well as, EG. Bian *et al.* [98] enhanced the flame retardancy of the rigid polyurethane foam (RPUF) composites by incorporating whisker silicon oxide (WSi) and EG. It was reported that the dynamic mechanical properties, as well as, the flame retardant properties, were enhanced on the incorporation of WSi and EG. In a study, Zhang *et al.* [56] synthesized a phosphorus-nitrogen based flame retardant namely DOPO-BA and incorporated it in a rosin-based RPUFs. Results showed that the incorporation of DOPO-BA improved the physical, thermal and flame retardant properties of RPUF.

In a similar study, Yang *et al.* [99] employed hexachlorocyclotriphosphazene, p-hydroxybenzaldehyde and diethyl phosphite to synthesize hexa(phosphitehydroxylmethylphenoxy) cyclotriphosphazene (HPHPCP). HPHPCP was incorporated into the rigid polyurethane foams prepared by the reaction of polyester polyol and polyether polyol with polymethylene polyphenyl isocyanate. Incorporation of the HPHPCP into the RPUF increased the percentage LOI (limiting oxygen index), while the heat release rate was found to decrease continuously on increasing the concentration of HPHPCP. Granular silica aerogel has also been used to enhance the flame retardancy of RPUF prepared by organic/inorganic polyisocyanurate. It was observed that on increasing the concentration of aerogel from 0 to 8 wt%, increased the percentage LOI from 29.4% to 34.6% [100]. 3,3',4,4'-

biphenyltetracarboxylic di anhydride and 9,10- dihydro-9-oxa-(10-glycidoxypropylene)-10-phosph-phenanthrene-10-oxide were incorporated in RPUF for enhancing the flame retardancy of the foam. It was concluded from the results that the RPUF incorporated with flame retardant showed a small improvement in the thermal properties but the peak of heat release (PHRR) and total heat release (THR) decreased by approximately 20% [136]. Along with the incorporation of flame retardant, some functional filler such as aluminium diethyl phosphinate [137], calcium hypophosphite [138], and others may also be used to abate the flammability of RPUF. By selecting appropriate filler, the mechanical, thermal and fire properties of the RPUF may be tailored to the requisite conditions.

However, different types of vegetable oils have been used as polyol for the polyurethane production, castor oil is the most promising as it is the only vegetable oil, which contains hydroxyl groups in its structure naturally, that are essential for generating urethane linkage. Although many recent studies reported on the castor oil-based polyurethanes reinforced with different flame retardants, have shown enhanced flame retardancy, still the literature is devoid of much data on castor oil-based RPUF composites reinforced with ceramic fillers, such as alumina and zirconia powder. Alumina powder exhibits unique properties, such as, hardness, resistance to strong acid and alkali attack at elevated temperatures, excellent dielectric properties, wear-resistant, high strength, and stiffness, etc. Studies show that high purity alumina is suitable for use up to the temperature of 1925°C [139]. Zirconia (ZrO_2 , Zirconium dioxide) is chemically inactive and acid resistant filler, used as thermal barrier coating (TBC) in gas turbine blades, diesel engine parts owing to its low thermal conductivity and in dentistry to prepare dental crown due to its high strength [140]. Owing to these remarkable properties as well as low cost, these fillers are considered as potential engineering ceramics materials for the properties enhancement [141].

Verdolotti *et al.* [142] incorporated the alumina powder in flexible PU foam to enhance its hydrophobicity and thermal stability. Swain *et al.* [143] investigated the influence of nano-silica and nano-alumina on the properties of PU composites. It was observed that both the nanoparticles of alumina and zirconia demonstrated improvement in tensile, as well as, thermal properties of the composite up to a fixed concentration, then properties start to deteriorate due to the agglomeration of the particles. A few researchers employed ZrO_2 to enhance the mechanical and thermal properties of PU coatings due to the advantageous properties of ZrO_2 , such as, excellent thermal stability, chemical inertness and high hardness [144–146]. Hybrid of α - zirconium phosphate and nano-graphene oxide has also been incorporated in the rigid polyvinyl chloride foam to enhance the flame retardancy of the foam [147]. So, alumina and zirconia powder may prove to be better additives to enhance the mechanical and thermal properties of the RPUF. But still, no study has been conducted on RPUF incorporated with ceramic fillers to enhance its flame retardancy.

The present study is an attempt to overcome such research gaps, with an aim to produce RPUF composite with enhanced mechanical and structural properties, using these ceramic fillers. Additionally, the effect of variation in concentration of zirconia and alumina powder on the thermal, mechanical and fire performance of RPUF has also been analyzed.

3.2 RESULTS AND DISCUSSION

The foam performance depends on its structure, which in turn is affected by the particle size, dispersion and the properties of the filler incorporated in the reaction mixture. The ceramic fillers can impart stiffness to the material, consequently enhance the mechanical strength of the rigid foam [19, 94]. RPUF was prepared from the polyol derived from the castor oil and the ceramic fillers were added as reinforcement, so that the requisite strength and thermal

properties may be achieved. Effect of the incorporation of these fillers on the properties of RPUF is discussed in the subsequent sections:

3.2.1 FTIR and ^1H NMR Analysis

Figure 3.1 shows the ^1H NMR spectrum of the modified and virgin castor oil. The sharp singlet at 1.23 ppm is attributed to the proton associated with the hydroxyl group. The signal obtained as a multiplet at 1.50 ppm is attributed to the methylene protons of aliphatic chain. NMR spectrum of the modified castor oil shows signals at 2.26 ppm and 3.29 ppm respectively, which is assigned to the presence of proton α to carbonyl carbon of the ester bond. The multiplet signal at 4.25 ppm correspond to the proton α to oxygen atom. The signal obtained at 5.20 ppm is associated with the proton attached to alkene carbon. A signal at 0.87 ppm is assigned to the terminal methyl proton. Similar results were obtained by Narwal *et al.* [148].

The modified castor oil shows the similar peaks, except the increase in intensity of the peak at 1.23 ppm, due to the hydroxyl proton, which confirms the increase in hydroxyl value of the castor oil by transesterification reaction. In addition, the peaks get broadened in the NMR spectrum of the modified castor oil, which is attributed to the broad range of different molecular weight compounds in the modified polyol.

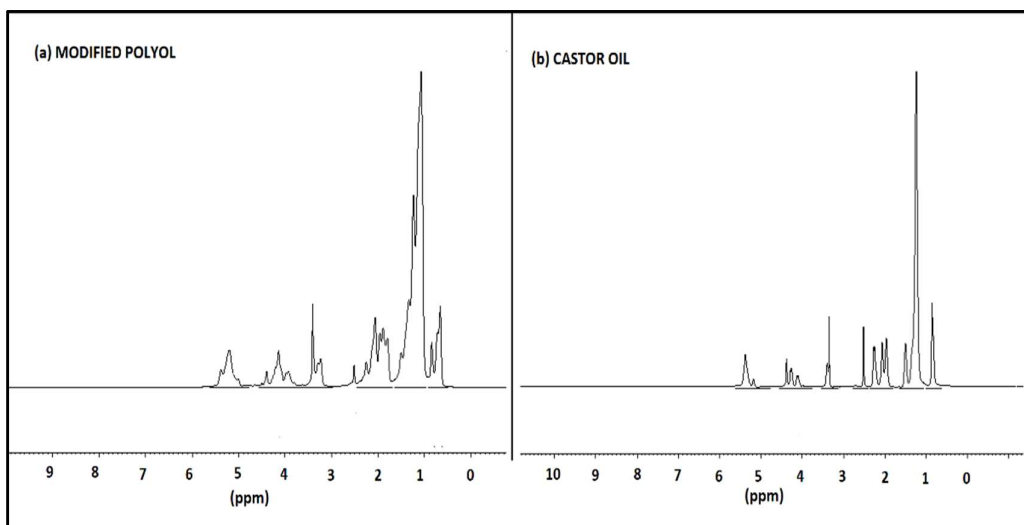


Figure 3.1: ^1H NMR of (a) Modified Polyol and (b) Castor Oil

The FTIR spectra of the polyol samples confirmed the presence of the C-H symmetric and asymmetric stretching vibrations of CH₂ groups at 2925.3 cm⁻¹ and 2854.2 cm⁻¹ respectively. The intense band at 1742.9 cm⁻¹ was due to C=O stretching of ester groups and the absorption bands at 1480.3 and 1373.8 cm⁻¹ were attributed to CH₂ bending and C-H bending vibration, respectively. As illustrated in Figure 3.2, the broad and strong band corresponding to the OH group (3357.3 cm⁻¹) in the castor oil was also noted and the intensity of this peak increases in the spectra of the polyol, which confirms the increase in the hydroxyl number by the transesterification reaction [148].

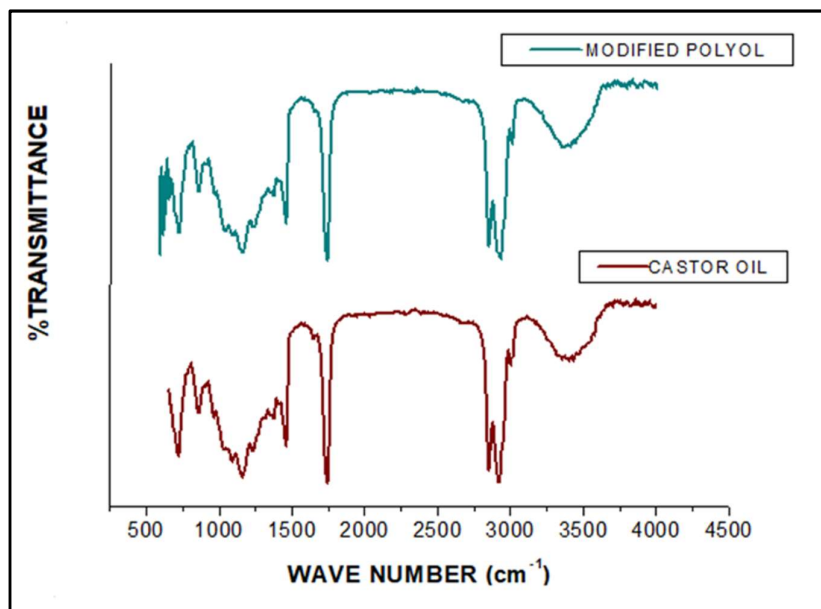


Figure 3.2: FTIR of Castor Oil and Modified Polyol

3.2.2 Mechanical Testing

Figures 3.3 and 3.4 show the variation in mechanical properties and specific strength (strength/density) of RPUF on the incorporation of the ceramic fillers. Upon reinforcing RPUF with 10% alumina and 6% zirconia powder, flexural strength reached up to 2.18 MPa and 5.72 MPa respectively, as compared to 0.79 MPa of unreinforced polyurethane foam. So, the

percentage increase in the flexural strength was 176% and 624% respectively. The alumina and zirconia powder reinforced PU foam also showed an increase in the compressive strength up to 3.62 MPa and 6.61 MPa respectively, as compared to 1.77 MPa for unreinforced polyurethane foam, before the failure occurs, which was respectively 104% and 273% higher than that of unreinforced foam.

High-density urethane cellular foam shows little deflection on applying heavy structural loads during construction applications. It also has applications in hand-carved models, prototypes, CNC-machined topographical maps, and industrial patterns [149].

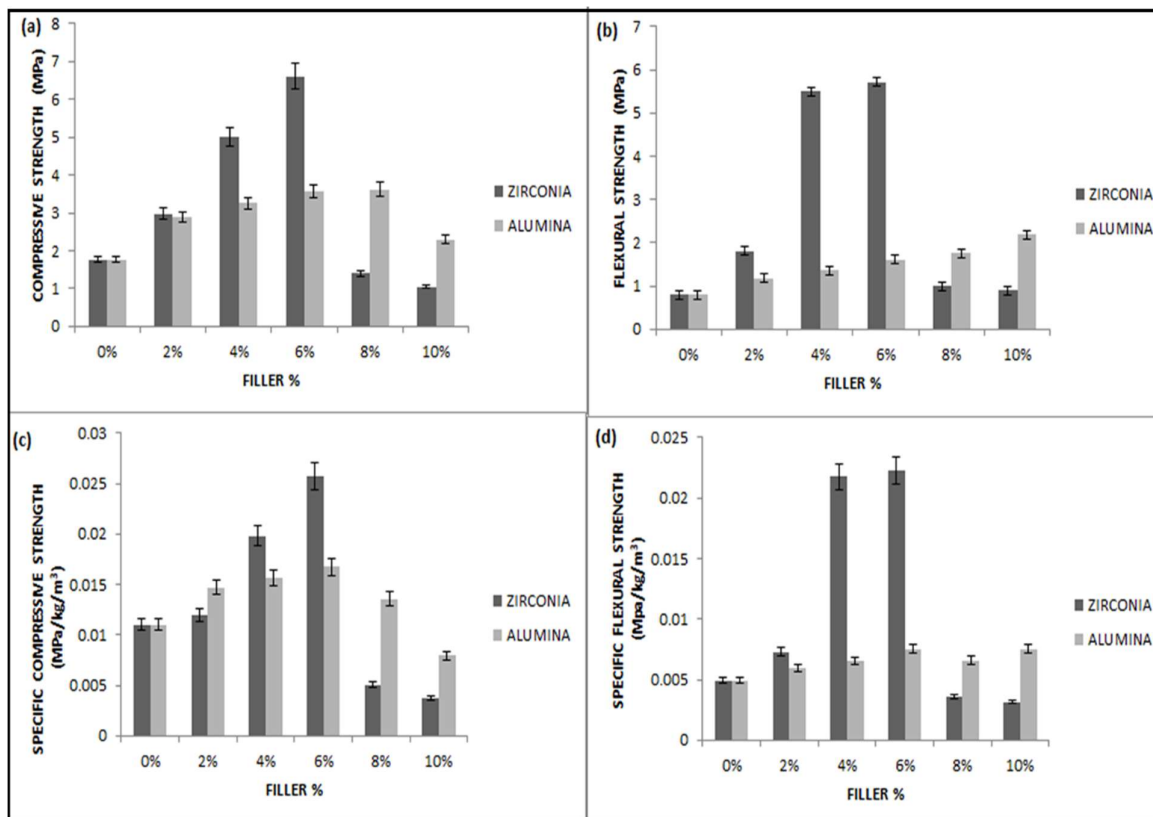


Figure 3.3: Plots of (a) Compressive Strength vs. Filler Percentage, (b) Flexural Strength vs. Filler Percentage, (c) Specific Compressive Strength vs. Filler Percentage and (d) Specific Flexural Strength vs. Filler Percentage

It is observed that the addition of ceramic filler increases the viscosity of the polyol, which indicates more interfacial interaction of the filler with the polyol. APTES treated ceramic fillers have better interaction with the polyol due to the presence of a terminal amino group [150].

APTES can be chemically bonded to the surfaces of the filler by the condensation of its alkoxy groups with the surface hydroxyl groups of the ceramic filler as shown in Figure 3.5. On increasing the concentration of the zirconia powder up to 6%, and alumina powder up to 8%, increases the interfacial interaction, consequently enhancing the mechanical properties of the RPUF. Beyond these concentrations, the particles get agglomerated with each other which, deteriorates the mechanical properties of the RPUF [143]. It is also observed that the incorporation of zirconia powder shows a much higher increase in the compressive strength as compared to that of alumina powder. This behaviour is attributed to the finer particle size and larger surface area of zirconia powder, which leads to better interaction between the zirconia powder and the polyol. Additionally, the alumina powder does not get agglomerated at 8% concentration due to its lower surface area, which promotes better dispersion at a higher concentration in comparison to the zirconia powder, consequently enhancing the mechanical properties.

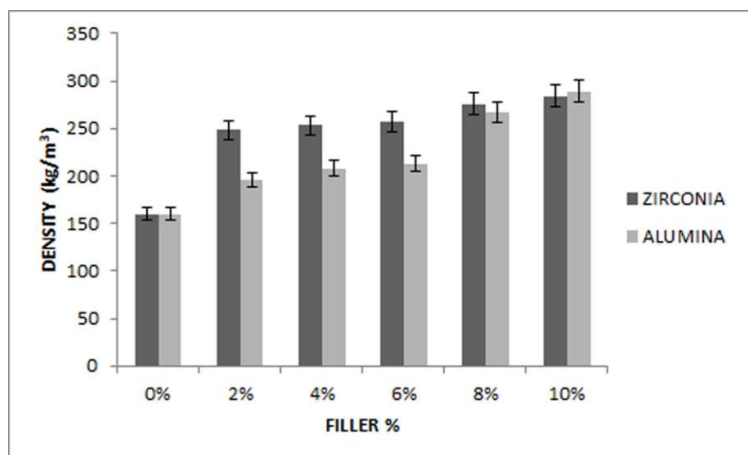


Figure 3.4: Plots of Density vs. Concentration of Ceramic Fillers

3.2.3 Scanning Electron Microscopy

Figure 3.6 shows the variation in the cellular morphology of the unreinforced and ceramic filler reinforced RPUF composites. It is evident from the figure that the incorporation of the ceramic fillers decreased the cell size from $350 \pm 50 \mu\text{m}$ to 280 ± 20 and $320 \pm 20 \mu\text{m}$ for zirconia and alumina powder respectively.

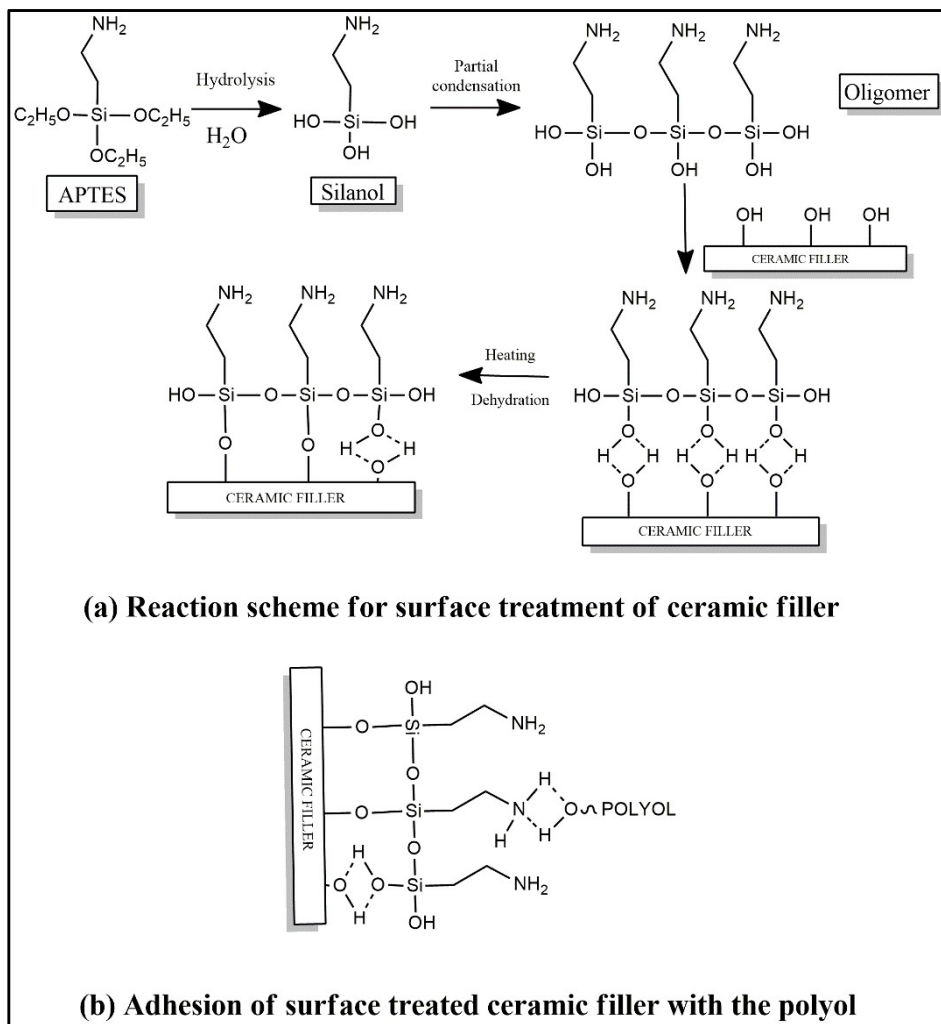


Figure 3.5: Scheme for Surface Treatment and Adhesion of Filler with Polyol

The cell structure was also more homogeneous and round in shape after the addition of ceramic fillers. It is attributed to the fact that the incorporation of ceramic fillers provides more nucleation sites for bubble formation. It is also observed that the ceramic fillers increase the

viscosity of the polyol, which prevents the bubble from being coalesced and consequently reduce the cell size [143].

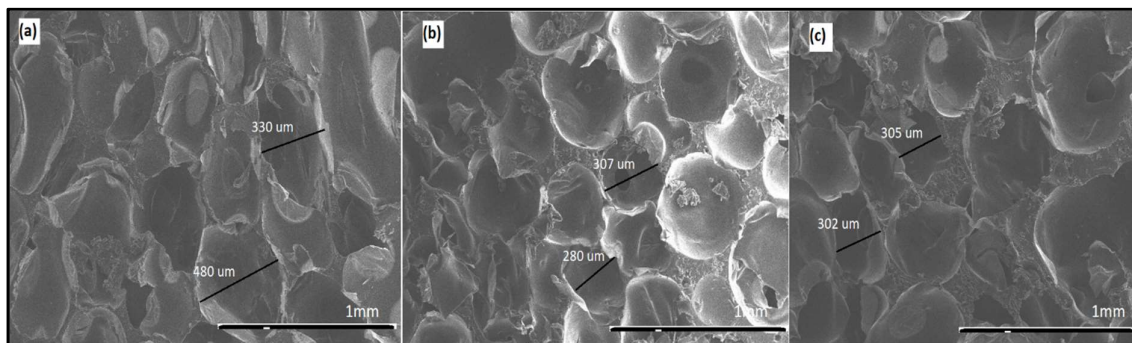


Figure 3.6: SEM Images of RPUF with (a) 0% Filler, (b) 6% Zirconia and (c) 8% Alumina

3.2.4 Thermo-Gravimetric Analysis (TGA)

To evaluate the thermal stability of these foam composites, TGA is conducted under the flow of nitrogen. Results showed the enhanced thermal properties of RPUFs on the incorporation of alumina and zirconia fillers. Maximum char residue was observed for the alumina at 6% and zirconia at 8% concentration. Usually, the thermal stability of RPUFs is characterized by the temperatures of 5% weight loss ($T_{5\%}$) which is considered as the temperature for the onset of degradation [56]. It was noticed that 5% weight loss temperature increased from 192°C to 251°C and 265°C by the incorporation of alumina and zirconia powder respectively, while there is almost no change in the peaks of T_{MAX1} and T_{MAX2} . The TGA and DTG analysis of the ceramic fillers incorporated RPUF composites are illustrated in Figure 3.7 and the parameters are summarized in Table 3.1.

It was observed that the RPUF show two weight loss stages, the first peak at around 300°C - 350°C is related to the degradation of the flexible phase and the decomposition of the urethane linkages in the hard segments. The second peak observed at 450°C – 500°C is attributed to the degradation of soft segments and the thermolysis of the organic residues. The

improvement in the thermal stability is associated with the strong interfacial interaction between the polyol and the ceramic filler phases. If the surface area of the filler is high, a high polyol-filler interaction restricts the polymer chain mobility, which increases the glass transition temperature, consequently increasing the temperature of 5% weight loss ($T_{5\%}$).

Additionally, the zirconia powder can act as a cross-linker between the PU backbones, consequently enhancing the thermal properties of the foam. The improved thermal stability could also be attributed to the homogeneous dispersion of ZrO_2 within the polyol which acts as a thermal insulator due to its low thermal conductivity [145].

Table 3.1: Thermal Characteristics of the RPUF Incorporated with Ceramic Fillers

Concentration of Filler	$T_{5\%}$ (°C)	T_{Max1} (°C)	T_{Max2} (°C)	Residual Mass (%)
0%	192±2	330±4	488±4	8.1±2.0
2% Alumina	235±2	326±2	465±2	11.3±1.0
4% Alumina	246±1	325±2	474±2	11.2±1.0
6% Alumina	251±1	336±1	474±1	14.9±2.0
8% Alumina	251±2	334±1	475±1	12.8±1.0
10% Alumina	233±2	325±2	480±2	12.5±2.0
2% Zirconia	259±2	338±2	478±2	12.5±1.0
4% Zirconia	263±2	339±2	480±1	14.3±1.0
6% Zirconia	265±2	344±1	477±1	16.6±2.0
8% Zirconia	260±2	337±2	471±2	18.4±1.0
10% Zirconia	196±2	340±2	481±2	15.7±2.0

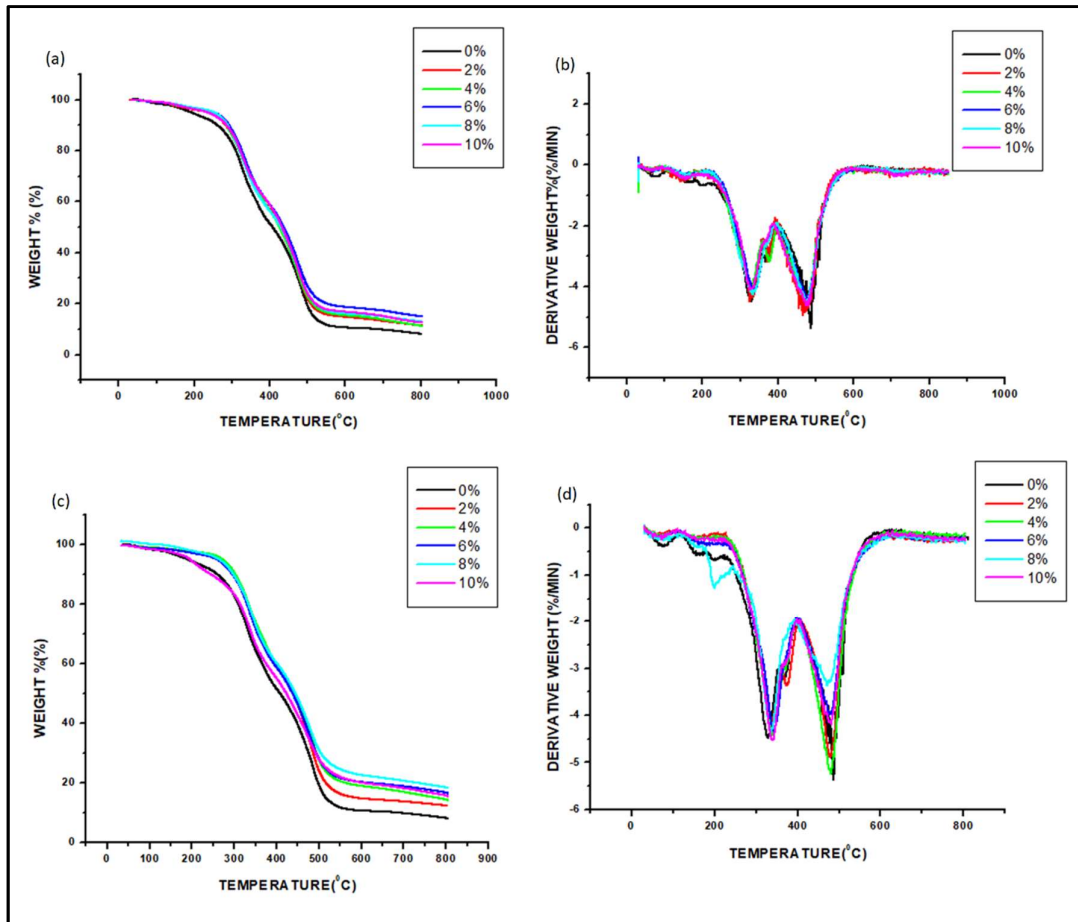


Figure 3.7 (a): TGA Curve of RPUF Incorporated with Alumina Powder, (b) DTG Curve of RPUF Reinforced with Alumina Powder, (c) TGA Curve of RPUF Incorporated with Zirconia Powder, (d) DTG curve of RPUF Reinforced with Zirconia Powder (Test conditions: Nitrogen atmosphere, heating rate 10°C/min)

3.2.5 Cone Calorimeter Testing

Figure 3.8 and 3.9 show the cone calorimeter performance of the RPUF composites containing a varied concentration of the ceramic fillers and the results are compiled in Table 3.2. The cone calorimeter test provides a quantitative analysis of the flame retardancy and smoke release of foams. TTI is an important fire behaviour parameter to judge the flammability

of the polymeric foams. It is evident that the TTIs of the ceramic filler incorporated RPUF composites have shown a considerable increase in comparison with the neat polyurethane foam. The incorporation of filler increased TTI from 2 s to 6 s, for both the foams incorporated with 6% alumina and 6% zirconia powder, which may be attributed to the high-temperature performance of these fillers. Conventionally, the intensity of the fire is correlated with the heat release rate (HRR). Figure 3.8 (a) and 3.9 (a) show the trends in the change in the HRR with time. Two peaks are exhibited for most of the formulations, which are attributed to the formation of a protective charred layer during the burning of the foam [151].

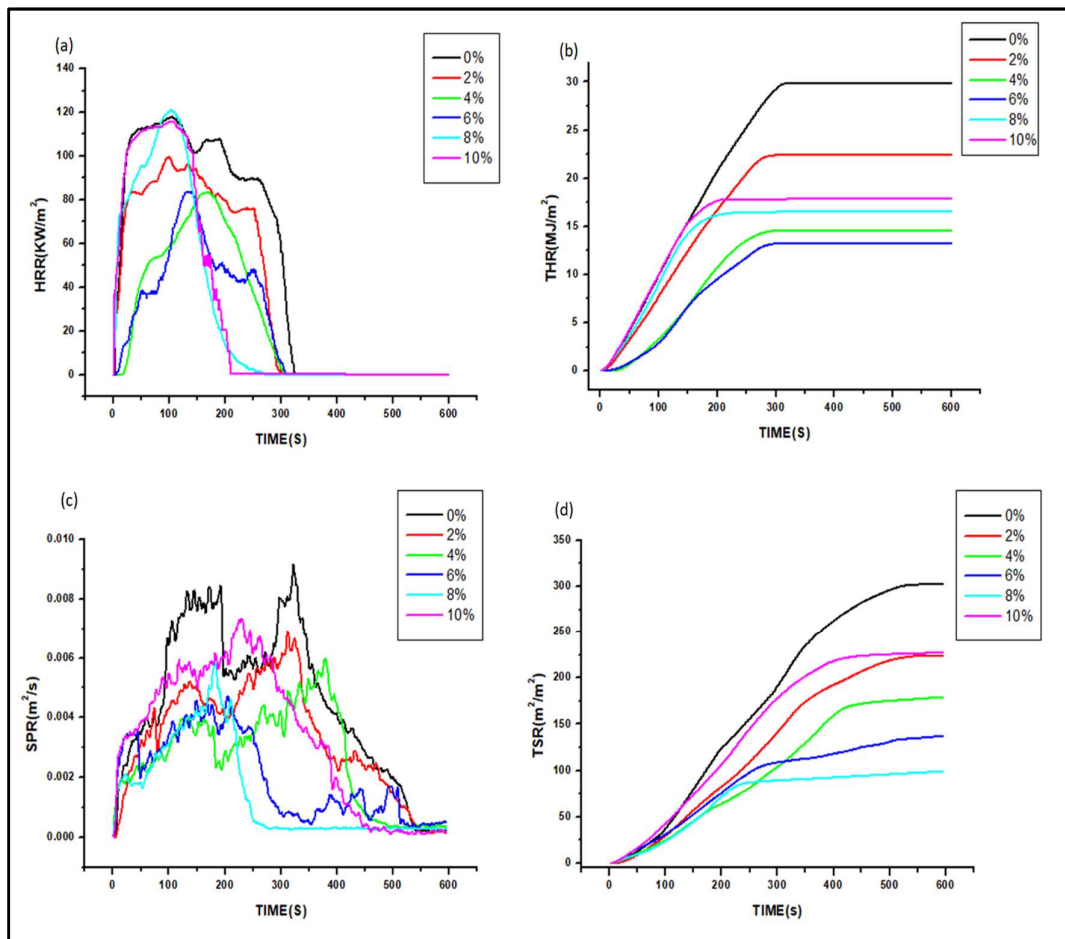


Figure 3.8: (a) HRR (Heat Release Rate), (b) THR (Total Heat Release), (c) SPR (Smoke Production Rate) and (d) TSR (Total Smoke Release) of RPUFs Incorporated with Alumina Powder (Test conditions: incident heat flux of 35kW/m²)

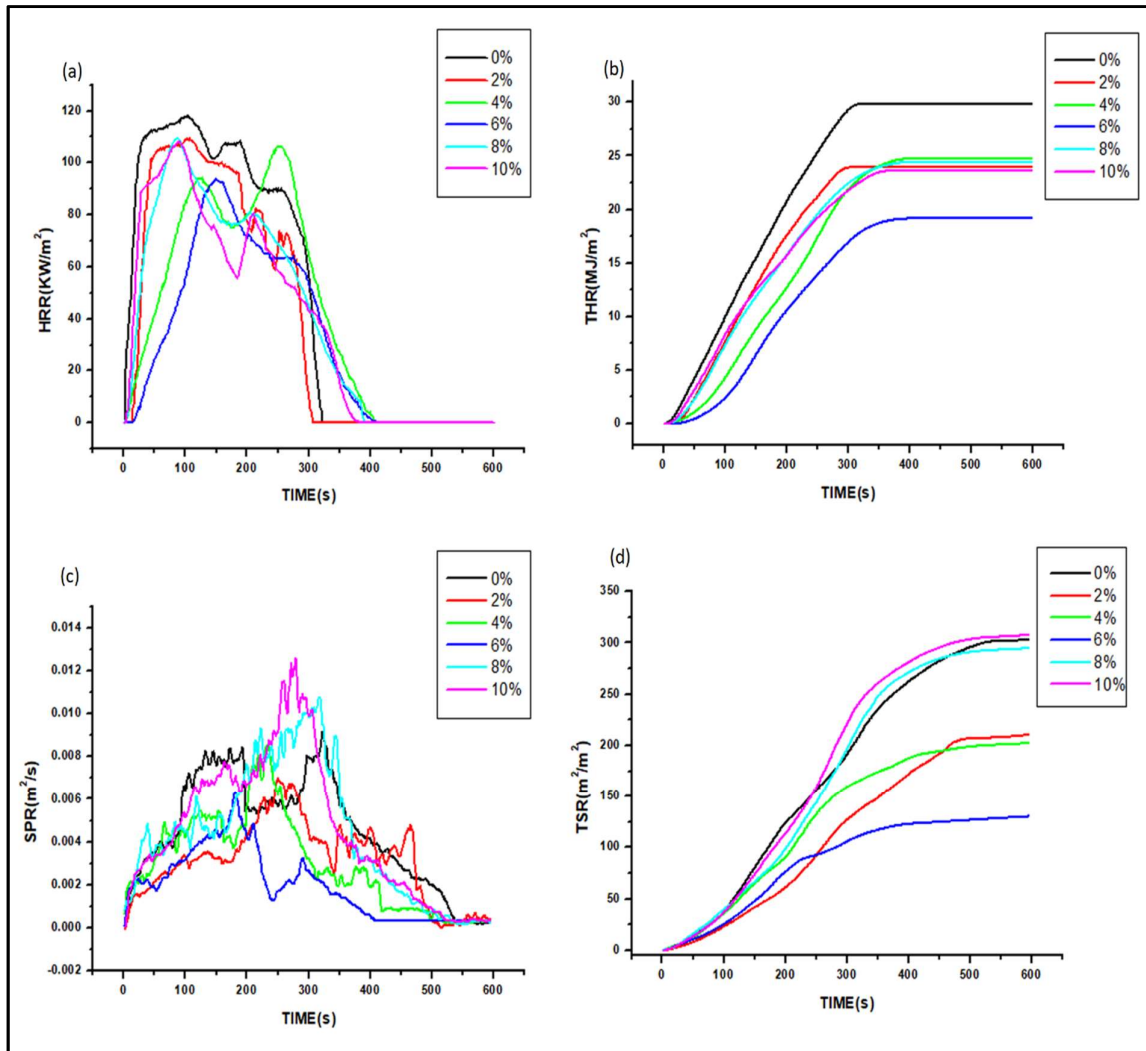


Figure 3.9: (a) HRR (Heat Release Rate), (b) THR (Total Heat Release), (c) SPR (Smoke Production Rate) and (d) TSR (Total Smoke Release) of RPUFs Incorporated with Zirconia Powder (Test conditions: incident heat flux of 35kW/m²)

Results show that the peak heat-release rate (PHRR) was 84 kW/m² and 94 kW/m² for the foam composite containing 6% alumina powder and 6% zirconia powder respectively, which were less than that of the neat RPUF (118 kW/m²). PHRR signifies the surface pyrolysis of the rigid polyurethane foam and the evolution of a large quantity of flammable low molecular weight by-products, such as, primary or secondary amine, isocyanate, alcohol and

olefin [152]. Ceramic fillers are high-temperature performance fillers and demonstrate better thermal insulation at elevated temperature, which reduces the rate of heat release. Furthermore, on increasing the concentration of filler, agglomeration of the particles deteriorates the insulating effect. Additionally, the APTES treated ceramic fillers restrains the segmental motion of the PU backbone owing to an increased crosslink density in the RPUF [150].

Table 3.2: Fire Characteristics of the RPUF Incorporated with Ceramic Fillers

Concentration of Filler	PHRR (kW/m²)	THR (MJ/m²)	TSR (m²/m²)	Residue (%)
0%	118±2	29.8±1.0	302±3	11.5±2.0
2% Alumina	100±3	22.4±2.0	224±2	16.4±2.0
4% Alumina	83±2	14.5±1.0	179±3	18.3±1.0
6% Alumina	84±2	13.2±1.0	137±3	20.4±1.0
8% Alumina	121±3	16.5±1.0	99±2	21.4±2.0
10% Alumina	116±2	17.8±2.0	227±2	23.1±1.0
2% Zirconia	109±2	23.9±2.0	210±2	18.9±2.0
4% Zirconia	106±2	24.7±1.0	202±3	19.1±1.0
6% Zirconia	94±2	19.2±1.0	130±2	21.6±2.0
8% Zirconia	109±3	24.4±1.0	294±2	22.1±1.0
10% Zirconia	108±3	23.6±2.0	307±3	24.7±1.0

Figures 3.8 (b) and 3.9 (b) show that the total heat release (THR) also decreased on the incorporation of ceramic fillers. This result illustrates that ceramic powder hinders the heat transfer and flame spread, therefore decreasing the intensity of the fire. As the flame retardancy of an additive is also reliant on the augmented char residue yield [153], the observed char

residue increased from 11.47% for neat RPUF to 23.10% and 24.69% for RPUF with 10% alumina powder and 10% zirconia powder respectively.

The smoke production behaviour of the RPUFs can be predicted by the total smoke release (TSR) and smoke production rate (SPR). Figure 3.8 (c) and 3.9 (c) show the SPR and the first peak of SPR denotes that the smoke production decreased from 0.008 to 0.004 m²/s and 0.006 for 6% alumina powder and 6% zirconia powder respectively. The TSR also decreased from 302 m²/m² to 99 m²/m² and 130 m²/m² for 8% alumina powder and 6% zirconia powder respectively (Figure 3.8 (d) and 3.9 (d)). This smoke suppression is attributed to the protective charred layer that prevented the release of the smoke [154]. Increasing the concentration of alumina powder beyond 6% shows an increase in the rate of heat release due to the less insulation caused by the slight agglomeration of the alumina powder, whereas the smoke release decreases owing to the increased cross-linking density of the RPUF. Furthermore, at 10% concentration of the filler, total collapse in the structure demonstrates deteriorated flame retardant properties.

3.3 SIGNIFICANT FINDINGS

Rigid PU foams are prepared by incorporating alumina and zirconia powders to enhance the flame retardant and thermal properties of the foams. The compressive strength and the flexural strength of the ceramic filler incorporated foam were found to increase by 273% and 624% respectively. TGA and DTG curves showed an increase in the thermal stability of the ceramic filler reinforced foams. The 5% weight loss temperature (T_{5%}) increased from 192°C to 265°C for the 8% zirconia powder filled RPUF. TTI was also found to increase from 2 seconds to 6 seconds for the foam with 6% concentration of zirconia powder, as well as, alumina powder. The flame retardancy of the ceramic filler incorporated RPUFs was also

enhanced and 6% concentration of the ceramic fillers demonstrated the best properties with up to 29% decrease in heat release rate (HRR) and 71% suppression in the production of smoke. As the addition of ceramic powder improves the physical, thermal and fire properties of the vegetable oil-based RPUFs, the ceramic powder may be considered as a potential additive to improve these properties of the RPUF.

CHAPTER 4

DEVELOPMENT OF CONDUCTING RPUF USING CARBON FIBRE REINFORCEMENT

4.1 INTRODUCTION

Electromagnetic interference (EMI) is the disturbance generated by some undesirable radiated signals emitted by the electronic instruments, which may affect the performance of the other electronic devices. Nowadays, an expeditious rise in the use of wireless devices for communication, such as laptops, smartphones, routers, and others are polluting their surroundings in terms of electromagnetic pollution, which may be dangerous for the health of the human beings, as well, as for information security. An appropriate EMI shield is required to protect the environment from electromagnetic waves, used by many vital applications such as air traffic control, weather radar, satellite communications and others [155, 156]. These EMI shielding materials may also be used for evading radar detection by absorbing electromagnetic radiations. The metallic coatings have extensively been used as EMI shielding materials, but they always suffer from shortcomings of high density, poor resistance to corrosion and high cost of processing. As alternatives, polymeric foams incorporated with some conductive fillers are explored to fabricate lightweight and tough shielding materials. These polymeric foams are a suitable material for such applications due to their various better mechanical and electrical properties along with low density. A wide range of polymers, such as epoxies [157], poly (methyl methacrylate) (PMMA) [158, 159], polyurethane (PU) [160], polystyrene (PS) [161] and polypropylene (PP) [162] have been utilized to develop the EMI shielding foams.

Kuang *et al.* [163] prepared poly lactic acid – MWCNT nanocomposite foam for EMI shielding applications and observed that a conductivity of 3.4 S/m was obtained using the foam with 10 wt% of MWCNT and 0.3 g/cm³ density. Li *et al.* [164] fabricated epoxy-MWCNT

nanocomposite foam and obtained a conductivity of 3.04×10^{-2} S/m by the addition of 5wt% of MWCNT. Yan *et al.* [156] prepared polystyrene nanocomposite using reduced graphene oxide (rGO) and achieved electrical conductivity up to 43.5 S/m with 3.47 vol% loading of rGO. Hwang *et al.*[165] prepared polybutylene terephthalate (PBT) /carbon fibre composite and investigated the effect of carbon fibre on the EMI shielding performance. It was concluded from their studies that carbon fibre loading should be greater than 30 wt% to get better EMI shielding effectiveness.

Zhang *et al.* [166] fabricated PMMA based foam with density 0.22-0.38 g/cm³ , incorporated with Fe₃O₄ and MWCNT. It was observed that the foams with 1.63% hybrid filler loading showed an electrical conductivity of 2×10^{-4} S/m. Li *et al.* [167] fabricated ultrathin carbon foams by the pyrolysis of the polyimide/ graphene composite foams. It was observed that up to 24 dB electromagnetic interference (EMI) shielding effectiveness was exhibited by these graphene based foams, with conductivity up to 2300 S/cm.

Besides these materials, PU foam may be used as a promising material due to its low density and good mechanical properties. Commercially, the PU foams are available in different forms such as flexible, rigid or elastomeric, depending upon their structure. Rigid polyurethane foams (RPUFs) have been used in a wide variety of applications, such as, building and construction industry, transportation and others, for the insulation purpose. RPUF has also been used in radomes and high-speed aircrafts due to its ability to allow electric and magnetic waves to pass through it. Owing to its high dielectric constant and low weight it is being used in different fields of electronic industry such as potting and encapsulation of the electronic components, microwave absorbers, and others. RPUF may also be used for electromagnetic wave absorption by incorporating some functional filler. The functional fillers contribute the plastic materials with a much wider range of properties, including some unique properties, not normally associated with plastics, such as high electrical conductivity or low flame retardancy.

Li *et al.* [168] studied the effect of the sandwich and gradient configuration on the EMI shielding performance and concluded that the multilayered polyurethane graphene composite may be used as a high-performance material for microwave absorption and EMI shielding. Farhan *et al.* [169] prepared a different type of carbon foams using powdered PU and carbon precursors, novolac and pitch. Silicon carbide (SiC) nano-wires were grown to enhance the absorption properties of these carbon foam. A maximum EMI shielding of 79.50 dB cm³/g was achieved in the carbon foam containing 20% Si content, with very low conductivity. Esfahani *et al.* [170] incorporated the surface functionalized graphene sheets in the thermoplastic PU and their EMI shielding effect has been investigated. Results showed that higher electrical conductivity and improved dielectric properties were achieved due to the stronger interfacial interaction between the filler and the TPU matrix. The TPU film with 5 vol% graphene and thickness of 1 mm exhibited commercially relevant EMI shielding effectiveness of 25 dB in the X-band frequency range.

Commercially, the PU has been prepared by the reaction of polyols with the polyisocyanate, both of them are petroleum-based raw materials, but, due to the depletion in the petroleum resources and rising concern about the environment, bio-based raw materials are the requirement of the modern world [50, 171–173]. Ibrahim *et al.* [174] fabricated castor oil based PU films to be employed as a base material for electrolytes. It was observed that the conductivity of PU films increased from 1.18×10^{-9} S/m to 1.42×10^{-4} S/m, on the incorporation of 30 wt% of LiI salt. Nevertheless, the potential applications of bio-based conductive RPUF have not been explored so far. So, herein, we are exploring the electrical conductivity of the bio-based RPUF, incorporated with carbon fibre in varied proportion. The mechanical, thermal and flame retardant properties of these foams have been investigated.

4.2 RESULTS AND DISCUSSION

Carbon fibre in different proportion is added to the PU foam to provide some desired functional properties. The foam architecture depends on the particle size and the dispersion of the filler in the reacting mixture. Moreover, an interaction between the filler and the polymer matrix is the important parameter governing the mechanical properties of reinforced PU foam.

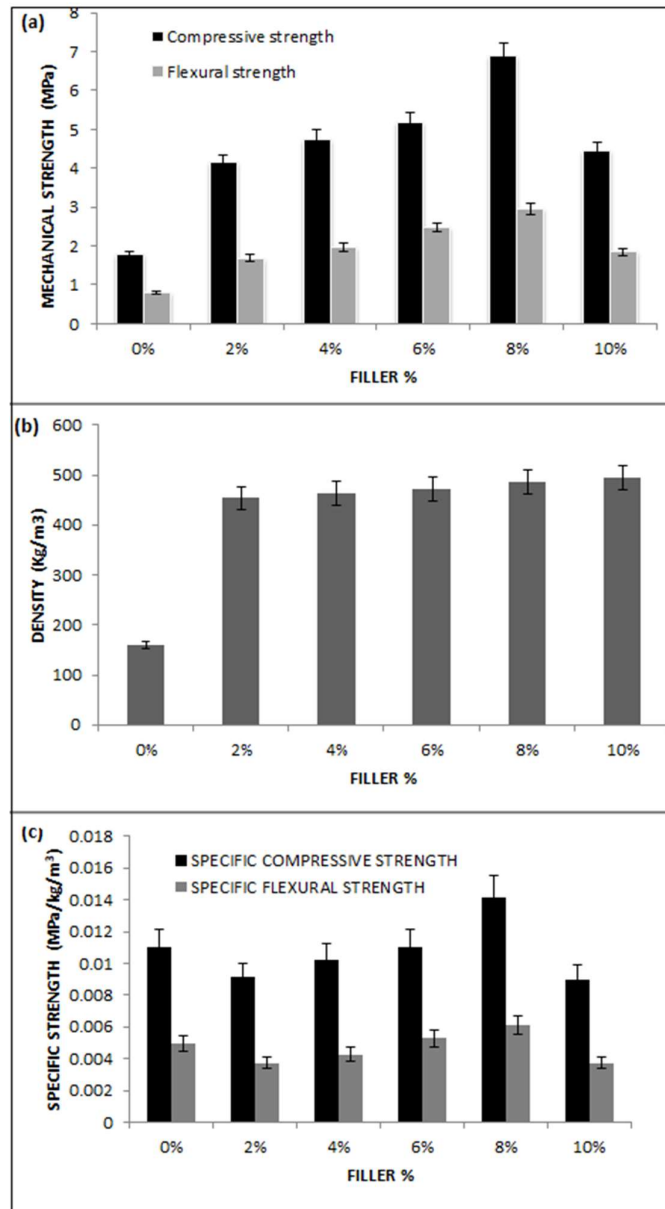


Figure 4.1: Plots of (a) Mechanical Strength vs. Filler Concentration, (b) Density vs. Filler Concentration, (c) Specific Strength vs. Filler Concentration

4.2.1 Mechanical Properties

Mechanical properties of the PU foam are influenced by several factors such as density of the foam, cell geometry, as well as, the number & size of cells. In general, the foams with higher density are expected to be more rigid, which in turn exhibit higher mechanical strength. PU foam without fillers has a large number of cells, with a comparatively larger cell size, but when carbon fibre is incorporated, it is evident from the SEM images that foam cell size decreased.

Figure 4.1 shows the change in the mechanical properties of the rigid polyurethane foam on the addition of carbon fibre powder. The foam with 8% concentration of carbon fibre shows higher mechanical properties, with compressive strength 6.88 MPa and flexural strength 2.97 MPa, which is almost 3 times in comparison to the unreinforced foams (Figure 4.1(a)). Figure 4.1(c) shows the variation in specific strength or reduced strength (strength/density) on increasing the concentration of the carbon fibre powder. It is observed that the specific strength decreases initially, but, again on increasing the concentration of the filler up to 8%, there is an increase in the specific compressive strength and the specific flexural strength by 28% and 24% respectively, as compared to the neat foam.

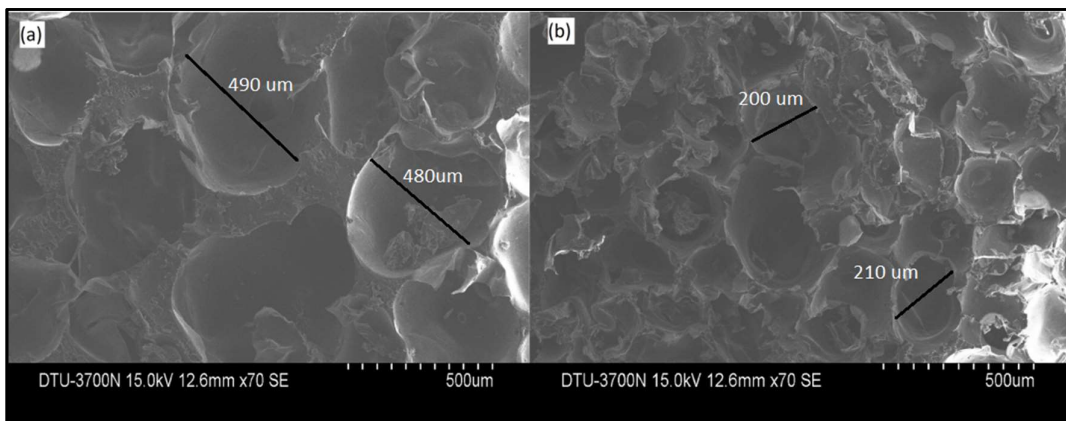


Figure 4.2: SEM Micrographs of RPUF with (a) 0% and (b) 8% Concentration of Carbon Fibre Powder

This behaviour is attributed to the decrease in cell size and increase in cell number as more cell walls and struts per unit area of PU foams are present to support the foam structure, under loading. This is also confirmed by the SEM images of RPUFs as shown in Figure 4.2. An initial slight decrease in the specific strength is attributed to the heterogeneity produced by the addition of the filler. It is also confirmed by the FTIR of carbon fibre incorporated RPUFs. Furthermore, the incorporation of the fillers in the cell walls and struts strengthened the foam structure, consequently increasing its mechanical strength. It is evident from the literature, that, the hydrogen bond formation among the urethane groups greatly contributes to the strength of the RPUFs. But the filler introduced may interfere with the hydrogen bond formation, thus causing a negative effect on the properties of RPUFs. The overall performance of the RPUFs depends on the competition between the positive effects of carbon fibre reinforcement and the negative effects of hydrogen bond formation [175]. A similar decrease in cell size has been reported in literature, for the addition of carbon nanotubes to the polyurethane foams [96].

4.2.2 Thermo-Gravimetric Analysis (TGA)

The Thermo-Gravimetric Analysis (TGA) and Derivative Thermo-gravimetry (DTG) of the carbon fibre powder incorporated RPUF are illustrated in figures 4.3 (a) and 4.3 (b) respectively. To evaluate the thermal stability of these foams, TGA is conducted under the flow of nitrogen.

Generally, the thermal stability of the RPUFs is described by the degradation onset temperature i.e., the temperature of 5% weight loss ($T_{5\%}$). The results show a decrease in 5% weight loss temperature ($T_{5\%}$) from 192°C to 148°C for the foam with 10% concentration of the carbon fibre. This behaviour of RPUF is attributed to the increased thermal conductivity of the foams, consequently increasing the heat to spread more rapidly, only on the percolation path made by the carbon fibre, and initializing some initial weight loss [176]. Similar decrease in 5% weight loss temperature was observed by Ciecierska *et al.* on the addition of graphite in

RPUF [96]. Char residue also increases on increasing the filler concentration. All the samples show three weight loss stages at 195°C, 330°C and 490°C respectively.

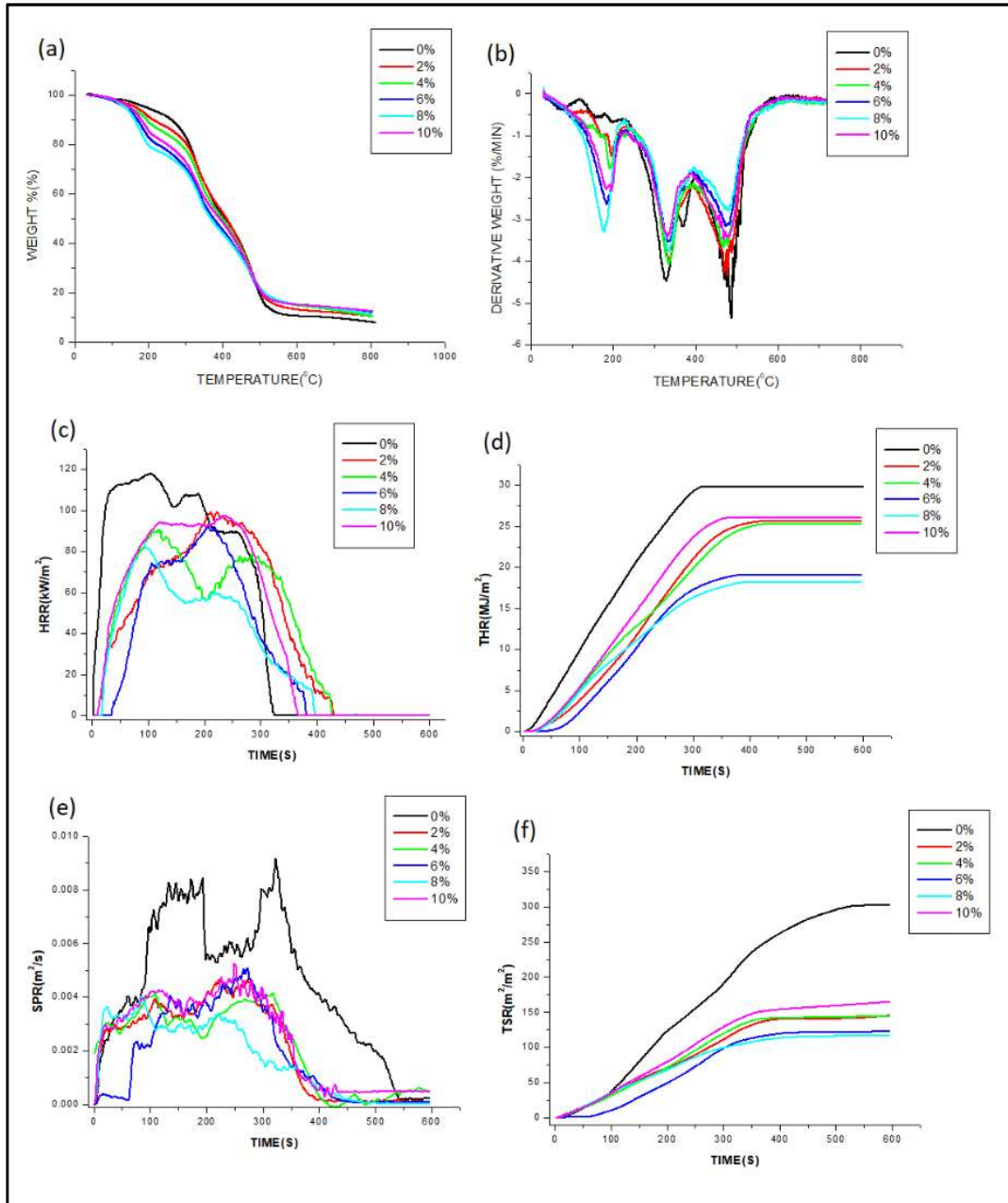


Figure 4.3: (a) TGA Plots, (b) DTG Plots, (Test conditions: Nitrogen atmosphere, heating rate 10°C/min) (c) HRR (Heat Release Rate), (d) THR (Total Heat Release), (e) SPR (Smoke Production Rate) and (f) TSR (Total Smoke Release) of the RPUFs Incorporated with Carbon Fibre (Test conditions: incident heat flux of 35kW/m²)

The beginning slow weight loss stage at 195°C is caused by the initial weight loss of some hard segments around the carbon fibres. The foam with 8% concentration of the carbon fibres shows the fastest degradation, which is attributed to the better dispersion of the carbon fibre, consequently, providing the longest percolation path for heat transfer. On the other hand, the foam with 10% concentration of the carbon fibre, though, possesses a higher concentration of the filler, the poor dispersion provides comparatively shorter percolation path for the heat transfer. The quick weight loss stage at 330°C is related to the degradation of the hard segments, resulting in the formation of isocyanate, alcohol, amine, olefin and CO₂.

The third slow weight loss stage at 490°C is attributed to the degradation of the soft segments and thermolysis of the organic residues. It was observed that the increase in the concentration of the filler slows down the degradation up to 8% filler concentration. On increasing the concentration of the carbon fibre beyond this limit, increases the rate of the degradation, owing to the poor dispersion of the filler.

4.2.3 Cone Calorimeter Testing

Figures 4.3 (c) to (f) show the cone calorimeter performance of the RPUF containing a varied concentration of the carbon fibre filler and the results are compiled in Table 4.1. It is evident that the TTIs (time to ignition) of the carbon fibre filler incorporated RPUFs have shown a slight increase from 2 s to 5 s for the foams incorporated with 8% carbon fibre powder. Conventionally, the intensity of the fire is correlated with the heat release rate (HRR) [151]. The results showed that the peak heat-release rate (PHRR) was decreased from 118 kW/m² to 85 kW/m², for the foam containing 8% carbon fibre powder (figure 4.3 (c)). PHRR signifies the surface pyrolysis of the RPUF and evolution of a large quantity of flammable low molecular weight by-products, such as primary or secondary amines, isocyanates, alcohols and olefins [152, 154].

Table 4.1: Cone Calorimeter Data of the RPUF Incorporated with Carbon Fibre

Concentration of Filler	PHRR (kW/m²)±2	THR (MJ/m²)±1.0	TSR (m²/m²)±3	Residue (%)±0.5	TTI (s)±1
0%	118	29.8	347	11.5	2
2% Carbon Fibre	99	25.7	144	31.6	3
4% Carbon Fibre	91	25.3	145	36.1	4
6% Carbon Fibre	92	19.0	123	40.5	5
8% Carbon Fibre	85	18.2	116	44.0	5
10% Carbon Fibre	97	26.0	165	44.4	4

Figure 4.3 (e) shows the smoke production rate (SPR), where, the first peak denotes that the rate of the smoke production decreased from 0.008 to 0.004 m²/s for 8% carbon fibre powder loading. The total smoke release (TSR) also decreases from 347 m²/m² to 116 m²/m² on the addition of 8% carbon fibre powder (Figure 4.3 (f)). This behaviour of the RPUF incorporated with carbon fibre powder is associated with the formation of the carbon layer on the surface, and consequently reduction in the combustion gases, which is analogous to the observations of Ciecierska *et al.*[96]

4.2.4 Conductivity Measurement

The incorporation of the carbon fibre in the RPUF generates conductivity in the foam. Figure 4.4 shows the change in the conductivity of RPUF on the incorporation of carbon fibre.

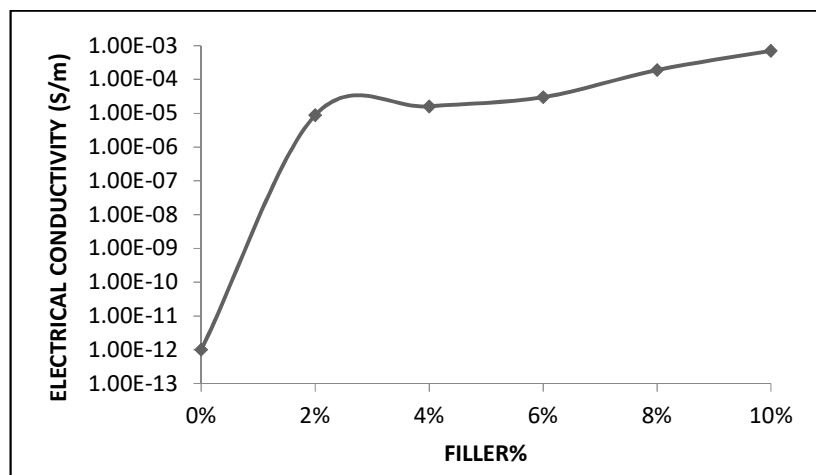


Figure 4.4: Plots of Electrical Conductivity of Carbon Fibre Reinforced RPUF (S/m) vs. Filler%

It is clearly observed by the results that the incorporation of the conducting carbon fibre in RPUF increased the conductivity of RPUFs and the foams with 8% & 10% carbon fibre contents exhibits a conductivity of 1.9×10^{-4} and 7.1×10^{-4} S/m respectively. A similar range of electrical conductivity was obtained by Ibrahim et al. in castor oil-based polyurethane films incorporated with LiI salt [174]. So, these resulted carbon fibre reinforced foams may be used in the applications where the conducting rigid foams are required.

4.3 SIGNIFICANT FINDINGS

RPUFs were prepared by incorporating the carbon fibre powder to develop the electromagnetic shields, using bio-based raw materials obtained by the transesterification of castor oil. FTIR and ^1H NMR spectra of the prepared polyol confirm the transesterification of castor oil. The mechanical, thermal and flame retardant properties of these foam shields have been studied. The foams with 8% and 10% carbon fibre concentration showed conductivity of 1.9×10^{-4} and 7.1×10^{-4} S/m respectively. The results concluded that the RPUF with 8% carbon fibre concentration showed higher mechanical properties, with a 3-fold increase in the

compressive and flexural strength respectively. Specific compressive strength was also found to increased by 28% for the foams with 8% concentration of the carbon fibre powder. The peak of heat release (PHRR) was found to decrease from 118 kW/m² to 85 kW/m² on the incorporation of carbon fibre powder. Additionally, the rate of smoke production was also observed to decrease for these composite RPUFs. As the incorporation of the carbon fibre in RPUF provides a reasonable amount of conductivity, without deteriorating the other properties of the vegetable oil based rigid PU foams, so carbon fibres are proved to be a potential additive to yield conducting PU foams.

CHAPTER 5

STUDIES ON THE MINERAL FILLER REINFORCED RPUF

5.1 INTRODUCTION

Rigid Polyurethane foam (RPUF) has its application in a wide variety of fields such as construction, transport, thermal insulation, packaging of electronic goods, radomes and others [177, 178]. High-density polyurethane cellular foam shows little deflection on applying heavy structural loads during the construction applications. The RPUF has applications in hand-carved models, prototypes, CNC-machined topographical maps and industrial patterns [149]. The polyurethane foams derived from the renewable sources are a requirement of the modern world due to the various issues related to the petroleum-based foams [8, 32]. Polyurethane (PU) foams are prepared by using polyols and polyisocyanate as raw materials. Although polyols have successfully been derived from the renewable sources [41, 42], the studies reveal that the functional properties (compressive strength, thermal stability and flammability etc.) of these renewable source-based foams are inferior to the foam derived from the petroleum-based raw materials. Numerous studies have been conducted in past to improve these functional properties of the renewable sources based foams by incorporating different fillers. Additives such as fibres or particulate fillers are used as reinforcement to increase the compressive strength, sound attenuation, thermal stability and flame retardancy, as well as. to decrease the density and water absorptivity of the PU foam.

Serban *et al.* [75] investigated the influence of the glass fibre incorporation on the mechanical properties of PU foam in terms of the variations in fibre length (12.5-50 mm) and fibre mass content (5-20%). Results concluded that the glass fibre reinforcement increases the elastic modulus more than two folds as compared to unreinforced PU foam, on the incorporation of 20% glass fibre with fibre length 25 mm. Xue *et al.* [57] developed a lignin-

based rigid polyurethane foams (LRPF), reinforced with different weight ratios (1-5 wt%) of the pulp fibre. The addition of the pulp fibre in the LRPF resulted in greater cell size, lower density and better thermal stability of the foam.

Apart from these fibrous fillers, some particulate fillers such as finely divided mineral fillers have additional advantages of providing high heat-deflection temperature, low thermal expansion, good moldability and low cost, which are the requirement of good rigid polyurethane foam. These additional advantages are strongly affected by the filler-to-resin ratio, the extent of dispersion and the particle size of the filler [153, 179]. Different types of mineral fillers such as calcium carbonate [85], talc [90] and nanoclay [19, 82] have been considered to improve the properties of the PU foams.

Czuprynski *et al.* [91] incorporated various particulate fillers in the rigid polyurethane-polyisocyanurate foams and analyzed their effects on the properties of the rigid foam. The addition of the aluminium hydroxide and talc into the foam improved its various functional properties, such as, increase in the compressive strength and closed cell content as well as decrease in the apparent density, flammability and brittleness, while the addition of the chalk, borax and the starch reportedly deteriorated its properties. Nik Pauzi *et al.* [86] considered modified di-aminopropanemontmorillonite (DAP-MMT) nanoclay (0-10 wt%) as a promising reinforcement material to be incorporate in the palm oil-based PU foam. An increase in the compressive strength and the thermal stability was observed, on increasing the concentration of DAP-MMT up to 4%.

Zheng *et al.* [112] introduced organically modified montmorillonite (OMMT) nanoclay as a filler in the polyurethane matrix to enhance the flame retardancy of the RPUF. Phosphorus-based flame retardant such as ammonium polyphosphate (APP) and triphenyl phosphate (TPP) were also used to enhance the char-forming property of RPUF. It was observed that the foam with 8% APP, 4% TPP, 5% OMMT exhibited maximum increase in the combustion duration

time as well as a decrease in the heat release rate and total smoke production. Zieleniewska *et al.* [94] introduced the egg shell waste (0-25%) into RPUF and investigated its effect on the material properties of the foam. Results indicated an increased compressive strength & density, better thermal stability, low water absorption and high dimensional stability in wet conditions.

Zhu *et al.* [18] incorporated cellulose microfibrils and nanoclay in the rigid PU foam to alter the cellular structure of the foams. The compressive strength of foam was found to be increased by using these fillers as reinforcement. Atabek *et al.* [138] analysed the effect of the calcium hypophosphite on the properties of some thermoplastic polymers including polyurethane. It was observed that the thermal stability and flame retardancy of the polyurethane was increased on the incorporation of the filler. The synergistic effect of some mixed inorganic flame retardant has also been studied. Mixture of the expandable graphite or red phosphorus with guanidinium phosphate was employed as a flame retardant and a noticeable improvement in the flame retardancy of the RPUF was observed [180]. Additionally, some flame retardants such as aluminium diethyl phosphinate [137], hydroxyl-terminated monomer containing phosphorus and nitrogen, tri(N, N-bis- (2-hydroxy-ethyl) acyloxyethyl) phosphate (TNAP) [181] or modified urea-formaldehyde resin [182] has also been used to improve the flame retardancy of the polyurethane.

Though, numerous studies have already been conducted for the enhancement of properties of RPUF using mineral fillers, such as calcium carbonate, talc and nanoclay, but some other low cost natural mineral fillers such as feldspar and kaolinite clay have not been explored so far to enhance the functional properties of the bio-based RPUF. Feldspar is an alumina-silicate mineral and being used as fillers in the adhesive, rubber and paint industries to improve the strength, toughness and durability of the final products. The beneficial properties of the feldspar include high chemical inertness, high resistance to abrasion, and low viscosity at high filler loading [183]. Kaolinite clay is used by many industries as a filler to reduce the cost and to

enhance the strength. Kaolinite clay is chemically inert, nonabrasive, has low plasticity & apparent bulk density, as well as, high refractory properties [184, 185]. So, in this chapter, mineral fillers kaolinite clay and feldspar have been used as reinforcement and their effects on the mechanical, thermal and flame retardant behaviours of bio-based RPUF has been investigated.

5.2 RESULTS AND DISCUSSION

5.2.1 Mechanical Properties

Mechanical properties of PU foam are influenced by several factors such as the size & shape of the cells along with the density of the foam. The foam structure also depends on the particle size and the dispersion of the filler in the reacting mixture. Moreover, the interaction between the filler and the polymer matrix is also an important parameter governing the mechanical properties of the reinforced PU foam [91].

Figure 5.1 and 5.2 show the change in the mechanical strength and the specific mechanical strength (strength/density) of the RPUF incorporated with different mineral fillers. The incorporation of these fillers in the rigid PU foam increases the compressive strength of the foam initially and then a decrease in the property was observed, with further increase of filler concentration.

The maximum compressive strength was shown on the addition of feldspar at 8% and kaolinite clay at 6% concentration, while the foams incorporated with 8% feldspar showed the highest compressive strength of 4.98 ± 0.25 MPa which is 182% greater than that of the neat foam (Figure 5.1 (a)). The flexural strength also demonstrated the similar trends and the foam with 6% kaolinite clay showed the highest flexural strength of 3.56 ± 0.18 MPa, which is 351% greater than that of the neat foam (Figure 5.1 (b)).

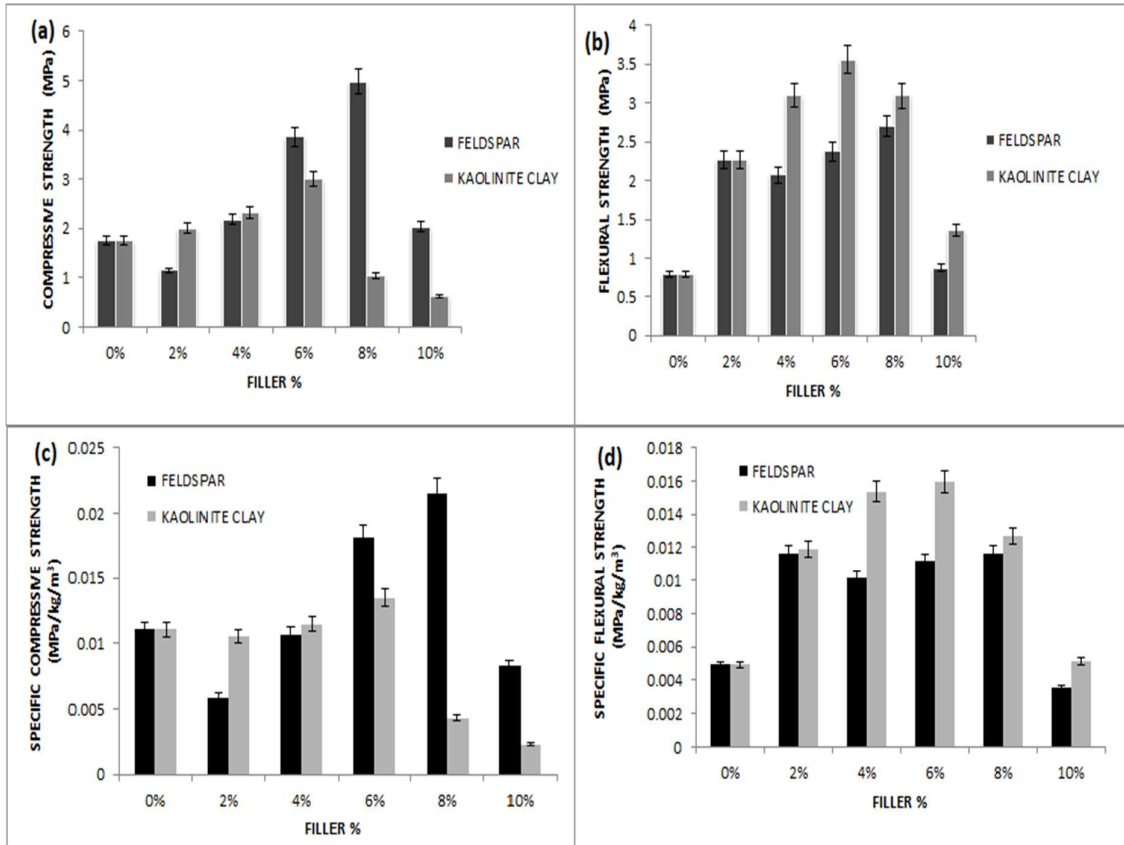


Figure 5.1: Plots of (a) Compressive Strength vs. Filler%, (b) Flexural Strength vs. Filler%, (c) Specific Compressive Strength vs. Filler%, (d) Specific Flexural Strength vs. Filler%

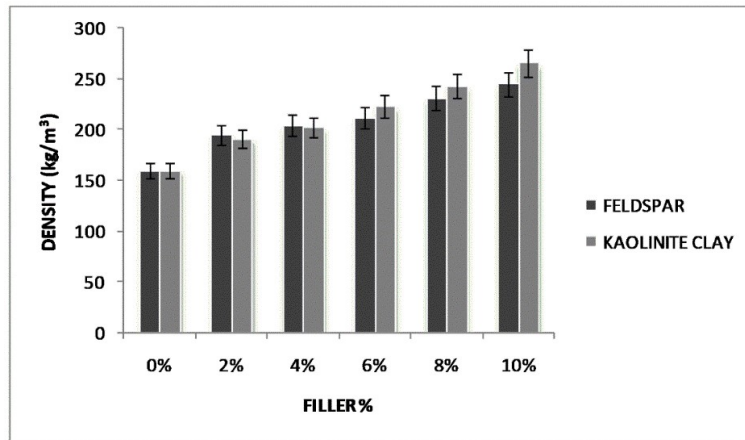


Figure 5.2: Plots of Density of the RPUF vs. Concentration of the Mineral Fillers

Further, on increasing the filler concentration beyond this limit, led to the agglomeration of the filler, which produces only filler –filler interaction, consequently deteriorating the mechanical properties of the foam. It is proved by the distorted structure of the foams at higher filler concentration, as shown by the SEM images. Similar findings have also been reported in the literature [86]. The density of the rigid foams also increases on increasing the concentration of mineral fillers (Figure 5.2). As, the density has a remarkable effect on the mechanical strength of the foam, so the specific mechanical strength has been studied to have an idea about the change in strength due to the incorporation of the mineral fillers in the rigid PU foam (Figure 5.1 (c) and 5.1 (d)).

The decrease in cell size and subsequent increase in the cell number contribute to a superior mechanical strength because the load applied is encountered by more cell walls per unit area of the foam. Furthermore, the incorporation of the fillers, in the cell walls, strengthened the foam structure, consequently increasing the mechanical strength [96]. Furthermore, as the feldspar possesses more percentage of silica in its composition, which, forms the restraining network and enhances the mechanical strength more in comparison to the kaolinite clay [185].

5.2.2 Scanning Electron Microscopy (SEM)

The physical and mechanical properties of the RPUF are remarkably affected by the morphology of the foams. Figure 5.3 shows the SEM images of the fractured surface of the rigid PU foam composites and reveals their cell structure. The neat PU foams showed cell size in the range of $400 \pm 20 \mu\text{m}$, while the incorporation of the mineral fillers decreased the cell size to $350 \pm 20 \mu\text{m}$ and $280 \pm 20 \mu\text{m}$ for the foams reinforced with 8% feldspar and 6% kaolinite clay, respectively. This behaviour is attributed to the fact that the fillers provide more nucleation sites for the bubble formation. In addition, the mineral fillers do not float easily with

the matrix, consequently, increasing the viscosity of the matrix while foaming, which causes the resistance to the increase in cell size.

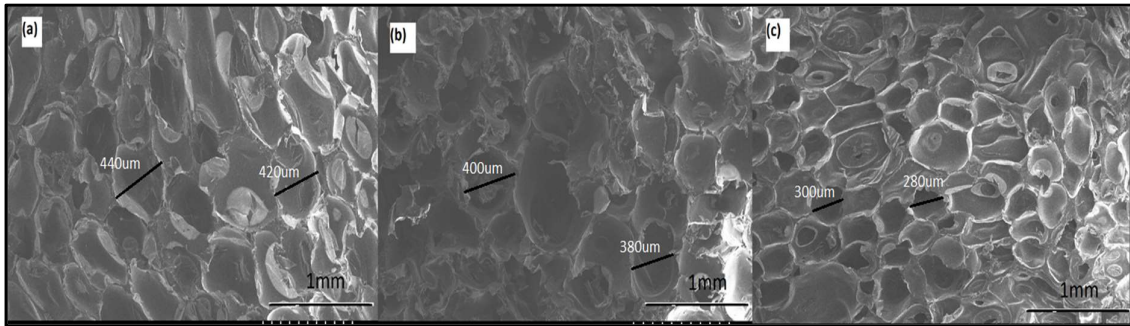


Figure 5.3: SEM Micrographs of the Foam Reinforced with (a) 0% Filler, (b) 8% Feldspar and (c) 6% Kaolinite Clay

Furthermore, the incorporation of the filler increases the viscosity of the reaction mixture, which prevents the bubble from being coalesced and consequently leading to the decrease in the cell size. The reduced cell size comes out with more packed foam structure that results in the increased foam density and mechanical strength, which is accredited to the availability of more struts per unit area of RPUF [86]. Increasing the concentration of the fillers beyond 8% for feldspar and 6% for the kaolinite clay deteriorates the cell structure, which is associated with the agglomeration of the mineral fillers after a certain concentration, due to the high viscosity of the matrix-filler premix.

5.2.3 Thermo-Gravimetric Analysis (TGA)

To evaluate the thermal stability of the prepared rigid foam composites, TGA is conducted under the flow of nitrogen. The TGA and DTG analysis of the mineral filler incorporated RPUF are illustrated in Figure 5.4 (a) to 5.4 (d) and the parameters are summarized in Table 5.1. The RPUFs showed two stages of weight loss, at 300 - 350°C and 450 - 500°C respectively. The first peak at around 300 - 350°C is attributed to the degradation of the urethane and urea linkages in the hard segments and the decomposition of the flexible

phase containing polyol. The second peak observed at 450 - 500°C is related to the thermolysis of the organic residues and the degradation of the soft segments [50].

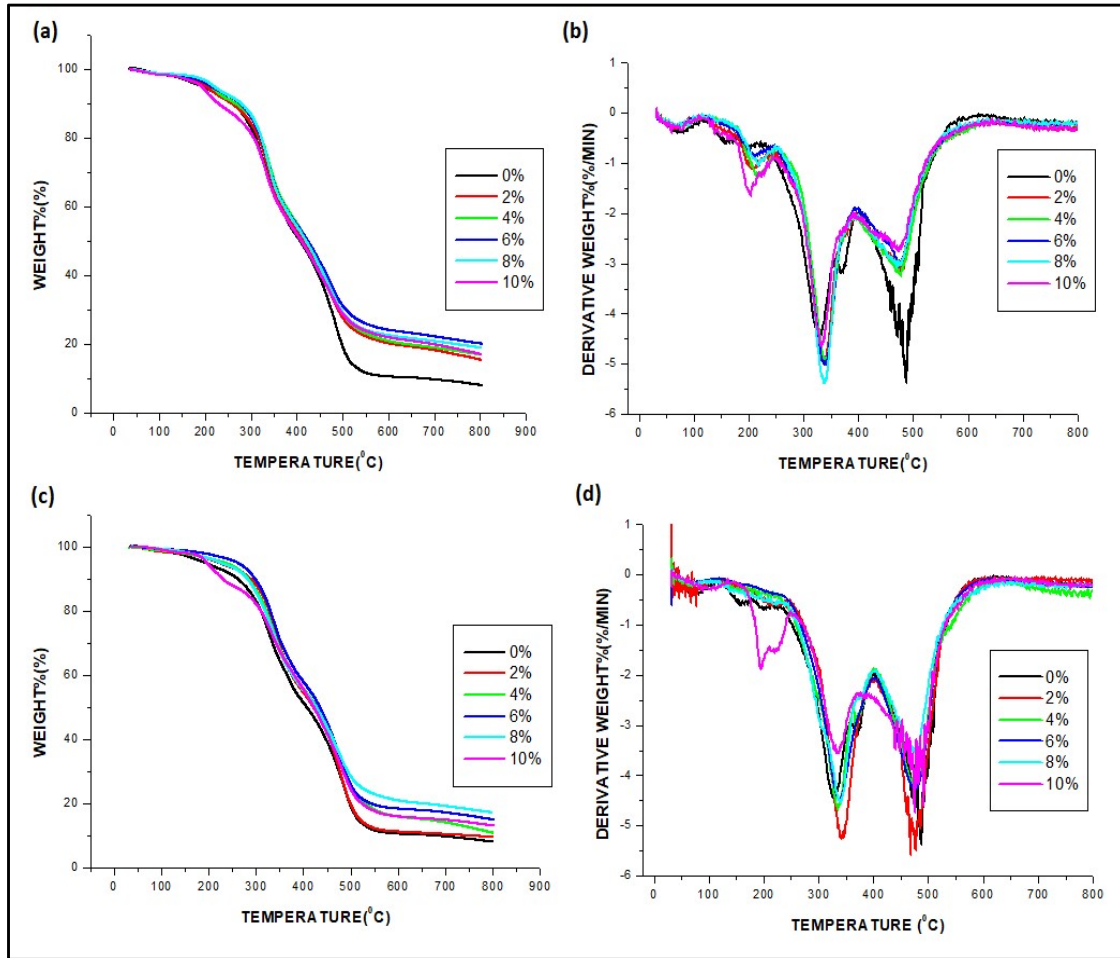


Figure 5.4: (a) TGA Curve of the RPUF Incorporated with Feldspar, (b) DTG Curve of RPUF Reinforced with Feldspar, (c) TGA Curve of RPUF Incorporated with Kaolinite Clay and (d) DTG Curve of RPUF Reinforced with Kaolinite Clay (Test conditions: Nitrogen atmosphere, Heating rate 10°C/min)

Conventionally, the thermal stability of the RPUFs is described by the temperatures of 5% weight loss ($T_{5\%}$), considered as the temperature for the onset of degradation [56]. The results showed that 5% weight loss temperature ($T_{5\%}$) increased from $192\pm 2^\circ\text{C}$ to $218\pm 2^\circ\text{C}$ for the foam with 8% feldspar and $260\pm 2^\circ\text{C}$ for the foam with 6% kaolinite clay, then again decreased due to the heterogeneity generated by the agglomeration of the filler at higher

concentration. T_{max1} increases slightly on the incorporation of the mineral filler, as the mineral fillers execute the function of the thermal barrier, which, prevents the rapid advancement of the heat and restricts the further degradation.

Table 5.1: Thermal Characteristics of RPUF Incorporated with Different Mineral Fillers

Concentration of Filler	$T_{5\%}$ (°C)±2	T_{Max1} (°C)±2	T_{Max2} (°C)±2	Residual Mass (%)±0.1
0%	192	330	488	8.1
2% Kaolinite Clay	220	344	467	9.5
4% Kaolinite Clay	233	335	474	10.9
6% Kaolinite Clay	260	339	476	15.0
8% Kaolinite Clay	224	341	477	17.3
10% Kaolinite Clay	196	335	475	13.1
2% Feldspar	202	339	480	15.5
4% Feldspar	212	342	478	16.9
6% Feldspar	212	337	475	18.1
8% Feldspar	218	337	470	18.9
10% Feldspar	190	332	473	17.1

Furthermore, bulk density of the foam material is increased by the exfoliation or the intercalation of kaolinite clay within the RPUF, which restricts the diffusion of volatile decomposition products within the RPUF consequently increasing the thermal stability of the foam. Owing to endothermic decomposition of the mineral fillers, they absorb heat and therefore keep the enclosing polymer cooler. Large aspect ratio of the kaolinite clay also

provides the more compact thermal barrier to the polymer chains. $T_{\max 2}$ decreases for the incorporation of kaolin due to the loss of water around 450°C, while feldspar does not decompose at this temperature so no visible changes were noticed in feldspar incorporated RPUF [186, 187]. For the foams with 10% concentration of the mineral filler, a degradation peak has been observed at around 200°C, which is attributed to the presence of the unreacted raw materials, owing to an incomplete reaction of the polyol with the polyisocyanate and the deterioration in the structure of the RPUF. The amount of residue produced was also found to be increased on increasing the filler concentration in RPUF, which supports early extinguish of the flame in real fire condition [188].

5.2.4 Cone Calorimeter Testing

Figure 5.5 and 5.6 show the fire behaviour of the RPUF composites containing varied concentration of the mineral fillers and relative data are summarized in Table 5.2. The cone calorimetry provides quantitative analysis of the fire behaviour of the foams. The heat release rate is considered as an indication to measure the intensity of the flame. The polyurethane foams exhibited two apparent heat release rate peaks: the first peak is attributed to the surface pyrolysis of foam and the release of flammable low molecular weight products, such as primary or secondary amines, isocyanates, alcohols and olefins, while the second one is probably due to the degradation of the previously formed charred protective layer and the release of the entrapped flammable gases [154]. The peak heat release rate (PHRR) decreased from 118±5 kW/m² to 89±5 kW/m² and 72±5 kW/m² on the incorporation of 8% kaolinite clay and 6% feldspar respectively, in comparison to the neat RPUF (Figure 5.5 (a) and 5.6(a)). This behaviour is probably due to the formation of a distended charred layer in the mineral filler incorporated foams, as, the protective char forms a barrier for the heat and mass transfer [152]. Furthermore, the mineral fillers decompose endothermically and release some non-flammable gases, which decreases the rate of heat release [153].

Table 5.2: Flammability Characteristics of the RPUF Incorporated with Mineral Fillers

Concentration of Filler	PHRR (kW/m²) ±5	THR (MJ/m²) ±0.5	TSR (m²/m²) ±10	Residue (%) ±0.5
0%	118	29.8	347	11.5
2% Kaolinite Clay	101	24.3	335	15.6
4% Kaolinite Clay	96	20.4	216	17.9
6% Kaolinite Clay	93	17.5	88	18.1
8% Kaolinite Clay	89	21.1	120	22.2
10% Kaolinite Clay	92	22.4	140	23.5
2% Feldspar	90	25.6	134	15.6
4% Feldspar	84	15.5	97	16.7
6% Feldspar	72	13.7	55	18.2
8% Feldspar	78	20.6	124	20.8
10% Feldspar	98	16.4	129	22.2

Figure 5.5 (b) and 5.6 (b) showed that the neat RPUF exhibited greater total heat release (THR) than the foams with mineral fillers and the 6% feldspar incorporated foam showed minimum THR amongst all the samples. This indicates that the mineral fillers prevent the heat transfer, consequently protecting the material beneath the charred layer from further burning. The formation of residue is another important parameter to quantify the fire properties. The incorporation of the mineral fillers increased the amount of the residue from 11.5±0.5% to 23.5±0.5% and 22.2±0.5% for the RPUF containing maximum filler concentration of 10% kaolinite clay and 10% feldspar, respectively. The higher residue for the filler incorporated

foams is probably due to the formation of more residue from the endothermal decomposition of the mineral fillers [153].

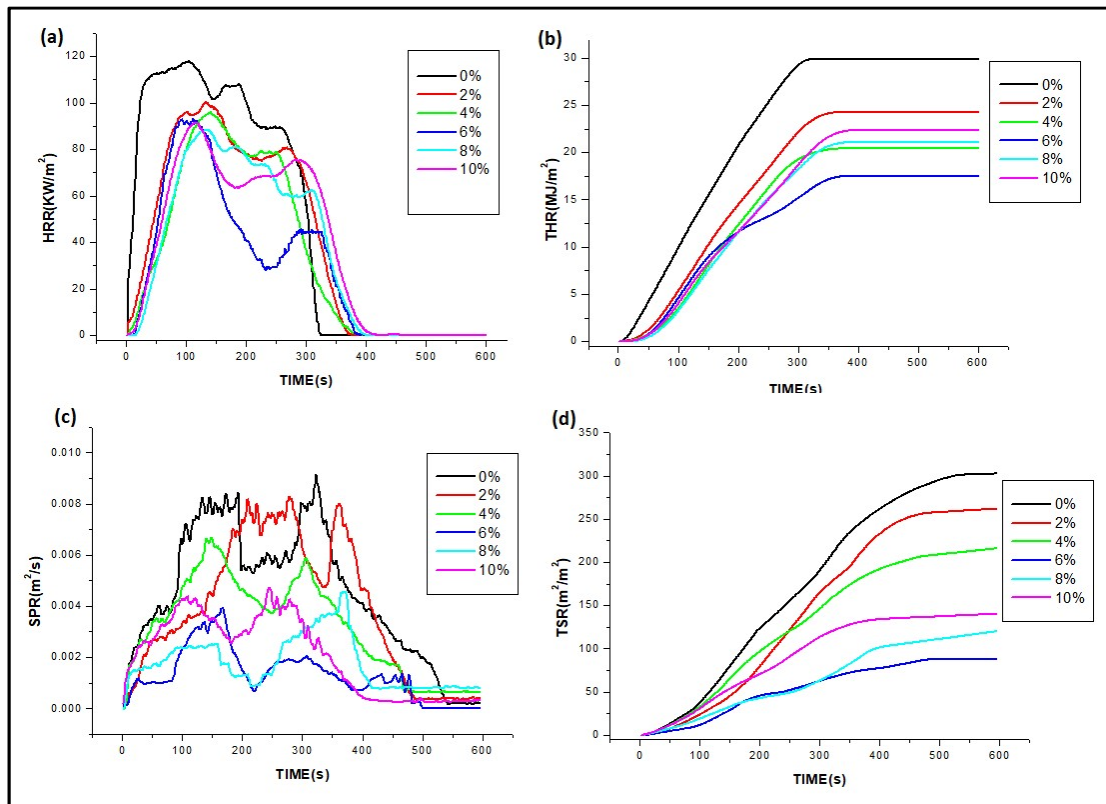


Figure 5.5: (a) HRR (Heat Release Rate), (b) THR (Total Heat Release), (c) SPR (Smoke Production Rate) and (d) TSR (Total Smoke Release) of the RPUFs Incorporated with Kaolinite Clay (Test conditions: incident heat flux of 35kW/m²)

Incorporation of the mineral fillers decreases the release of the toxic gases such as carbon monoxide, carbon dioxide and others. The feldspar starts to melt and decompose at 1150°C, while the kaolinite clay dehydrates at a temperature around 450°C to give metakaolinite, which turns into mullite and the amorphous silica on the heating above 1000°C, which, supports the high temperature performance of the mineral fillers and reduces the flammability of the RPUF [186, 187]. The smoke production is the another important parameter to evaluate the fire behaviour of any material, which is determined by the smoke production rate (SPR) and the total smoke release (TSR).

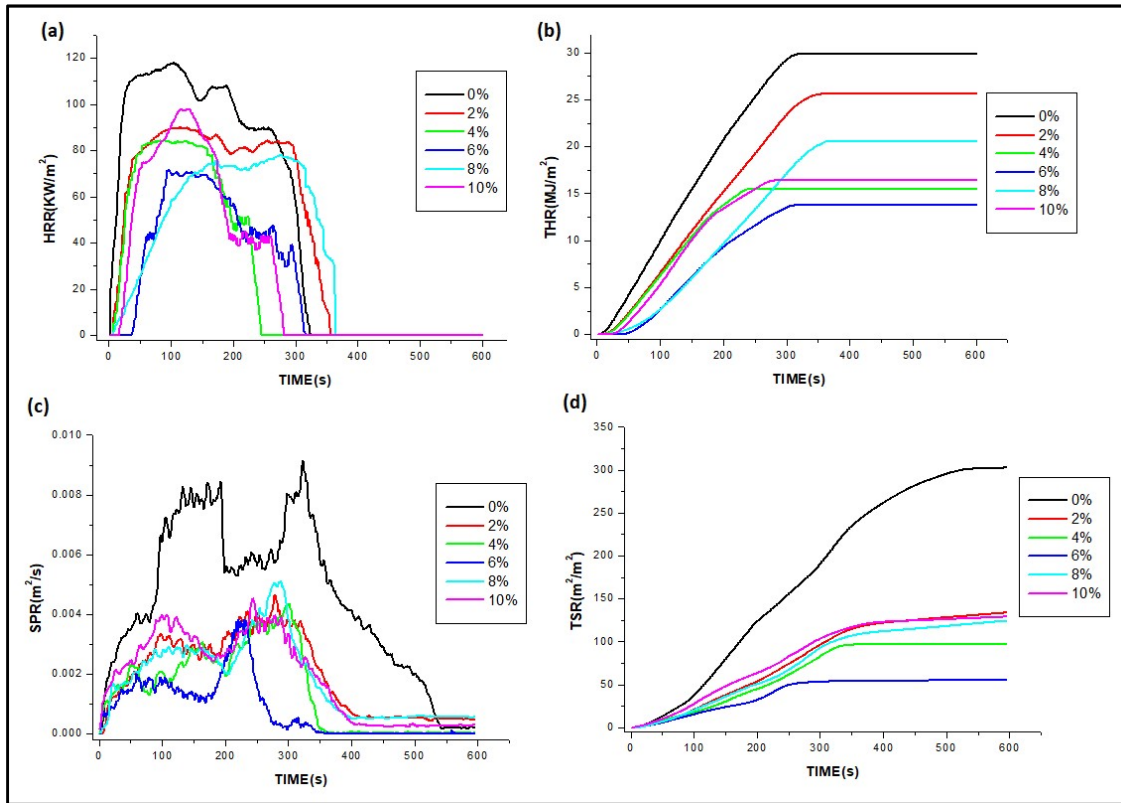


Figure 5.6: (a) HRR (Heat Release Rate), (b) THR (Total Heat Release), (c) SPR (Smoke Production Rate) and (d) TSR (Total Smoke Release) of RPUFs Incorporated with Feldspar (Test conditions: incident heat flux of 35kW/m²)

Figure 5.5 (c) and 5.6 (c) show the rate of the smoke production, which exhibits the similar trend as shown by the HRR. The smoke production rate corresponding to the first peak, decreased from 0.008 to 0.004 m²/s and 0.003 m²/s for the foams with 6% kaolinite clay and 8% feldspar respectively. The TSR of these foams were decreased to 88±10 m²/m² and 55±10 m²/m² for 6% feldspar and 6% kaolin respectively, in comparison to 347±10 m²/m² for the neat foam (Figure 5.5 (d) and 5.6 (d)). This behavior of the RPUFs attributes to the denser structure of the charred layer which restricts the spread of the flame and diluted the gas phase. The smoke suppression is attributed to the generation of the charred protective layer that, hinders the release of the smoke.

As the mineral fillers are non-combustible fillers, the incorporation of these fillers reduces the flammability of RPUF, by reducing the total amount of the flammable materials, as well as, by hindering the rate of diffusion of oxygen. The performance of the filler in flame retardancy application is highly dependent on the compatibility of the filler and the heat absorbed by it during the decomposition. Owing to the endothermic decomposition of the kaolinite clay, the heat required to vaporise the same amount of the polymeric mass is increased, additionally the existence of the gas phase flame diluents (e.g. water) also tend to reduce the temperature of the flame, consequently, reducing the fraction of the heat transmitting to the foam. Since, a critical concentration of the free radicals is required for the self-sustaining flame. So, the flame can be extinguished by reducing the concentration of the free radicals, which, is performed by the release of water in the decomposition of the kaolinite clay [153, 186].

As, feldspar deposits as inert layer on the surface of the decomposing RPUF, due to its non-combustible behaviour, it prevents the incoming radiation and oxygen reaching the decomposing RPUF, as well, restricts the release of the flammable pyrolysis products and smoke to the gas phase [187].

5.3 RPUF INCORPORATED WITH CALCIUM CARBONATE NANOPARTICLES

Apart from the feldspar and kaolinite clay, calcium carbonate nanoparticles were also prepared and incorporated in the RPUF. The characterization of the prepared nanoparticles is summarized in the following section:

5.3.1 FTIR Analysis

Figure 5.7 shows the FTIR spectra of the prepared calcium carbonate nanoparticles. It confirms the formation of the aragonite structure of the calcium carbonate. The FTIR spectra of the calcium carbonate nanoparticles shows peaks at 712.6, 858, 1082.5, and 1485.1 cm^{-1}

respectively, attributed to the in-plane bending vibration, the out-of-plane bending vibration, the symmetric stretch, and the asymmetric stretch of CO_3^{2-} , which is characteristic for the aragonite crystal structure. The band located at 1787 cm^{-1} was assigned to the vibrations of the $\text{C}=\text{O}$ stretching. Moreover, the peaks of OH (3433.5 cm^{-1}) and C–H stretching (2921.4 cm^{-1}), as the organic matrix characteristics and the peak of HCO_3^- (2526 cm^{-1}) were confirmed. Since the carbonate ions and the similar molecules have four normal modes of vibration peaks, symmetric stretching, out-of-plane bending, doubly degenerate planar asymmetric stretching and doubly degenerate planar bending, the spectral data obtained for the samples reveal a broad absorption peak at $\sim 1485\text{ cm}^{-1}$, $\sim 1082\text{ cm}^{-1}$, $\sim 1788\text{ cm}^{-1}$, $\sim 856\text{ cm}^{-1}$, and $\sim 713\text{ cm}^{-1}$, which have been reported to be the common characteristic features of the carbonate ions in the calcium carbonate, and are the fundamental modes of vibration for this molecule. The peak at 1082.5 cm^{-1} was only observed in the spectrum of aragonite-phase calcium carbonate, is in accordance with that reported in the literature [85].

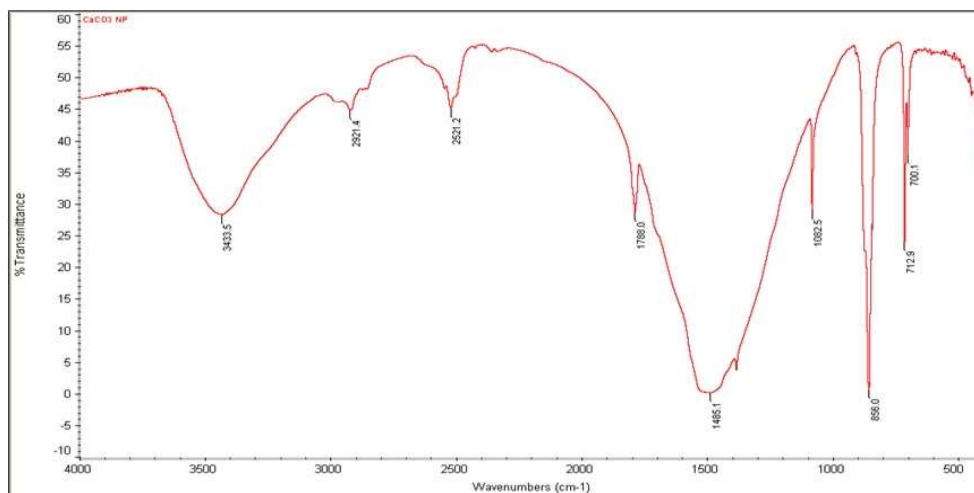


Figure 5.7: FTIR Spectra of the Prepared Calcium Carbonate Nanoparticles

5.3.2 Transmission Electron Microscopy

Figure 5.8 shows the TEM analysis of the calcium carbonate nanoparticles. The results showed that the particle size of the prepared nanoparticles was in the range of 250 nm. In addition, the shape of the nanoparticles was needle like, which confirms the aragonite structure

of the nanoparticles. It was also found that the particles formed were of uniform size and shape [153].

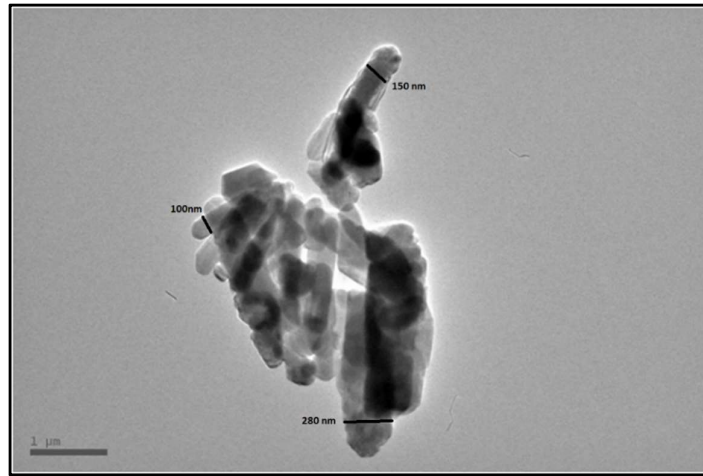


Figure 5.8: TEM Analysis of the Calcium Carbonate Nanoparticles

5.3.3 XRD Analysis

Figure 5.9 demonstrates the XRD pattern of calcium carbonate nanoparticles, and by comparing the XRD graph obtained from literature, aragonite structure of the calcium carbonate is confirmed.

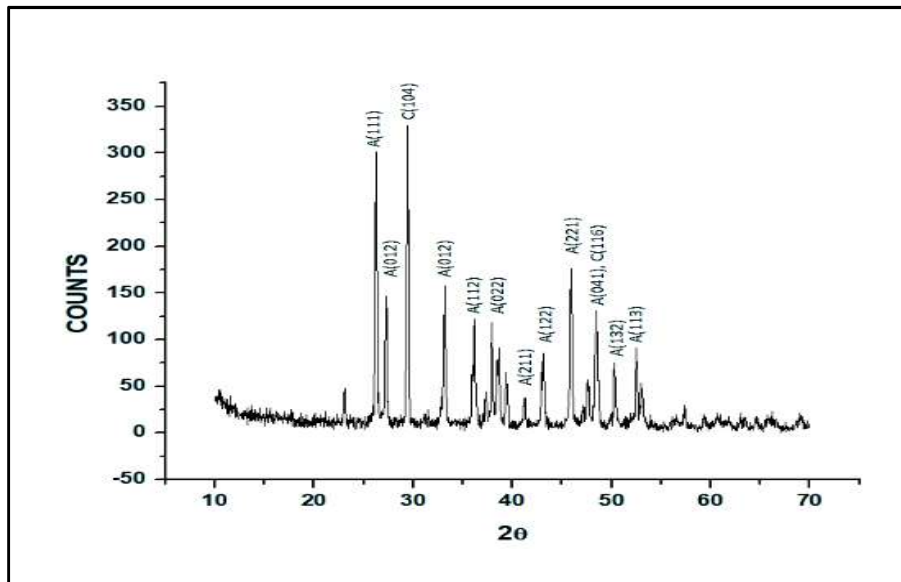


Figure 5.9: XRD Pattern of the Calcium Carbonate Nanoparticles

5.3.4 Scanning Electron Microscopy (SEM)

The scanning electron microscopy gives an idea about the cell structure of the rigid PU foam. Figure 5.10 shows the SEM images of the internal structure of the rigid polyurethane foams incorporated with calcium carbonate nanoparticles. As evident, the neat PU foams show pore size in the range of 400 μm , while with the incorporation of 2% CaCO_3 nanoparticles increases the pore size up to 600 μm , which may be explained by the poor dispersion of the CaCO_3 nanoparticles in the PU matrix. Again on increasing the filler concentration, the pore size starts to decrease due to the more nucleation sites available for the bubble formation. In addition, the solid filler are difficult to flow, thus causing resistance to the increase in the pore size [135].

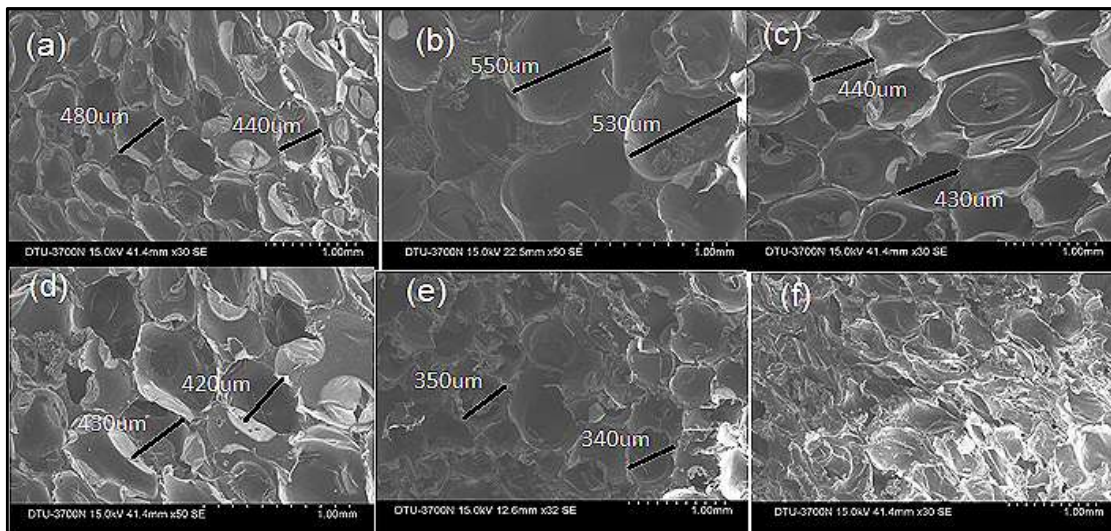


Figure 5.10: SEM Micrographs of the RPUF with (i) 0%, (ii) 2%, (iii) 4%, (iv) 6%, (v) 8% and (vi) 10% Concentration of the CaCO_3 Nanoparticles.

5.3.5 Thermo-Gravimetric Analysis (TGA)

TGA of RPUF incorporated with calcium carbonate nanoparticles is conducted under the flow of the nitrogen to analyze the thermal stability of these foams. Figure 5.11 shows the thermogravimetric analysis results of the foams prepared by the incorporation of the calcium

carbonate nanoparticles. Results show that the 5% weight loss temperature ($T_{5\%}$) increases from 218°C to 284°C for the foam with 8% nanoparticles concentration, then again decreases due to the poor dispersion of the filler, at higher concentration. The char residue also increases on increasing the CaCO_3 nanoparticles, which shows early extinguish of the flame in real fire conditions. It also aids in the thermal stability of the resulted RPUF.

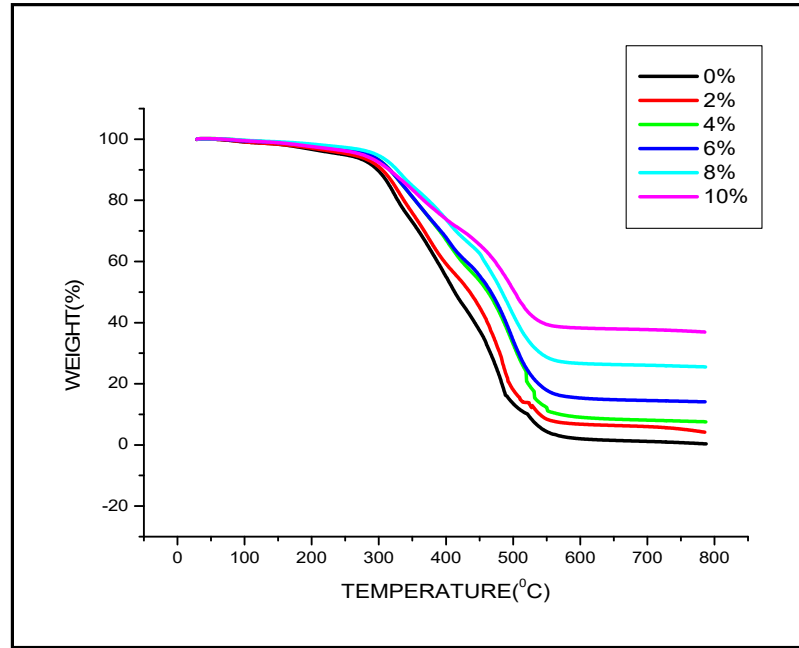


Figure 5.11: TGA Plots of the RPUF Incorporated with CaCO_3 Nanoparticles (Test conditions: Nitrogen atmosphere, heating rate 10°C/min)

5.3.6 Cone Calorimeter Testing

Figure 5.12 show the fire behaviours of the calcium carbonate nanoparticles filled RPUFs, measured by the cone calorimetry. The results are also summarized in Table 5.3. The cone calorimetry gives quantitative analysis of the flammability and smoke emission of the materials. The time to ignition (TTI) increased from 2 s for the neat RPUF to 10 s for the calcium carbonate nanoparticles incorporated foams.

HRR is considered as an indicator for quantifying the severity of the fire [154]. The Figure 5.12 (a) shows the trends in the heat release rate of RPUF incorporated with calcium

carbonate nanoparticles. It was concluded that, the peak heat release rate (PHRR) decreased from 118 kW/m² to 93 kW/m² for the foam incorporated with 8% concentration of calcium carbonate nanoparticles. The HRR graph shows mainly two peaks, the first peak is originated due to the surface pyrolysis of the RPUF, while, the second peak is attributed to the collapse of the charred structure and the burning of the material beneath. Figure 5.12 (b) shows that the neat RPUF demonstrated higher total heat release (THR) in comparison to the foams incorporated with calcium carbonate nanoparticles, which is attributed to the endothermic decomposition and non-reactivity of the mineral fillers.

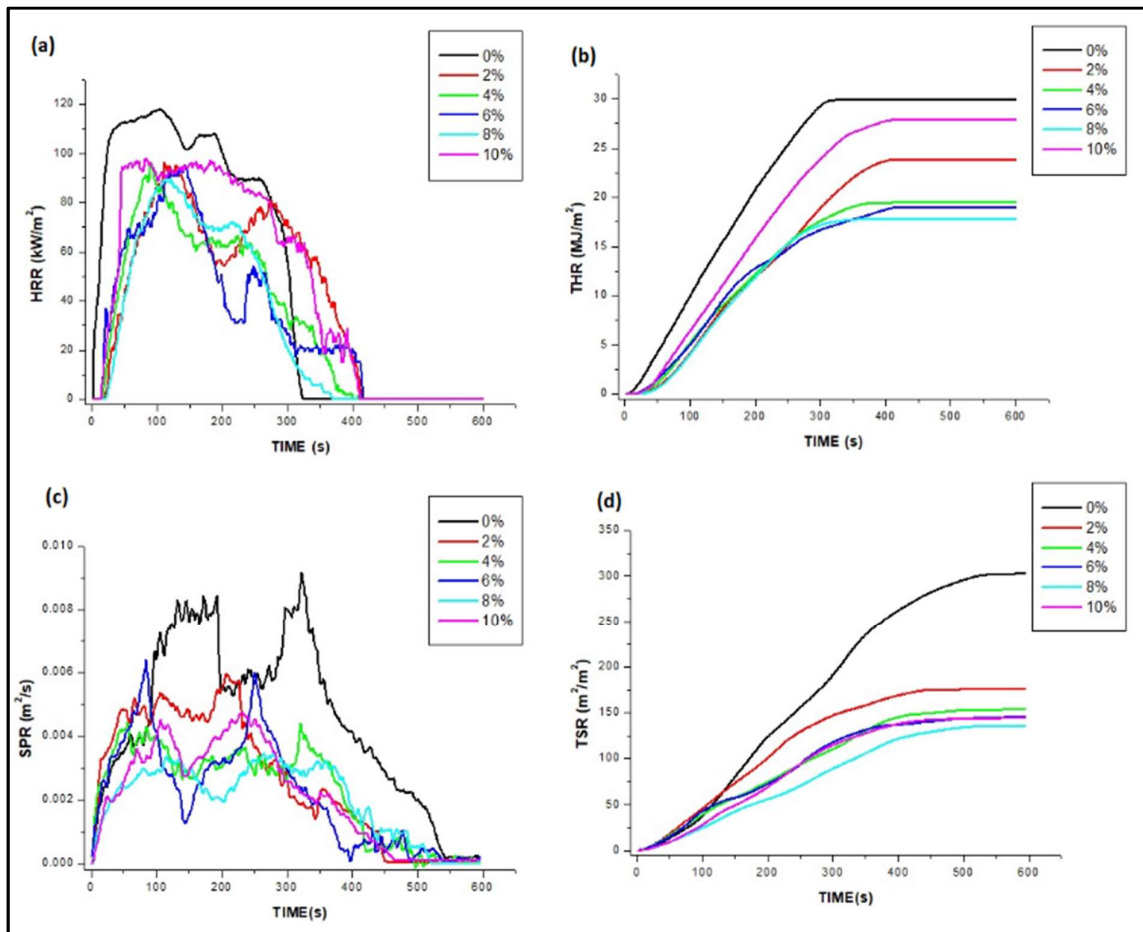


Figure 5.12: (a) HRR (Heat Release Rate), (b) THR (Total Heat Release), (c) SPR (Smoke Production Rate) and (d) TSR (Total Smoke Release) of RPUFs Incorporated with CaCO₃ Nanoparticles (Test conditions: incident heat flux of 35kW/m²)

The smoke emission behaviours of the neat RPUF and the calcium carbonate nanoparticles incorporated foams were characterized by the smoke production rate (SPR) and the total smoke release (TSR). It was clearly seen from the Figure 5.12 (c) and 5.12 (d) that, the addition of the calcium carbonate nanoparticles shows remarkable reduction in the SPR, as well as, TSR. The reduction in the smoke emission, on the incorporation of the filler is accredited to the dilution of the gas phase by the release of small molecules such as water vapours as well as by the occurrence of the non-reactive barrier by mineral fillers [153].

Table 5.3: Cone Calorimeter Data of the RPUFs Incorporated with the Calcium Carbonate Nanoparticles

Concentration of Filler	PHRR (kW/m²)±5	THR (MJ/m²)±0.5	TSR (m²/m²)±10	TTI (s)
0%	118	29.8	303	2
2% CaCO₃	105	23.8	176	6
4% CaCO₃	102	19.4	154	7
6% CaCO₃	98	18.9	145	8
8% CaCO₃	93	17.7	135	10
10% CaCO₃	104	27.8	144	8

5.4 SIGNIFICANT FINDINGS

Rigid PU foams were prepared by incorporating different mineral fillers to enhance the mechanical, thermal and flame retardant properties of the foams. The experimental results showed that the RPUF incorporated with 8% feldspar demonstrated maximum compressive strength of 4.98 MPa, which is 182% greater than that of the unreinforced RPUF. The thermal stability and flame retardancy of the foams were also found to be improved on the addition of the mineral fillers. The RPUF incorporated with clay demonstrated the best thermal properties and showed an increase in the 5% weight loss temperature from 192°C to 260-270°C. The char

residue was also found to be increased from 8 wt% to 16 wt% on the incorporation of the mineral fillers. Cone calorimeter test of the RPUF with varied concentrations of the mineral fillers demonstrated a fair enhancement in the flame retardancy of the RPUF, and among all the samples, the best properties were shown by the foams with 6% concentration of any of the mineral filler. Of these fillers, feldspar showed higher flame retardancy, that suggests its better fire performance among the mineral filler studied in this research. The 8% feldspar showed the best mechanical properties but, the thermal properties as well as the fire performance deteriorated on the incorporation of 8% feldspar. This behaviour is accredited to the fact that the agglomeration of the filler commences at 8% concentration of the filler, but the cellular structure of the foam is not affected considerably as evident from the SEM micrographs. The thermal and fire performance starts to deteriorate due to the lesser barrier effect of the filler, resulting from the filler agglomeration. The presence of the more concentration of the filler in the cell walls of RPUF strengthens the structure, consequently, increasing its compressive strength. The cone calorimetry shows an improvement in the fire performance of the rigid polyurethane foam incorporated with CaCO_3 nanoparticles. The HRR increases from 118 kW/m^2 to 93 kW/m^2 for the foams with 8% concentration of filler. Total heat release (THR), smoke production rate (SPR) and total smoke release (TSR) were also found to reduce on the addition of CaCO_3 nanoparticles. As the substitution of petroleum based feedstock with agricultural oils for the production of polymers is a potential field of research and the improvement of their properties is the need of the hour, this study shows that the incorporation of the mineral fillers improves the mechanical, thermal and flame retardant properties of vegetable oil based rigid PU foams, so, the mineral fillers may be utilized as unique flame retardant, with good mechanical and thermal properties. These mineral fillers incorporated RPUFs may be used for the fire safety applications in buildings, for carving models & prototypes.

CHAPTER 6

DEVELOPMENT OF THE METALLIC FILLER REINFORCED RPUF AND OPTIMIZATION OF THE REINFORCING FILLER COMPOSITION

6.1 INTRODUCTION

During past few decades, the rigid polyurethane foams (RPUFs) have been the subject of intense research due to a wide range of applications in construction & refrigeration industry, prototypes and industrial patterns [29, 96, 177]. Commercially, polyurethane (PU) foam is prepared by the reaction of polyol with polyisocyanate, which are the petroleum based raw materials. A lot of studies have been executed for the preparation of PU foam using the polyols derived from different vegetable oils, and reinforced with different natural and synthetic fillers [27, 97, 154]. Although various studies have already been reported on the castor oil based polyurethanes, and their reinforced with different fillers for the enhanced mechanical and thermal properties [173, 189], but still the literature is devoid of investigations on castor oil based RPUF reinforced with metallic fillers such as copper, iron and others. Of these, copper powder may be used to impart good mechanical and thermal properties, in castor oil based RPUF [176]. The present study investigates the influence of the copper powder in RPUF.

6.2 RESULTS AND DISCUSSION

6.2.1 Compressive Strength Measurement

Figure 6.1 shows the changes in the compressive strength, specific compressive strength and the density of RPUF on the incorporation of the metallic fillers. The unique material characteristics shown by the metallic filler are the results of the strong ionic interatomic bonds. The copper powder reinforced RPUF showed an increase in compressive strength up to 3.83 MPa on the addition of 8% copper powder, as compared to 1.77 MPa for the unreinforced

polyurethane foam. As the strength of the copper powder filler is higher than that of the RPUF matrix, so the copper powder filler can dissipate the load of the polymer matrix and act as a barrier for the growth of the fracture. When a growing fracture meets a copper powder particle, the dissipation of the energy at the filler site prevents the fracture converting into an unstable one, consequently increasing the toughness of the foam.

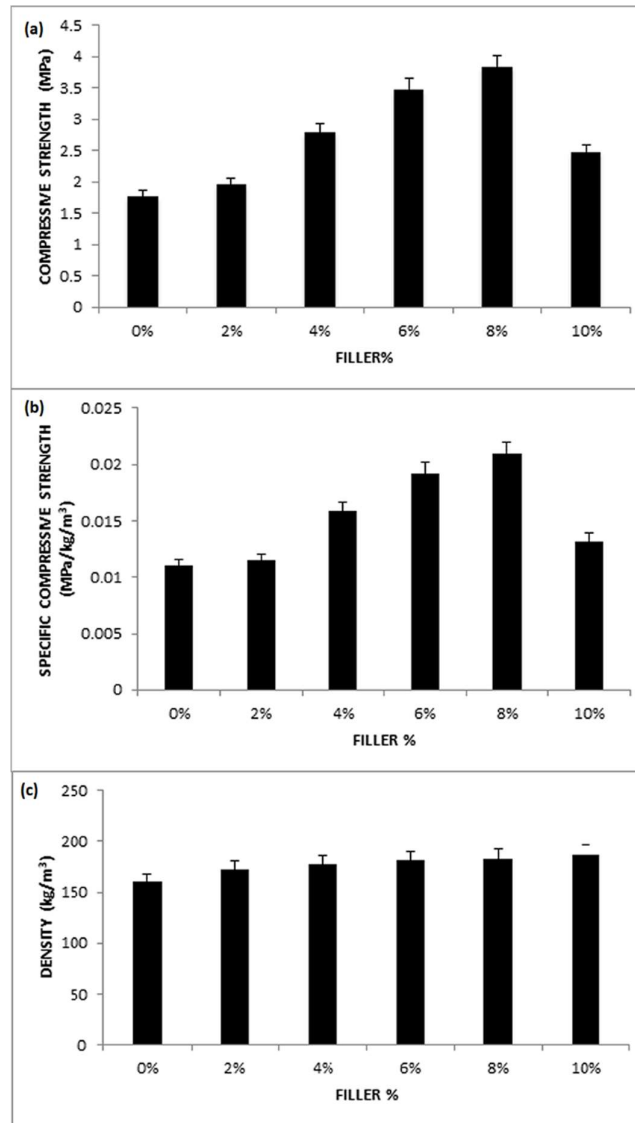


Figure 6.1: Plots of (a) Compressive Strength vs. Concentration of Copper Filler, (b) Specific Compressive Strength vs. Concentration of Copper Filler and (c) Density vs. Concentration of Copper Filler

6.2.2 Thermo-Gravimetric Analysis (TGA)

To evaluate the thermal stability of the RPUF incorporated with the copper powder, the TGA is conducted under the flow of nitrogen. The TGA analysis of the metallic filler incorporated RPUF are illustrated in Figure 6.2 and the results are summarized in Table 6.1. The results indicated that the thermal properties enhanced on the incorporation of the copper powder. The maximum char residue is observed for the copper filled foams, at 10% filler concentration. Usually, the thermal stability of the RPUFs is characterized by the temperatures of the 5% weight loss ($T_{5\%}$), considered as the temperature for the onset of degradation [56]. It is seen that, the 5% weight loss temperature increases from 192°C to 257°C by the incorporation of the copper powder from 0% to 8%. This behaviour of the metallic filler reinforced RPUF may be accredited to the better thermal properties and high temperature performance of the copper powder filler.

Table 6.1: Thermal Characteristics of the RPUF Incorporated with the Metallic Fillers

Concentration of Filler	$T_{5\%} \pm 2$ (°C)	$T_{Max1} \pm 2$ (°C)	$T_{Max2} \pm 2$ (°C)	Residual Mass ± 0.05 (%)
Neat PU with 0% Copper	192	330	488	8.08
2% Copper	245	335	476	10.99
4% Copper	248	337	475	12.02
6% Copper	253	338	479	13.20
8% Copper	257	340	475	14.37
10% Copper	256	334	480	15.00

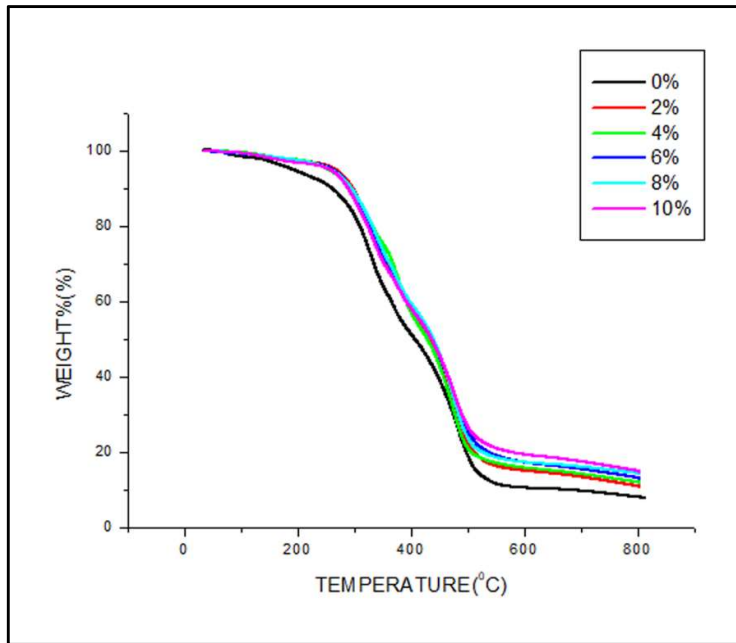


Figure 6.2: TGA Curves of the Neat and the Copper Powder Reinforced RPUF (Test conditions: Nitrogen atmosphere, heating rate 10°C/min)

6.2.3 Cone Calorimeter Testing

Figure 6.3 (a) to 6.3 (d) show the plots of the cone calorimeter experiment performed on the RPUF containing varied concentration of the metallic filler and data are summarized in Table 6.2. Conventionally, the intensity of the fire is correlated with the heat release rate (HRR) and total heat release (THR) [151, 152]. Figure 6.3 (a) shows that the peak heat-release rate (PHRR) is decreased from 118 kW/m² to 93 kW/m² on the incorporation of 8% copper powder in the RPUF. Fig. 6.3 (b) shows that the total heat release (THR) also decreases from 29.8 MJ/m² to 17.0 MJ/m² on the incorporation of the copper fillers. Figure 6.3 (c) reveals the smoke production rate (SPR) and the first peak of SPR indicates that the smoke production decreased from 0.008 to 0.004 m²/s for the introduction of 8% copper powder. The total smoke release (TSR) also decreases from 302 m²/m² to 141 m²/m² for 8% copper powder filling (Figure 6.3 (d)).

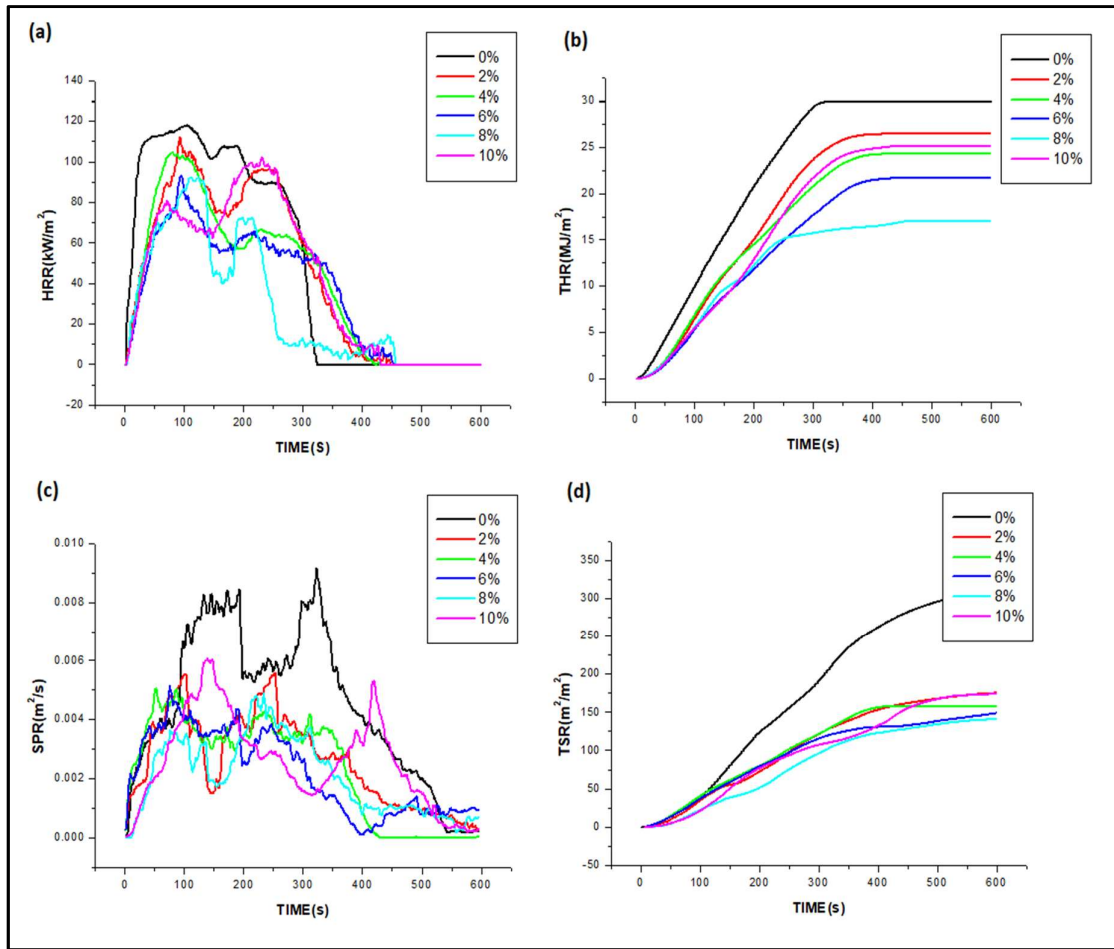


Figure 6.3: (a) HRR (Heat Release Rate), (b) THR (Total Heat Release), (c) SPR (Smoke Production Rate) and (d) TSR (Total Smoke Release) of RPUFs Incorporated with Copper Powder (Test conditions: incident heat flux of 35kW/m²)

The results are accredited to the fact that the formation of the metallic protective layer hinders the flame spread, release of the flammable by-products and toxic smoke. It is concluded that the RPUF incorporated with 8% copper powder shows the best mechanical, thermal and flame retardant properties among all the other formulations studied in this project, for which the **patent has been applied by Delhi Technological University, Application no.: 201911027962**, and the same is used for performing the drilling experiments to ascertain the machining ability of the foams.

Table 6.2: Cone Calorimeter Data of the RPUF Incorporated with the Metallic Fillers

Concentration of Filler	PHRR (kW/m ²) ±5	THR (MJ/m ²) ±0.5	TSP (m ² /m ²) ±10	Residue (%) ±0.5
0%	118	29.8	347	11.5
2%	114	26.5	175	28.7
4%	105	24.2	158	38.9
6%	97	21.7	148	47.5
8%	93	16.9	141	51.8
10%	104	25.0	173	38.5

Table 6.3: Data for Optimization of the Filler Concentration

Sample ID	Compressive Strength (MPa)	Flexural Strength (MPa)	Density (kg/m ³)	T _{5%}	PHRR (kW/m ²)	THR (MJ/m ²)	TSR (m ² /m ²)
0% Filler	1.77	0.79	160	192	118	29.8	302
8% CaCO ₃	2.45	1.39	216	296	93	17.7	134
6% Alumina	3.56	1.60	213	251	84	13.2	137
6% Clay	3.01	3.558	223	260	93	17.5	88
8% Feldspar	4.98	2.697	231	218	78	20.6	124
6% Zirconia	6.61	5.717	257	265	94	19.2	130
8% Carbon Fibre	6.875	2.966	486	136	85	18.2	116
8% Copper	3.83	4.717	183	257	93	16.9	141
Commercial Foam (FR-7112)	2.76	3.45	192	260	No data available	No data available	No data available
Commercial Foam (FR-7115)	3.489	4.544	240	265	No data available	No data available	No data available

6.2.4 Optimization of the Filler Concentration

To optimize the concentration of the filler showing the best mechanical, thermal and flame retardant properties, all the data with the concentration of each filler showing best combination of properties, is summarized in Table 6.3.

6.3 SIGNIFICANT FINDINGS

The rigid PU foams were prepared by incorporating the copper powder in varied concentration and the mechanical, flame retardant and thermal properties of the resulted foam were studied. The incorporation of the copper filler enhanced the mechanical properties of the vegetable oil based foam. The 5% weight loss temperature increased from 192°C to 257°C for the 8% copper powder filled RPUF. It was concluded from the analysis of the data for the optimization of the filler concentration, that the RPUF with 8% copper powder filler demonstrated the best combination of mechanical, thermal and flame retardant properties, with the density comparable with the commercial RPUF.

CHAPTER 7

RESPONSE SURFACE METHOD FOR THE EVALUATION AND OPTIMIZATION OF THE DRILLING PARAMETERS FOR THE BIO- BASED RPUF COMPOSITES

7.1 INTRODUCTION

From the analysis of the data for the optimization of the filler concentration, It has been concluded that the RPUF incorporated with 8% copper powder shows the best mechanical, thermal and flame retardant properties among all the other formulations studied in this research, so the same formulation is used for performing the drilling experiments, to ascertain the machining ability of the foams. This chapter investigates the influence of the drilling parameters, i.e. feed rate, drill diameter, spindle speed and density of RPUF, on the residual compressive strength, thrust force and delamination of the copper powder reinforced RPUF. The response surface method based approach has been employed to accomplish the optimized parameters for the drilling of the RPUF. Figure 7.1 shows the images of samples employed for the drilling test.



Figure 7.1: Samples Used for Drilling Test



Figure 7.2: Drilled Holes after Performing Drilling Test at Various Factor Levels

7.2 RESULTS AND DISCUSSION

Drilling-induced damages and consequently residual compressive strength is controlled by the thrust force, which is believed to have a threshold value after which the delamination occurs. According to the literature, exit side of the drilled specimen presents more severe delamination in the composite materials, so the images of the holes were obtained at the exit

side of the specimen. The maximum and the nominal diameters of the drilled holes were measured using an image processing software, image j. Figure 7.2 shows the images of the drilled holes after performing the drilling test at various factor levels.

Residual compressive strength was determined as the force per unit section area remaining after drilling,

$$\sigma_r = \frac{F}{(l - d)t}$$

where F , t , d , and l are the force applied at 10% compression, specimen thickness, hole diameter and the specimen width, respectively. To conduct the experiments, central composite design model was used. The details of the experiment design and obtained results of the thrust force, delamination and the residual compressive strength are presented in Table 7.1.

Table 7.1: Experimental Results for Drilling of RPUF Composites

Std	Run	Density (kg/m ³)	Spindle Speed (rpm)	Feed Rate (mm/rev)	Drill Diameter(mm)	Thrust(N)	Delamination	Residual Compressive Strength(MPa)
1	6	302.5	342	0.34	6	14.70	1.27	3.81
2	28	387.5	342	0.34	6	35.45	1.19	4.56
3	5	302.5	914	0.34	6	20	1.22	4.35
4	15	387.5	914	0.34	6	45.62	1.15	6.45
5	21	302.5	342	0.78	6	15.23	1.31	3.86
6	25	387.5	342	0.78	6	35.34	1.26	5.1
7	23	302.5	914	0.78	6	15.38	1.20	3.78
8	1	387.5	914	0.78	6	35.32	1.14	5.96
9	13	302.5	342	0.34	10	18.36	1.18	1.89

10	19	387.5	342	0.34	10	35.56	1.12	4.2
11	11	302.5	914	0.34	10	32.56	1.09	2.96
12	14	387.5	914	0.34	10	46.68	1.05	6.5
13	10	302.5	342	0.78	10	26.95	1.18	2.26
14	18	387.5	342	0.78	10	42.92	1.16	4.87
15	4	302.5	914	0.78	10	36.53	1.06	2.2
16	12	387.5	914	0.78	10	48.54	1.02	6.2
17	2	260	628	0.56	8	17.54	1.29	2.28
18	7	430	628	0.56	8	52.38	1.19	7.2
19	24	345	56	0.56	8	20.73	1.19	3.22
20	30	345	1200	0.56	8	39.56	1.03	5.12
21	26	345	628	0.12	8	30.67	1.13	4.5
22	8	345	628	1	8	32.85	1.14	4.12
23	29	345	628	0.56	4	17.89	1.3	4.98
24	16	345	628	0.56	12	36.98	1.07	3.12
25	22	345	628	0.56	8	28.84	1.09	3.54
26	9	345	628	0.56	8	28.72	1.08	3.19
27	3	345	628	0.56	8	33.91	1.09	3.24
28	27	345	628	0.56	8	29.82	1.06	2.5
29	17	345	628	0.56	8	28.09	1.09	3.17
30	20	345	628	0.56	8	31.01	1.13	3.26

The efficiency of the developed regression models has been established by assessing the level of significance for the model, as well as, lack of fit. It was concluded from the fit summary that the quadratic model is the most efficient model for anticipating the effect of the drilling parameters on the residual compressive strength of the RPUF composite. The ANOVA and the fit statistics for the thrust force, delamination and residual compressive strength are shown in Table 7.2, 7.3 and 7.4 respectively and the effect of the drilling on the responses is summarized in the subsequent sections.

7.2.1 Thrust Force Analysis

The plots for actual versus predicted thrust force, the delamination and the residual compressive strength are shown in Figures 7.3, 7.4 and 7.5 respectively, which signifies that the values of the response predicted by the developed quadratic model fit well with the actual values of the responses and suggests a good correlation between the experimental values and the developed quadratic model.

ANOVA of the reduced quadratic model for the thrust force is summarized in the Table 7.2. The significance of the model is established by the F-value of the model, as well as, the lack of fit, which are 93.32 and 0.72 respectively. The p-value for the model is less than 0.05, which establishes the statistical significance of the model at 95% confidence interval. The difference of less than 0.2 between the predicted R^2 (0.9519) and the adjusted R^2 (0.9663) values shows that the developed quadratic model suggests an appropriate relationship between the drilling parameters and the responses. Adequate precision provided by the model is above 35, which ascertains the significance of the model in terms of signal to noise ratio.

Table 7.2: ANOVA and Fit Statistics for Thrust Force on RPUF Composite

Source	Sum of Squares	df	Mean Square	F-value	p-value	
Model	3058.96	9	339.88	93.32	< 0.0001	Significant
ρ -Density	1933.21	1	1933.21	530.78	< 0.0001	
v -Spindle Speed	366.45	1	366.45	100.61	< 0.0001	
f -Feed Rate	5.65	1	5.65	1.55	0.2275	
d -Drill Diameter	497.22	1	497.22	136.52	< 0.0001	
ρd	45.97	1	45.97	12.62	0.0020	
vf	40.51	1	40.51	11.12	0.0033	
vd	38.81	1	38.81	10.66	0.0039	
fd	82.26	1	82.26	22.59	0.0001	
ρ^2	48.87	1	48.87	13.42	0.0015	
Residual	72.84	20	3.64			
Lack of Fit	49.90	15	3.33	0.7248	0.7132	Not Significant
Pure Error	22.95	5	4.59			
Cor Total	3131.80	29				
Std. Dev.	1.91				R²	0.9767
Mean	31.14				Adjusted R²	0.9663
C.V. %	6.13				Predicted R²	0.9519
PRESS	150.75				Adequate Precision	35.9585

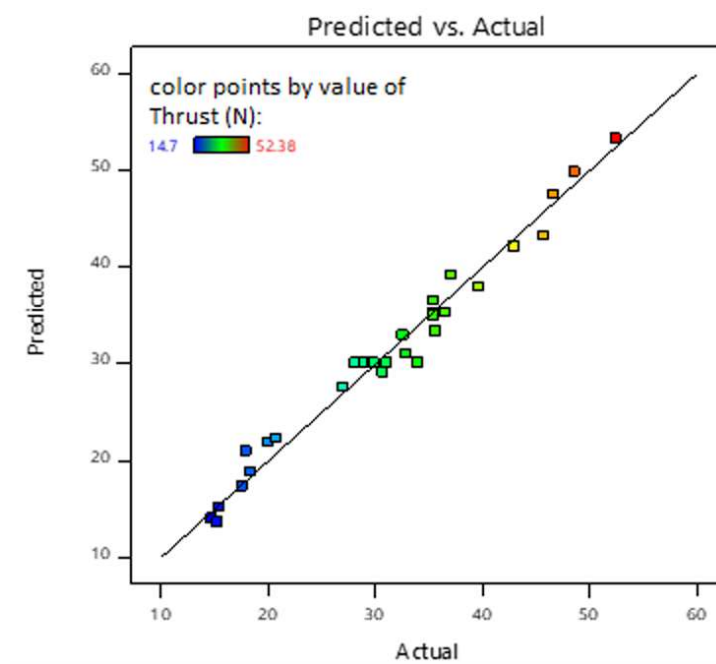


Figure 7.3: Predicted vs Actual Plot for Thrust Force on RPUF Composite

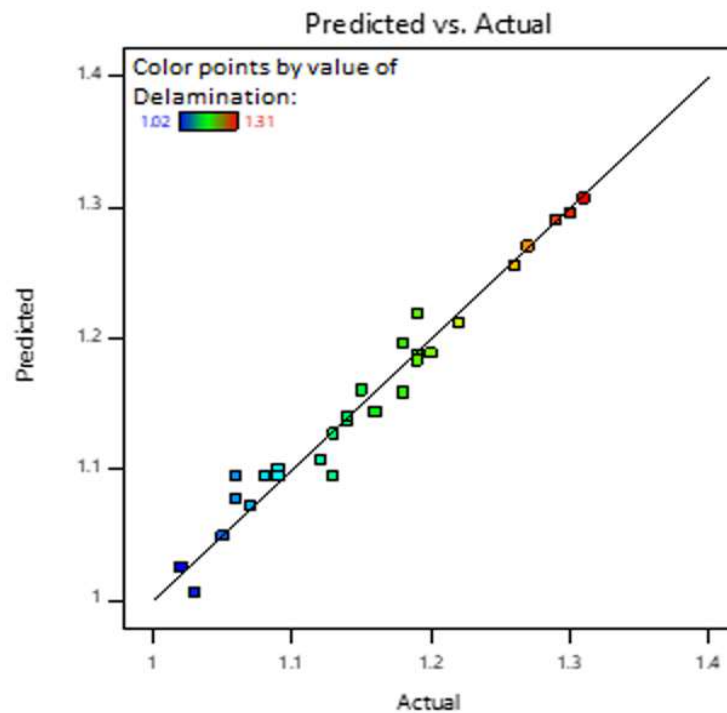


Figure 7.4: Predicted vs Actual Plot for Delamination of RPUF Composite

The p-value shows that the density, drill diameter and the spindle speed have shown significant effects on the thrust force generated in the course of the drilling, while, the feed rate

is insignificant in determining the thrust force. Among these factors, the density is the most influential factor whereas, the influence of the spindle speed is the least significant. The insignificance of feed rate in determining the thrust force is attributed to the higher density of the foam, which reduces the influence of other factors.

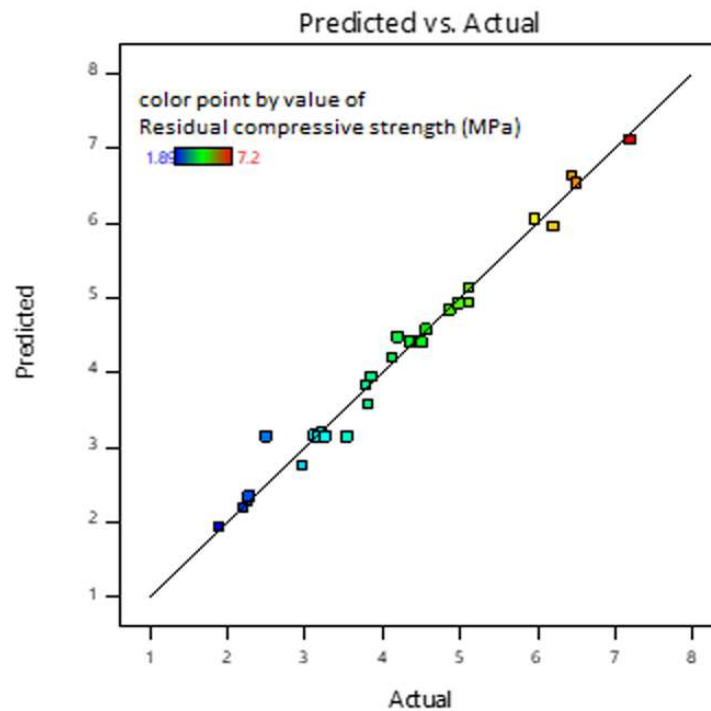


Figure 7.5: Predicted vs Actual Plot for Residual Compressive Strength of RPUF Composite

It was also noticed that the interaction of the density with the drill diameter, the spindle speed with the feed rate or the drill diameter, the feed rate with the drill diameter and the second order term of density, also have shown significant effect on the developed thrust force. Figure 7.6 shows the 3D response surfaces of the developed quadratic model for the thrust force. The higher value of the thrust force is accredited to the resistance to cut the polyurethane composite materials with increase in the density, which results in the higher drilling forces. It was also observed that the thrust force increases slightly on increasing the spindle speed or drill diameter

while the feed rate shows no effect on the thrust force. A similar increase in the thrust force were obtained by Debnath *et al.* [120, 190] for the thrust force at higher feed rate.

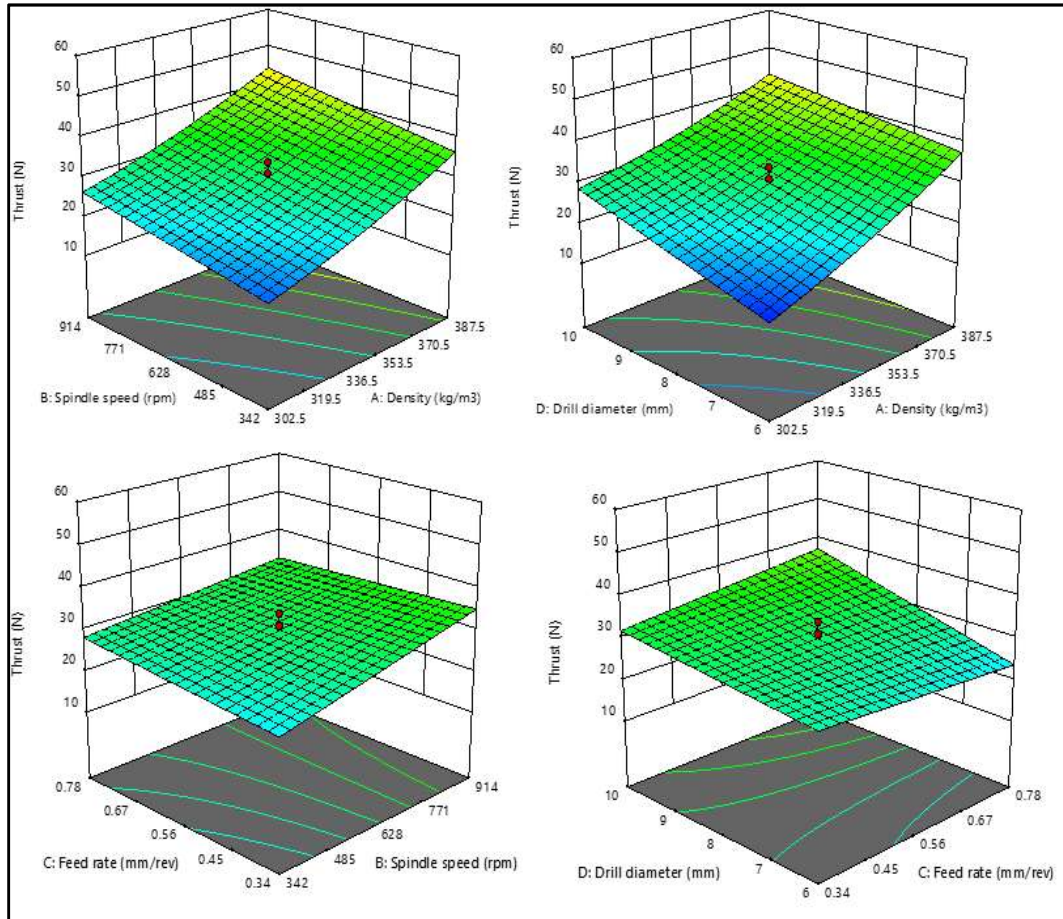


Figure 7.6: Response Surface for the Effect of Drilling on Thrust Force for RPUF Composite

7.2.2 Delamination Analysis

ANOVA of the reduced quadratic model for the delamination is summarized in the Table 7.4. the F-value of the model and its lack of fit values are 80.69 and 0.42 respectively, which ascertain the significance of the developed quadratic model. The p-value for the model is less than 0.05, which establish the statistical significance of the model at 95% confidence interval. The difference of less than 0.2 between the predicted R^2 (0.9484) and the adjusted R^2 (0.9565)

values shows that, the developed quadratic model suggests an appropriate relationship between the drilling parameters and the delamination. Adequate precision provided by the model is above 32 which ascertains the significance of the model in terms of the signal to noise ratio.

Table 7.3: ANOVA and Fit Statistics for Delamination of RPUF Composite

Source	Sum of Squares	df	Mean Square	F-value	p-value	
Model	0.1873	8	0.0234	80.69	< 0.0001	Significant
ρ -Density	0.0160	1	0.0160	55.20	< 0.0001	
v -Spindle Speed	0.0468	1	0.0468	161.36	< 0.0001	
f -Feed Rate	0.0003	1	0.0003	0.9191	0.3486	
d -Drill Diameter	0.0748	1	0.0748	257.87	< 0.0001	
Vf	0.0036	1	0.0036	12.41	0.0020	
ρ^2	0.0364	1	0.0364	125.57	< 0.0001	
f^2	0.0027	1	0.0027	9.31	0.0061	
d^2	0.0140	1	0.0140	48.08	< 0.0001	
Residual	0.0061	21	0.0003			
Lack of Fit	0.0035	16	0.0002	0.4198	0.9149	Not Significant
Pure Error	0.0026	5	0.0005			
Cor Total	0.1934	29				
Std. Dev.	0.0170				R²	0.9685
Mean	1.15				Adjusted R²	0.9565
C.V. %	1.48				Predicted R²	0.9484
PRESS	0.0100				Adequate Precision	32.2324

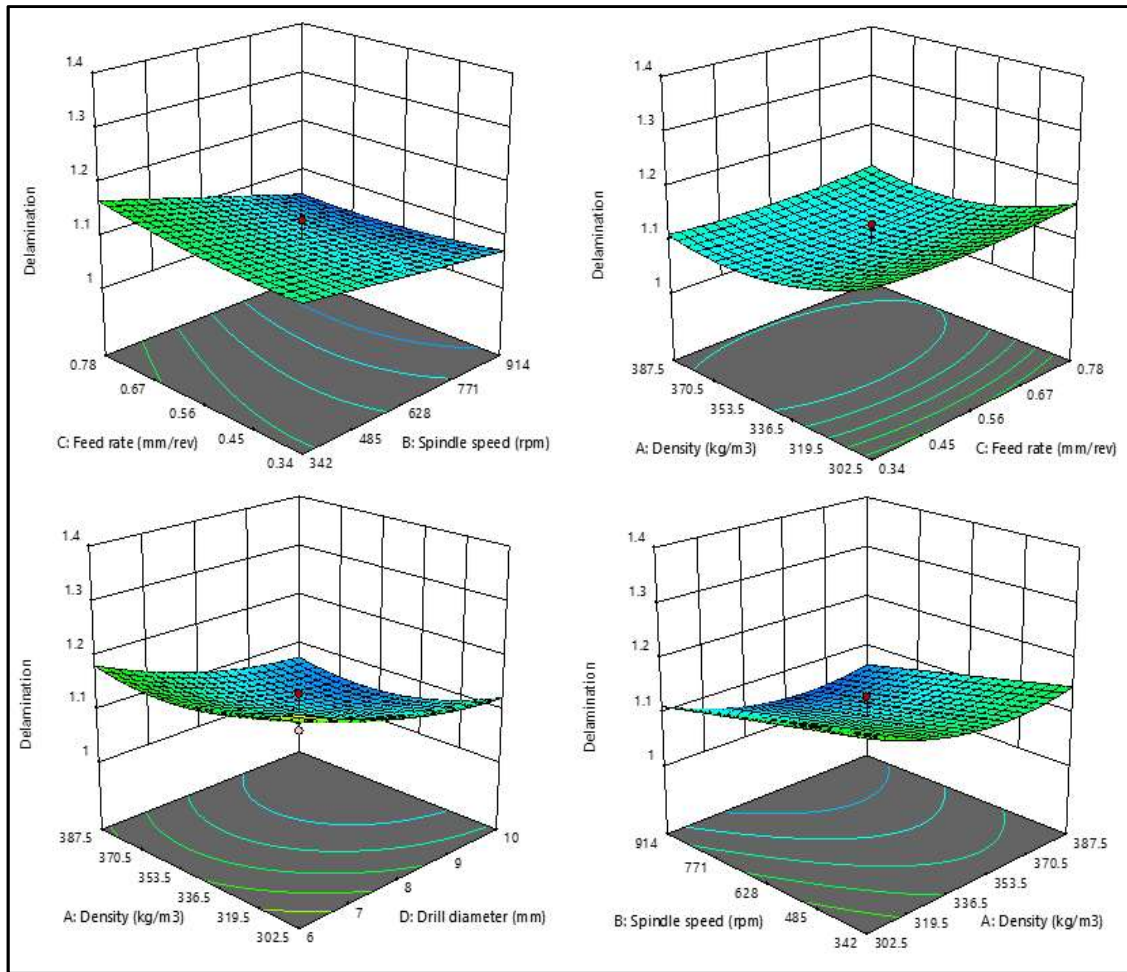


Figure 7.7: Response Surfaces for the Effect of Drilling on Delamination of RPUF Composite

The p-value shows that the density, spindle speed and the drill diameter have shown significant effect on the delamination generated during the drilling, while the feed rate is insignificant in causing the delamination. Among these factors, the drill diameter is the most influential factor whereas, the influence of the density is the least amongst all. It was also noticed that the interaction of the spindle speed with the feed rate, second order of density, feed rate and drill diameter also have shown significant effects on the generated delamination.

The drilling parameters, as well as, the characteristics of the matrix and the filler ascertain the extent of the delamination during drilling. Figure 7.7 shows the 3D response

surfaces of the developed quadratic model for the delamination. It was observed that the delamination decreases on increasing the spindle speed or density while the feed rate shows no effect on the delamination. Similar result were observed by Xing *et al.* [191] while drilling the carbon fibre reinforced carbon and silicon carbide composites. J. Miguel Silva *et al.* [134] also observed that the drilling with high spindle speed and step geometry drill bits provides higher bearing strength in the carbon/epoxy cross-ply composite plates. Additionally, by increasing the drill diameter, slight decrease in the delamination is observed. It is concluded from these plots that the variability in the delamination is little affected by the drilling parameters.

7.2.3 Residual Compressive Strength Analysis

ANOVA of the reduced quadratic model for the residual compressive strength is summarized in the Table 7.5. The F-value of the model and the lack of fit values are 97.20 and 0.22 respectively, which ascertain the significance of the developed quadratic model. The p-value for the model is less than 0.05, which establish the statistical significance of the model at 95% confidence interval. The difference of less than 0.2 between the predicted R^2 (0.9664) and the adjusted R^2 (0.9733) values shows that the developed quadratic model suggests an appropriate relationship between the drilling parameters and the residual compressive strength. The adequate precision provided by the model is above 35 which ascertains the significance of the model in terms of signal to noise ratio.

The p-value shows that the density, spindle speed and the drill diameter have shown significant effect on the residual compressive strength of the drilled RPUFs. Among these factors, the density is the most influential factor whereas, the influence of drill diameter is least amongst all.

Table 7.4: ANOVA and Fit Statistics for Residual Compressive Strength of RPUF Composite

Source	Sum of Squares	df	Mean Square	F-value	p-value	
Model	56.14	11	5.10	97.20	< 0.0001	Significant
ρ -Density	34.01	1	34.01	647.74	< 0.0001	
v -Spindle Speed	5.66	1	5.66	107.70	< 0.0001	
f -Feed Rate	0.0651	1	0.0651	1.24	0.2801	
d -Drill Diameter	4.60	1	4.60	87.66	< 0.0001	
ρv	1.51	1	1.51	28.70	< 0.0001	
ρd	2.39	1	2.39	45.61	< 0.0001	
$v f$	0.8789	1	0.8789	16.74	0.0007	
ρ^2	4.30	1	4.30	81.98	< 0.0001	
v^2	1.76	1	1.76	33.61	< 0.0001	
f^2	2.29	1	2.29	43.52	< 0.0001	
d^2	1.37	1	1.37	26.13	< 0.0001	
Residual	0.9451	18	0.0525			
Lack of Fit	0.3483	13	0.0268	0.2245	0.9861	Not Significant
Pure Error	0.5968	5	0.1194			
Cor Total	57.08	29				
Std. Dev.	0.2291				R²	0.9834
Mean	4.08				Adjusted R²	0.9733
C.V. %	5.62				Predicted R²	0.9664
PRESS	1.92				Adeq Precision	35.7390

It was also noticed that the interaction of the density with the spindle speed or the drill diameter and the interaction of the spindle speed with the feed rate, second order terms of density, spindle speed, feed rate and the drill diameter also have shown significant effects on the residual compressive strength.

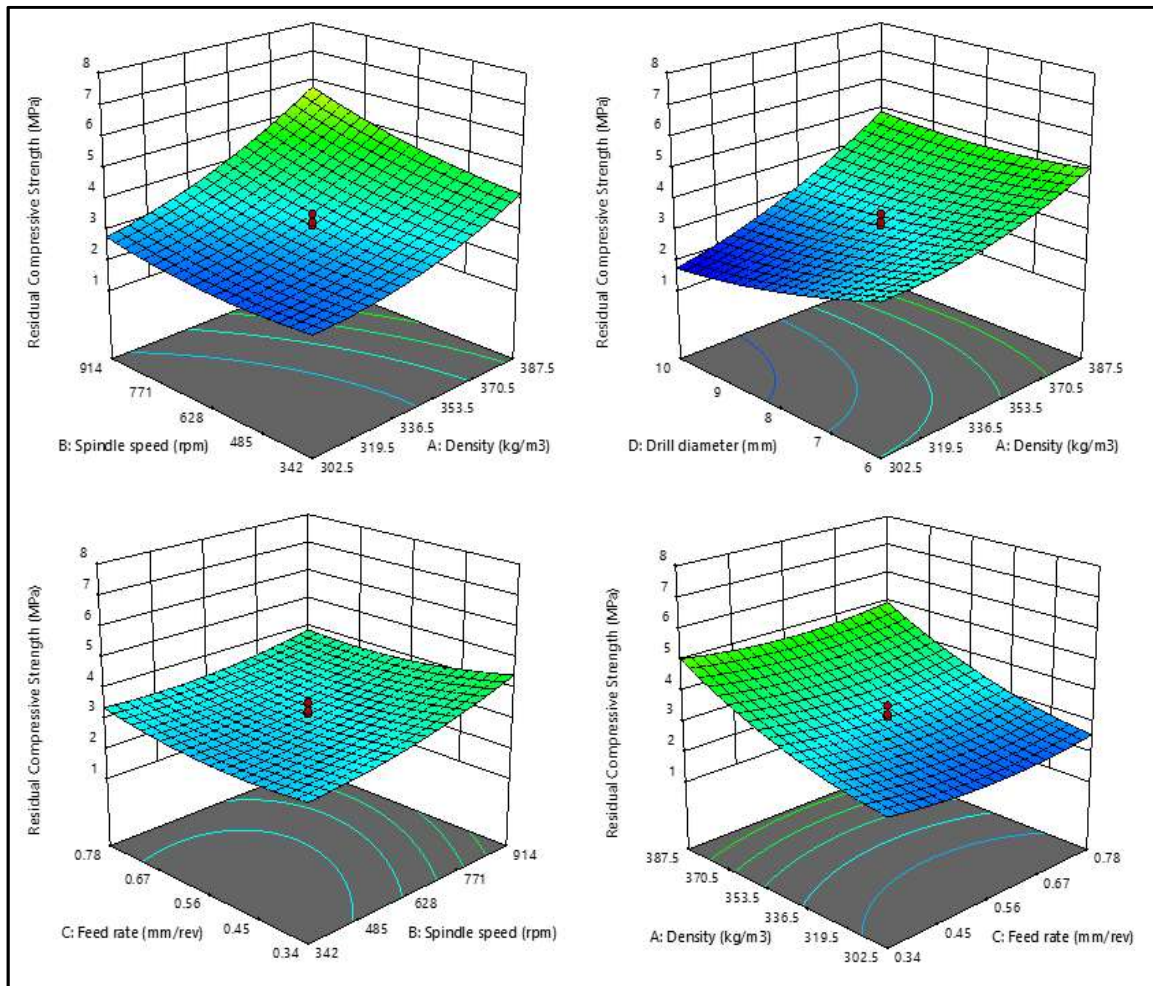


Figure 7.8: Response Surface for the Effect of Drilling on Residual Compressive Strength of RPUF Composite

Figure 7.8 shows the response surfaces of the developed quadratic model for the variation of the residual compressive strength with the drilling parameters. An increase in the residual compressive strength was observed on increasing the spindle speed. This behaviour is accredited to the lower impact of the spindle speed on the generation of the delamination which,

consequently, increases the residual compressive strength of the drilled RPUF. J. Miguel Silva et al. [134] also observed similar conclusions while drilling carbon/epoxy cross-ply composite plates.

7.2.4 Optimization Employing Desirability Function

The numerical optimization of the process parameters was performed by employing desirability function. The aim of the optimization was to maximize the residual compressive strength with minimized delamination. The desirability function of 1 is required to achieve the goal of optimization. Some best solutions with desirability function 1 are presented in the Table 7.5. It was concluded from the results that, the high spindle speed and the low feed rate are the optimized drilling parameters to obtain the maximum residual compressive strength for varied density or drill diameter.

Table 7.5: Optimized Values of Factors and Responses after Numerical Optimization

S. No.	Density (kg/m ³)	Spindle Speed (rpm)	Feed Rate (mm/rev)	Drill Diameter (mm)	Thrust Force (N)	Delamination	Residual Compressive Strength (MPa)	Desirability Function
1.	387.5	914	0.34	10	47.534	1.049	6.530	1
2.	387.5	914	0.34	6	43.240	1.160	6.632	1
3.	302.5	914	0.34	10	32.974	1.100	2.762	1
4.	302.5	914	0.34	6	21.90	1.212	4.411	1

The developed quadratic model to predict responses i.e., the thrust force, delamination and the residual compressive strength, for the factor levels at which the experiment is performed, are presented in the form of coded equations (1), (2) and (3) respectively. The relative impact of the drilling factors can be identified by comparing the factor coefficients provided by these equations.

Thrust force (N) =

$$+30.10 + 8.97\rho + 3.91v + 0.4850f + 4.55d - 1.69\rho d - 1.59vf + 1.56vd + 2.27fd + 1.30\rho^2 \quad (1)$$

Delamination =

$$+1.09 - 0.0258\rho - 0.0442v + 0.0033f - 0.0558d - 0.0150vf + 0.0361\rho^2 + 0.0098f^2 + 0.0223d^2 \quad (2)$$

Residual compressive strength (MPa) =

$$+3.15 + 1.19\rho + 0.4854v - 0.0521f - 0.4379d + 0.3069\rho v + 0.3869\rho d - 0.2344vf + 0.3961\rho^2 + 0.2536v^2 + 0.2886f^2 + 0.2236d^2 \quad (3)$$

7.3 SIGNIFICANT FINDINGS

The rigid PU foams were prepared by incorporating the copper powder to enhance the mechanical, flame retardant and thermal properties of the foams. The drilling experiments were performed on the resulted RPUF composites to assess their machining ability. In addition, the effect of the drilling parameters on the thrust force, delamination and the residual compressive strength of the drilled RPUFs was investigated experimentally. Four drilling parameters, namely, foam density, feed rate, drill bit diameter and the spindle speed, at five levels, based on the central composite design, were studied. The conclusions drawn from the present investigation are as follows:

- It was noticed that the density is the most influential factor for the optimization of the thrust force, delamination and the residual compressive strength, while the feed rate shows the negligible effect on the responses.
- The residual compressive strength increases with the increase in the spindle speed.

- After numerical optimization, the optimal process parameters were selected as the spindle speed, 914 rpm and the feed rate, 0.34 mm/rev to maximize the residual compressive strength.
- A polynomial regression model showing the impact of the density, feed rate, spindle speed and the drill diameter on the responses was presented in the form of the coded equations.

CHAPTER 8

CONCLUSIONS AND THE FUTURE PROSPECTS

8.1 CONCLUSIONS

The substitution of the petroleum based feedstock with agricultural oils for the production of polymers is a potential field of research and the improvement of their properties is the need of the hour. The rigid PU foams were prepared by using castor oil based-polyol and incorporated with different reinforcing fillers. The fillers considered in the present investigation exhibited considerable improvement in the mechanical, thermal and fire properties of the RPUFs. FTIR and ¹H NMR spectra of the prepared polyol confirm the transesterification of the castor oil. The compressive strength and the flexural strength of the ceramic filler incorporated foam were found to increase by 273% and 624% respectively. TGA and DTG curves showed an increase in the thermal stability of the ceramic filler reinforced foams. The 5% weight loss temperature ($T_{5\%}$) increased from 192°C to 265°C for the 8% zirconia powder filled RPUF. The flame retardancy of the ceramic filler incorporated RPUFs was also enhanced and 6% concentration of the ceramic fillers demonstrated the best properties, with up to 29% decrease in heat release rate (HRR) and 71% suppression in the production of smoke.

Foams with 8% and 10% carbon fibre concentration show conductivity of 1.9×10^{-4} and 7.1×10^{-4} S/m respectively. Results concluded that the RPUF with 8% carbon fibre concentration showed higher mechanical properties, with 3-fold increase in compressive and flexural strength respectively. Specific compressive strength was also found to increase by 28% for the foams with 8% concentration of the carbon fibre powder. The peak of heat release (PHRR) was found to decrease from 118 kW/m² to 85 kW/m² on the incorporation of carbon fibre powder. Additionally, the rate of smoke production was also observed to decrease for

composite RPUFs. Experimental results showed that the RPUF incorporated with 8% feldspar demonstrates maximum compressive strength of 4.98 MPa, which is 182% greater than that of the unreinforced RPUF. RPUF incorporated with clay demonstrated best thermal properties and showed increase in 5% weight loss temperature from 192°C to 260-270°C. The char residue was also found to be increased from 8 wt% to 16 wt% on the incorporation of mineral fillers. Cone calorimeter test of RPUF with varied concentration of mineral fillers demonstrated a fair enhancement in the flame retardancy of the RPUF and among all the samples, best properties were shown by the foams with 6% concentration of any of the mineral filler. Of these fillers, feldspar showed higher flame retardancy, thus suggesting its better fire performance in the mineral fillers studied in this research.

Copper powder reinforced rigid PU foams were prepared to enhance its mechanical, flame retardant and thermal properties and the drilling was performed to assess their machining ability. Conclusions drawn from the present investigation are as follows:

- As the incorporation of the carbon fibre in RPUF provides a reasonable amount of conductivity, without deteriorating the other properties of the vegetable oil based rigid PU foams, so the carbon fibres are a potential additive to yield conducting PU foams.
- The incorporation of the mineral fillers or ceramic fillers improve the mechanical, thermal and flame retardant properties of the vegetable oil based rigid PU foams, so these fillers may be utilized as unique flame retardants with additional benefits of good mechanical and thermal properties. These RPUF composites, thus produced, may be used for fire safety applications in buildings, for carving models & prototypes.
- The incorporation of metallic filler also enhances the mechanical properties of the vegetable oil-based foam and the best combination of the mechanical, thermal and flame retardant properties of RPUF composite was obtained by the incorporation of 8% copper powder filler.

- It is observed that the density is the most influential factor for the optimization of thrust force, delamination, and residual compressive strength during drilling, while the feed rate shows a negligible effect on the responses.
- The studies reveal that the residual compressive strength of the metallic filler reinforced RPUF increases with an increase in spindle speed during drilling experiments.
- After numerical optimization of the drilling process performed on metallic filler reinforced RPUF, the optimal process parameters were selected as spindle speed 914 rpm and feed rate 0.34 mm/rev to maximize the residual compressive strength.
- A polynomial regression model showing the impact of density, feed rate, spindle speed and drill diameter on the responses was presented in the form of coded equations.

8.2 FUTURE PROSPECTS OF WORK

The resulted RPUF incorporated with reinforcing fillers and anti-flamming agents possesses enhanced mechanical and structural properties. Being light weight, thermal and flame resistant material, and with low thermal conductivity, comparable or better to the commercial petroleum based polyurethane foams, the resulted RPUF can be employed for the multipurpose uses in various engineering and defence applications. Due to their high strength, ease of processing and property to adhere with other surface, these rigid polyurethane foams are expected to be used in many diverse fields where the combination to strength to weight ratio and excellent thermal insulation are the main requirements e.g. manufacture of the light weight roofs, doors and floors in road, rail and air transport. Being light weight, strong and machinable material, it can successfully replace the wood in many conventional applications. As Polyurethane rigid form is reported to have a low thermal conductivity, so resulted material could be used as artificial roof or wall panels for various air conditioned structures.

REFERENCES

- [1] Sivertsen K. Polymer foams. *3063 Polym Phys*.
- [2] Polyurethane chemicals and products in asia pacific (APAC), www.ialconsultants.com (2015, accessed 22 September 2016).
- [3] Yang W, Dong Q, Liu S, et al. Recycling and disposal methods for polyurethane foam wastes. *Procedia Environ Sci* 2012; 16: 167–175.
- [4] Polyurethane – PU Waste Recycling of Plastics, www.plastemart.com/upload/literature/PUrecycling.asp (2016, accessed 22 September 2016).
- [5] Green Polyurethane, www.nanotechindustriesinc.com/GPU-technical.php (2016, accessed 2 December 2016).
- [6] Thébault M, Pizzi A, Essawy HA, et al. Isocyanate free condensed tannin-based polyurethanes. *Eur Polym J* 2015; 67: 513–526.
- [7] Lee A, Deng Y. Green polyurethane from lignin and soybean oil through non-isocyanate reactions. *Eur Polym J* 2015; 63: 67–73.
- [8] Miao S, Wang P, Su Z, et al. Vegetable-oil-based polymers as future polymeric biomaterials. *Acta Biomater* 2014; 10: 1692–1704.
- [9] Dave VJ, Patel HS. Synthesis and characterization of interpenetrating polymer networks from transesterified castor oil based polyurethane and polystyrene. *J Saudi Chem Soc* 2013; 36: 1–7.
- [10] Kreye O, Mutlu H, Meier MAR. Sustainable routes to polyurethane precursors. *Green Chem* 2013; 15: 1431–1455.
- [11] Alagi P, Choi YJ, Hong SC. Preparation of vegetable oil-based polyols with controlled hydroxyl functionalities for thermoplastic polyurethane. *Eur Polym J* 2016; 78: 46–60.

-
- [12] Ronda JC, Lligadas G, Galia M, et al. Vegetable oils as platform chemicals for polymer synthesis. *Eur J Lipid Sci Technol* 2011; 113: 46–58.
- [13] Cornille A, Dworakowska S, Bogdal D, et al. A new way of creating cellular polyurethane materials: NIPU foams. *Eur Polym J* 2015; 66: 129–138.
- [14] Desroches M, Escouvois M, Auvergne R, et al. vegetable oils to polyurethanes: synthetic routes to polyols and main industrial products. *Polym Rev* 2012; 52: 38–79.
- [15] Lligadas G, Ronda JC, Galia M, et al. Plant oils as platform chemicals for polyurethane synthesis: current state-of-the-art. *Biomacromolecules* 2010; 11: 2825–2835.
- [16] Karimi MB, Khanbabaie G, Sadeghi GMM. Vegetable oil-based polyurethane membrane for gas separation. *J Memb Sci* 2017; 527: 198–206.
- [17] Miao S, Sun L, Wang P, et al. Soybean oil based polyurethane networks as candidate biomaterials: synthesis and biocompatibility. *Eur J Lipid Sci Technol* 2012; 114: 1165–1174.
- [18] Zhu M, Bandyopadhyay-Ghosh S, Khazabi M, et al. Reinforcement of Soy Polyol-Based Rigid Polyurethane Foams by Cellulose Microfibers and Nanoclays. *J Appl Polym Sci* 2012; 124: 4702–4710.
- [19] Fan H, Tekeci A, Suppes GJ, et al. Properties of biobased rigid polyurethane foams reinforced with fillers: Microspheres and nanoclay. *Int J Polym Sci* 2012; 2012: 1–8.
- [20] Miao S, Wang P, Su Z, et al. Soybean oil-based shape-memory polyurethanes: synthesis and characterization. *Eur J Lipid Sci Technol* 2012; 114: 1345–1351.
- [21] Luo X, Mohanty A, Misra M. Green composites from soy-based biopolyurethane with microcrystalline cellulose. *Macromol Mater Eng* 2013; 298: 412–418.
- [22] Somani KP, Kansara SS, Patel NK, et al. Castor oil based polyurethane adhesives for wood-to-wood bonding. *Int J Adhes Adhes* 2003; 23: 269–275.

-
- [23] Carriço CS, Fraga T, Pasa VMD. Production and characterization of polyurethane foams from a simple mixture of castor oil, crude glycerol and untreated lignin as bio-based polyols. *Eur Polym J* 2016; 85: 53–61.
- [24] Ionescu M, Radojicic D, Wan X, et al. Highly functional polyols from castor oil for rigid polyurethanes. *Eur Polym J* 2016; 84: 736–749.
- [25] Zieleniewska M, Leszczynski MK, Kuranska M, et al. Preparation and characterisation of rigid polyurethane foams using a rapeseed oil-based polyol. *Ind Crop Prod* 2015; 74: 887–897.
- [26] Kairyte A, Vejelis S. Evaluation of forming mixture composition impact on properties of water blown rigid polyurethane (PUR) foam from rapeseed oil polyol. *Ind Crop Prod* 2015; 66: 210–215.
- [27] Fourati Y, Hassen RB, Bayramoglu G, et al. A one step route synthesis of polyurethane network from epoxidized rapeseed oil. *Prog Org Coatings* 2017; 105: 48–55.
- [28] Rojek P, Prociak A. Effect of different rapeseed-oil-based polyols on mechanical properties of flexible polyurethane foams. *J Appl Polym Sci* 2012; 125: 2936–2945.
- [29] Zhou X, Sain MM, Oksman K. Semi-rigid biopolyurethane foams based on palm-oil polyol and reinforced with cellulose nanocrystals. *Compos Part A Appl Sci Manuf* 2016; 83: 56–62.
- [30] Ng WS, Lee CS, Chuah CH, et al. Preparation and modification of water-blown porous biodegradable polyurethane foams with palm oil-based polyester polyol. *Ind Crop Prod* 2017; 97: 65–78.
- [31] Das B, Konwar U, Mandal M, et al. Sunflower oil based biodegradable hyperbranched polyurethane as a thin film material. *Ind Crop Prod* 2013; 44: 396–404.
- [32] Ribeiro Da Silva V, Mosiewicki MA, Yoshida MI, et al. Polyurethane foams based on

- modified tung oil and reinforced with rice husk ash I: Synthesis and physical chemical characterization. *Polym Test* 2013; 32: 438–445.
- [33] Ribeiro Da Silva V, Mosiewicki MA, Yoshida MI, et al. Polyurethane foams based on modified tung oil and reinforced with rice husk ash II: Mechanical characterization. *Polym Test* 2013; 32: 665–672.
- [34] Kong X, Liu G, Curtis JM. Novel polyurethane produced from canola oil based poly(ether ester) polyols: Synthesis, characterization and properties. *Eur Polym J* 2012; 48: 2097–2106.
- [35] Kwon OJ, Yang SR, Kim DH, et al. Characterization of polyurethane foam prepared by using starch as polyol. *J Appl Polym Sci* 2006; 103: 1544–1553.
- [36] Ertas M, Fidan MS, Alma MH. Preparation and characterization of biodegradable rigid polyurethane foams from the liquified eucalyptus and pine woods. *Wood Res* 2014; 59: 97–108.
- [37] Tavares LB, Boas CV, Schleder GR, et al. Bio-based polyurethane prepared from Kraft lignin and modified castor oil. *eXPRESS Polym Lett* 2016; 10: 927–940.
- [38] Bernardini J, Cinelli P, Anguillesi I, et al. Flexible polyurethane foams green production employing lignin or oxypropylated lignin. *Eur Polym J* 2015; 64: 147–156.
- [39] Cinelli P, Anguillesi I, Lazzeri A. Green synthesis of flexible polyurethane foams from liquefied lignin. *Eur Polym J* 2013; 49: 1174–1184.
- [40] Hakim AAA, Nassar M, Emam A, et al. Preparation and characterization of rigid polyurethane foam prepared from sugar-cane bagasse polyol. *Mater Chem Phys* 2011; 129: 301–307.
- [41] Piszczyk L, Strankowski M, Danowska M, et al. Preparation and characterization of rigid polyurethane-polyglycerol nanocomposite foams. *Eur Polym J* 2012; 48: 1726–1733.

-
- [42] Piszczyk L, Strankowski M, Danowska M, et al. Rigid polyurethane foams from a polyglycerol-based polyol. *Eur Polym J* 2014; 57: 143–150.
- [43] Bio-Based Polyurethanes That Work, www.myriant.com/pdf/myriant-polyol-technical-bulletin-2013.pdf (2017, accessed 17 March 2017).
- [44] Soares B, Gama N, Freire CSR, et al. Spent coffee grounds as a renewable source for ecopolyols production. *J Chem Technol Biotechnol* 2015; 90: 1480–1488.
- [45] Hu S, Wan C, Li Y. Production and characterization of biopolyols and polyurethane foams from crude glycerol based liquefaction of soybean straw. *Bioresour Technol* 2012; 103: 227–233.
- [46] Li YY, Luo X, Hu S. Polyols and Polyurethanes from Oils and their Derivatives. In: *Bio-based Polyols and Polyurethanes*. Springer briefs in Green Chemistry for Sustainability, 2015, pp. 15–43.
- [47] Zhang L, Zhang M, Zhou Y, et al. The study of mechanical behavior and flame retardancy of castor oil phosphate-based rigid polyurethane foam composites containing expanded graphite and triethyl phosphate. 2013; 98: 2784–2794.
- [48] Mosiewicki MA, Dell’Arciprete GA, Aranguren MI, et al. Polyurethane Foams Obtained from Castor Oil-based Polyol and Filled with Wood Flour. *J Compos Mater* 2009; 43: 3057–3072.
- [49] Veronese VB, Menger RK, Forte MMC, et al. Rigid polyurethane foam based on modified vegetable oil. *J Appl Polym Sci* 2011; 120: 530–537.
- [50] Malik M, Kaur R. Mechanical and Thermal Properties of Castor Oil-Based Polyurethane Adhesive: Effect of TiO₂ Filler. *Adv Polym Technol* 2018; 37: 24–30.
- [51] Vanbesien T, Hapiot F, Monflier E. Hydroformylation of vegetable oils and the potential use of hydroformylated fatty acids. *Lipid Technol* 2013; 25: 175–178.
- [52] Arniza MZ, Hoong SS, Idris Z, et al. Synthesis of Transesterified Palm Olein-Based

- Polyol and Rigid Polyurethanes from this Polyol. *J Am Oil Chem Soc* 2015; 92: 243–255.
- [53] Lozada Z, Suppes GJ, Tu YC, et al. Soy-based polyols from oxirane ring opening by alcoholysis reaction. *J Appl Polym Sci* 2009; 113: 2552–2560.
- [54] Omrani I, Farhadian A, Babanejad N, et al. Synthesis of novel high primary hydroxyl functionality polyol from sunflower oil using thiol-yne reaction and their application in polyurethane coating. *Eur Polym J* 2016; 82: 220–231.
- [55] Lligadas G. Renewable polyols for polyurethane synthesis via thiol-ene/yne couplings of plant oils. *Macromol Chem Phys* 2013; 214: 415–422.
- [56] Zhang M, Luo Z, Zhang J, et al. Effects of a novel phosphorus-nitrogen flame retardant on rosin-based rigid polyurethane foams. *Polym Degrad Stab* 2015; 120: 427–434.
- [57] Xue B, Wen J, Sun R. Lignin-Based Rigid Polyurethane Foam Reinforced with Pulp Fiber: Synthesis and Characterization. *ACS Sustain Chem Eng* 2014; 2: 1474–1480.
- [58] Singhal P, Small W, Cosgriff-Hernandez E, et al. Low density biodegradable shape memory polyurethane foams for embolic biomedical applications. *Acta Biomater* 2014; 10: 67–76.
- [59] Blattmann H, Fleischer M, Bähr M, et al. Isocyanate- and Phosgene-Free Routes to Polyfunctional Cyclic Carbonates and Green Polyurethanes by Fixation of Carbon Dioxide. *Macromol Rapid Commun* 2014; 35: 1238–1254.
- [60] Cornille A, Auvergne R, Figovsky O, et al. A perspective approach to sustainable routes for non-isocyanate polyurethanes. *Eur Polym J* 2017; 87: 535–552.
- [61] Cornille A, Guillet C, Benyahya S, et al. Room temperature flexible isocyanate-free polyurethane foams. *Eur Polym J* 2016; 84: 873–888.
- [62] Calle M, Lligadas G, Ronda JC, et al. Non-isocyanate route to biobased polyurethanes

- and polyureas via AB-type self-polycondensation. *Eur Polym J* 2016; 84: 837–848.
- [63] Guan J, Song Y, Lin Y, et al. Progress in Study of Non-Isocyanate Polyurethane. *Ind Eng Chem Res* 2011; 50: 6517–6527.
- [64] Drechsel EK, Groszos SJ. *Method of preparing a polyurethane*. US Patent 2802022 A, 1957.
- [65] Sheng X, Ren G, Qin Y, et al. Quantitative synthesis of bis(cyclic carbonate)s by iron catalyst for non-isocyanate polyurethane synthesis. *Green Chem* 2015; 17: 373–379.
- [66] Bähr M, Mülhaupt R. Linseed and soybean oil-based polyurethanes prepared via the non-isocyanate route and catalytic carbon dioxide conversion. *Green Chem* 2012; 14: 483.
- [67] Bähr M, Bitto A, Mülhaupt R. Cyclic limonene dicarbonate as a new monomer for non-isocyanate oligo- and polyurethanes (NIPU) based upon terpenes. *Green Chem* 2012; 14: 1447–1454.
- [68] Lombardo VM, Dhulst EA, Leitsch EK, et al. Cooperative Catalysis of Cyclic Carbonate Ring Opening: Application Towards Non-Isocyanate Polyurethane Materials. *European J Org Chem* 2015; 13: 2791–2795.
- [69] Kathalewar M, Sabnis A, D’Mello D. Isocyanate free polyurethanes from new CNSL based bis-cyclic carbonate and its application in coatings. *Eur Polym J* 2014; 57: 99–108.
- [70] Chawla KK. Foams, fibers, and composites: Where do we stand? *Mater Sci Eng A* 2012; 557: 2–9.
- [71] Aramid fiber characteristics - Aramid Fiber, www.aramid.eu/characteristics.html (2016, accessed 23 September 2016).
- [72] Semmes EB, Frances A. *Nano-Aramid Fiber Reinforced Polyurethane Foam*.
- [73] Kim SH, Park HC, Jeong HM, et al. Glass fiber reinforced rigid polyurethane foams. *J*

-
- Mater Sci* 2010; 45: 2675–2680.
- [74] Yu YH, Choi I, Nam S, et al. Cryogenic characteristics of chopped glass fiber reinforced polyurethane foam. *Compos Struct* 2014; 107: 476–481.
- [75] Serban DA, Weissenborn O, Geller S, et al. Evaluation of the mechanical and morphological properties of long fibre reinforced polyurethane rigid foams. *Polym Test* 2016; 49: 121–127.
- [76] Kuranska M, Prociak A. Porous polyurethane composites with natural fibres. *Compos Sci Technol* 2012; 72: 299–304.
- [77] Shalwan A, Yousif BF. In state of art: mechanical and tribological behaviour of polymeric composites based on natural fibres. *Mater Des* 2013; 48: 14–24.
- [78] Gu RJ, Sain MM, Konar SK. Feasibility study of polyurethane composite foam with added hardwood pulp. *Ind Crop Prod* 2013; 42: 273–279.
- [79] El-Shekeil YA, Sapuan SM, Abdan K, et al. Influence of fiber content on the mechanical and thermal properties of Kenaf fiber reinforced thermoplastic polyurethane composites. *Mater Des* 2012; 40: 299–303.
- [80] Nirmal U, Hashim J, Lau ST, et al. Betelnut fibres as an alternative to glass fibres to reinforce thermoset composites: A comparative study. *Text Res J* 2012; 82: 1107–1120.
- [81] Dixit S, Verma P. The effect of surface modification on the water absorption behaviour of coir fibers. *Adv Appl Sci Res* 2012; 3: 1463–1465.
- [82] Estravís S, Tirado-Mediavilla J, Santiago-Calvo M, et al. Rigid polyurethane foams with infused nanoclays: Relationship between cellular structure and thermal conductivity. *Eur Polym J* 2016; 80: 1–15.
- [83] Dolomanova V, Rauhe JC. Mechanical properties and morphology of nano reinforced rigid PU foam. *J Cell Plast* 2011; 47: 81–93.

-
- [84] Rostami M, Ranjbar Z, Mohseni M. Investigating the interfacial interaction of different aminosilane treated nano silicas with a polyurethane coating. *Appl Surf Sci* 2010; 257: 899–904.
- [85] Gao X, Zhou B, Guo Y, et al. Synthesis and characterization of well-dispersed polyurethane/CaCO₃ nanocomposites. *Colloids Surfaces A Physicochem Eng Asp* 2010; 371: 1–7.
- [86] Nik Pauzi NNP, A. Majid R, Dzulkifli MH, et al. Development of rigid bio-based polyurethane foam reinforced with nanoclay. *Compos Part B Eng* 2014; 67: 521–526.
- [87] Sengupta R, Bhattacharya M, Bandyopadhyay S, et al. A review on the mechanical and electrical properties of graphite and modified graphite reinforced polymer composites. *Prog Polym Sci* 2011; 36: 638–670.
- [88] Otorugust G, Dodiuk H, Kenig S, et al. Important insights into polyurethane nanocomposite-adhesives; a comparative study between INT-WS₂ and CNT. *Eur Polym J* 2017; 89: 281–300.
- [89] Babalola FU, Erhievuyere-dominic PO. A Comparative Analysis of The Effects of Calcium Carbonate and Dolomite as Fillers in Polyether Polyurethane Foam Production. 2012; 1964: 34–40.
- [90] Alavi Nikje MM, Garmarudi AB, Haghshenas M. Effect of Talc Filler on Physical Properties of Polyurethane Rigid Foams. *Polym Plast Technol Eng* 2006; 45: 1213–1217.
- [91] Czupryn'Ski B, Paciorek-Sadowska J, Liszkowska J. Properties of Rigid Polyurethane-Polyisocyanurate Foams Modified with the Selected Fillers. *J Appl Polym Sci* 2010; 115: 2460–2469.
- [92] Shah DU, Vollrath F, Porter D. Silk cocoons as natural macro-balloon fillers in novel polyurethane-based syntactic foams. *Polym (United Kingdom)* 2015; 56: 93–101.

-
- [93] Shan CW, Idris MI, Ghazali MI. Study of Flexible Polyurethane Foams Reinforced with Coir Fibres and Tyre Particles. *Int J Appl Phys Math* 2012; 2: 123–130.
- [94] Zieleniewska M, Leszczyński MK, Szczepkowski L, et al. Development and applicational evaluation of the rigid polyurethane foam composites with egg shell waste. *Polym Degrad Stab* 2016; 1–9.
- [95] Yang ZG, Zhao B, Qin SL, et al. Study on the mechanical properties of hybrid reinforced rigid polyurethane composite foam. *J Appl Polym Sci* 2004; 92: 1493–1500.
- [96] Ciecierska E, Jurczyk-Kowalska M, Bazarnik P, et al. Flammability, mechanical properties and structure of rigid polyurethane foams with different types of carbon reinforcing materials. *Compos Struct* 2016; 140: 67–76.
- [97] Hu X, Wang D, Cheng W. Effect of dosage of expandable graphite, dimethyl methylphosphonate, triethanolamine, and isocyanate on fluidity, mechanical, and flame retardant properties of polyurethane materials in coal reinforcement. *Int J Min Sci Technol* 2015; 26: 345–352.
- [98] Bian X-C, Tang J-H, Li Z-M. Flame Retardancy of Whisker Silicon Oxide/Rigid Polyurethane Foam Composites with Expandable Graphite. *J Appl Polym Sci* 2008; 110: 3871–3879.
- [99] Yang R, Hu W, Xu L, et al. Synthesis, mechanical properties and fire behaviors of rigid polyurethane foam with a reactive flame retardant containing phosphazene and phosphate. *Polym Degrad Stab* 2015; 122: 102–109.
- [100] Zhao C, Yan Y, Hu Z, et al. Preparation and characterization of granular silica aerogel/polyisocyanurate rigid foam composites. *Constr Build Mater* 2015; 93: 309–316.
- [101] Li X, Tabil LG, Panigrahi S. Chemical treatments of natural fiber for use in natural fiber-reinforced composites: A review. *J Polym Environ* 2007; 15: 25–33.

-
- [102] Xie Y, Hill CAS, Xiao Z, et al. Silane coupling agents used for natural fiber/polymer composites: A review. *Compos Part A* 2010; 41: 806–819.
- [103] Tayfun U, Kanbur Y, Abaci U, et al. Mechanical, flow and electrical properties of thermoplastic polyurethane/fullerene composites: Effect of surface modification of fullerene. *Compos Part B* 2015; 80: 101–107.
- [104] Nirmal U, Lau STW, Hashim J. Interfacial Adhesion Characteristics of Kenaf Fibres Subjected to Different Polymer Matrices and Fibre Treatments Interfacial Adhesion Characteristics of Kenaf Fibres Subjected to Different Polymer Matrices and Fibre Treatments. 2014; 2014: 1–12.
- [105] Tayfun U, Dogan M, Bayramli E. Investigations of the flax fiber/thermoplastic polyurethane eco-composites: Influence of isocyanate modification of flax fiber surface. *Polym Compos* 2017; 38: 2874–2880.
- [106] Semenzato S, Lorenzetti A, Modesti M, et al. A novel phosphorus polyurethane foam/montmorillonite nanocomposite: preparation, characterization and thermal behavior. *Appl Clay Sci* 2009; 44: 35–42.
- [107] Dasari A, Yu ZZ, Cai GP, et al. Recent developments in the fire retardancy of polymeric materials. *Prog Polym Sci* 2013; 38: 1357–1387.
- [108] Heinen M, Gerbase AE, Petzhold CL. Vegetable oil-based rigid polyurethanes and phosphorylated flame-retardants derived from epoxydized soybean oil. *Polym Degrad Stab* 2014; 108: 76–86.
- [109] Xu Z, Tang X, Zheng J. Thermal stability and flame retardancy of rigid polyurethane foams/organoclay nanocomposites. *Polym Plast Technol Eng* 2008; 47: 1136–1141.
- [110] Yan D, Xu L, Chen C, et al. Enhanced mechanical and thermal properties of rigid polyurethane foam composites containing graphene nanosheets and carbon nanotubes. *Polym Int* 2012; 61: 1107–1114.

-
- [111] Christou A, Stec AA, Ahmed W, et al. A review of exposure and toxicological aspects of carbon nanotubes, and as additives to fire retardants in polymers. *Crit Rev Toxicol* 2016; 46: 74–95.
- [112] Zheng X, Wang G, Xu W. Roles of organically-modified montmorillonite and phosphorous flame retardant during the combustion of rigid polyurethane foam. *Polym Degrad Stab* 2014; 101: 32–39.
- [113] Yang C, Fischer L, Maranda S, et al. Rigid polyurethane foams incorporated with phase change materials: A state-of-the-art review and future research pathways. *Energy Build* 2015; 87: 25–36.
- [114] What is Aerogel?, www.aerogel.org (2016, accessed 10 October 2016).
- [115] Acharya A, Joshi D, Gokhale VA. Aerogel – A promising building material for sustainable buildings. *Chem Process Eng Resour* 2013; 9: 1–7.
- [116] Findik F. Latest progress on tribological properties of industrial materials. *Mater Des* 2014; 57: 218–244.
- [117] Chegiani F, Mansori M El. Tribology International Friction scale effect in drilling natural fiber composites. *Tribol Int* 2018; 119: 622–630.
- [118] Hussain SA, Pandurangadu V, Kumar KP. Optimization of surface roughness in turning of GFRP composites using genetic algorithm. *Int J Eng Sci Technol* 2014; 6: 49–57.
- [119] Jahanian E, Zeinedini A. Influence of drilling on mode II delamination of E-glass / epoxy laminated composites. *Theor Appl Fract Mech* 2018; 96: 398–407.
- [120] Roy M, Shanmuka M, Debnath K. Experimental investigations on drilling of lignocellulosic fiber reinforced composite laminates. *J Manuf Process* 2018; 34: 51–61.
- [121] Xavier MA, Kumar JPA. Machinability of Hybrid Metal Matrix Composite - A

-
- Review. *Procedia Eng* 2017; 174: 1110–1118.
- [122] Machining Instructions for Engineering Plastics, https://www.theplasticshop.co.uk/plastic.../engineering_plastics_machining_guide.pdf (2017, accessed 26 December 2017).
- [123] Donohue BB. How it Works – Machining Plastics. 2016; 7: 1–13.
- [124] Boedeker Plastics : Guide to Plastics Machining, <http://www.boedeker.com/fabtip.htm> (2016, accessed 26 December 2017).
- [125] Balani K, Verma V, Agarwal A, et al. Physical, Thermal, and Mechanical Properties of Polymers. In: *Biosurfaces*. Hoboken, NJ, USA: John Wiley & Sons, Inc, pp. 329–344.
- [126] Kumar D, Singh KK. ScienceDirect Experimental analysis of Delamination , Thrust Force and Surface roughness on Drilling of Glass Fibre Reinforced Polymer Composites Material Using Different Drills. 2017; 4: 7618–7627.
- [127] Geier N, Szalay T. Optimisation of process parameters for the orbital and conventional drilling of uni-directional carbon fibre-reinforced polymers (UD-CFRP). *Meas J Int Meas Confed* 2017; 110: 319–334.
- [128] Zarif N, Heidary H, Minak G. Critical thrust and feed prediction models in drilling of composite laminates. *Compos Struct* 2016; 148: 19–26.
- [129] Heidary H, Zarif N, Minak G. Investigation on delamination and fl exural properties in drilling of carbon nanotube / polymer composites. *Compos Struct* 2018; 201: 112–120.
- [130] Velaga M, Cadambi RM. ScienceDirect Drilling of GFRP Composites for Minimising Delamination Effect. *Mater Today Proc* 2017; 4: 11229–11236.
- [131] Zarif N, Heidary H, Fotouhi M, et al. Experimental analysis of GFRP laminates subjected to compression after drilling. *Compos Struct* 2017; 169: 144–152.
- [132] Díaz-álvarez A, Rodríguez-millán M, Díaz-álvarez J, et al. Experimental analysis of drilling induced damage in aramid composites. *Compos Struct* 2018; 1–9.

-
- [133] Xu J, Li C, Mi S, et al. Study of drilling-induced defects for CFRP composites using new criteria. *Compos Struct* 2018; 201: 1076–1087.
- [134] Miguel J, Ferreira F, Abreu SM, et al. Correlation of drilling damage with mechanical strength : A geometrical approach. *Compos Struct* 2017; 181: 306–314.
- [135] Guo C, Zhou L, Lv J. Effects of expandable graphite and modified ammonium polyphosphate on the flame-retardant and mechanical properties of wood flour-polypropylene composites. *Polym Polym Compos* 2013; 21: 449–456.
- [136] Jia D, Hu J, He J, et al. Properties of a novel inherently flame-retardant rigid polyurethane foam composite bearing imide and oxazolidinone. *J Appl Polym Sci* 2019; 136: 47943.
- [137] Wang X, Zhang P, Huang Z, et al. Effect of aluminum diethylphosphinate on the thermal stability and flame retardancy of flexible polyurethane foams. *Fire Saf J* 2019; 106: 72–79.
- [138] Atabek LS. The flame - retardant effect of calcium hypophosphite in various thermoplastic polymers. *Fire Mater* 2019; 43: 294–302.
- [139] Shukla D, Srivastava R. Effect of alumina platelet reinforcement on dynamic mechanical properties of epoxy. *Proc World Congr Eng* 2011; III: 3–7.
- [140] Zirconium Oxide: Properties, Uses And Manufacturing Process, <https://www.articlecube.com/zirconium-oxide-properties-uses-and-manufacturing-process> (2017, accessed 18 September 2017).
- [141] Mishra TK, Kumar A, Verma V, et al. PEEK composites reinforced with zirconia nanofiller. *Compos Sci Technol* 2012; 72: 1627–1631.
- [142] Verdolotti L, Salerno A, Lamanna R, et al. A novel hybrid PU-alumina flexible foam with superior hydrophilicity and adsorption of carcinogenic compounds from tobacco smoke. *Microporous Mesoporous Mater* 2012; 151: 79–87.

-
- [143] Swain S, Sharma RA, Bhattacharya S, et al. Effects of nano-silica/nano-alumina on mechanical and physical properties of polyurethane composites and coatings. *Trans Electr Electron Mater* 2013; 14: 1–8.
- [144] Xu K, Hu YQ. Fabrication of transparent Pu/ZrO₂ nanocomposite coatings with high refractive index. *Chinese J Polym Sci (English Ed)* 2010; 28: 13–20.
- [145] Zhou S, Wu L. Phase separation and properties of UV-curable polyurethane/zirconia nanocomposite coatings. *Macromol Chem Phys* 2008; 209: 1170–1181.
- [146] Azemati AA, Khorasanizadeh H, Shirkavand Hadavand B, et al. Study on Radiation Properties of Polyurethane/Nano Zirconium Oxide Nanocomposite Coatings. *Mater Sci Forum* 2017; 894: 109–112.
- [147] Wang Z, Huang Z, Li X, et al. A nano graphene oxide/ α -zirconium phosphate hybrid for rigid polyvinyl chloride foams with simultaneously improved mechanical strengths, smoke suppression, flame retardancy and thermal stability. *Compos Part A Appl Sci Manuf* 2019; 121: 180–188.
- [148] Narwal SK, Saun NK, Dogra P, et al. Production and Characterization of Biodiesel Using Nonedible Castor Oil by Immobilized Lipase from *Bacillus aerius*. *BioMed Res Interntional* 2015; 2015: 281934.
- [149] Rigid Polyurethane Foam Sheets - High Density Hard Foam Blocks | General Plastics — General Plastics, <https://www.generalplastics.com/rigid-foams> (2018, accessed 29 June 2018).
- [150] Yang YC, Jeong SB, Kim BG, et al. Examination of dispersive properties of alumina treated with silane coupling agents, by using inverse gas chromatography. *Powder Technol* 2009; 191: 117–121.
- [151] Wang Y, Wang F, Dong Q, et al. Core-shell expandable graphite @ aluminum hydroxide as a flame-retardant for rigid polyurethane foams. *Polym Degrad Stab* 2017;

- 146: 267–276.
- [152] Zhang M, Zhang J, Chen S, et al. Synthesis and fire properties of rigid polyurethane foams made from a polyol derived from melamine and cardanol. *Polym Degrad Stab* 2014; 110: 27–34.
- [153] Hull TR, Witkowski A, Hollingbery L. Fire retardant action of mineral fillers. *Polym Degrad Stab* 2011; 96: 1462–1469.
- [154] Yang R, Wang B, Han X, et al. Synthesis and characterization of flame retardant rigid polyurethane foam based on a reactive flame retardant containing phosphazene and cyclophosphonate. *Polym Degrad Stab* 2017; 144: 62–69.
- [155] Nasouri K, Shoushtari AM, Mojtahedi MRM. Theoretical and experimental studies on EMI shielding mechanisms of multi-walled carbon nanotubes reinforced high performance composite nanofibers. *J Polym Res* 2016; 23: 3–10.
- [156] Yan DX, Pang H, Li B, et al. Structured reduced graphene oxide/polymer composites for ultra-efficient electromagnetic interference shielding. *Adv Funct Mater* 2015; 25: 559–566.
- [157] Huang Y, Li N, Ma Y, et al. The influence of single-walled carbon nanotube structure on the electromagnetic interference shielding efficiency of its epoxy composites. *Carbon N Y* 2007; 45: 1614–1621.
- [158] Aram E, Ehsani M, Khonakdar HA, et al. Functionalization of graphene nanosheets and its dispersion in PMMA/PEO blend: Thermal, electrical, morphological and rheological analyses. *Fibers Polym* 2016; 17: 174–180.
- [159] Tripathi SN, Saini P, Gupta D, et al. Electrical and mechanical properties of PMMA/reduced graphene oxide nanocomposites prepared via in situ polymerization. *J Mater Sci* 2013; 48: 6223–6232.
- [160] Stiebra L, Cabulis U, Knite M. Polyurethane foams obtained from residues of PET

- manufacturing and modified with carbon nanotubes. *J Phys Conf Ser* 2016; 709: 012002.
- [161] Yang Y, Gupta MC, Dudley KL, et al. Novel carbon nanotube - Polystyrene foam composites for electromagnetic interference shielding. *Nano Lett* 2005; 5: 2131–2134.
- [162] Ameli A, Jung PU, Park CB. Electrical properties and electromagnetic interference shielding effectiveness of polypropylene/carbon fiber composite foams. *Carbon N Y* 2013; 60: 379–391.
- [163] Kuang T, Chang L, Chen F, et al. Facile preparation of lightweight high-strength biodegradable polymer / multi-walled carbon nanotubes nanocomposite foams for electromagnetic interference shielding. *Carbon N Y* 2016; 105: 305–313.
- [164] Li J, Zhang G, Zhang H, et al. Applied Surface Science Electrical conductivity and electromagnetic interference shielding of epoxy nanocomposite foams containing functionalized multi-wall carbon nanotubes. *Appl Surf Sci* 2018; 428: 7–16.
- [165] Hwang S. Tensile , electrical conductivity and EMI shielding properties of solid and foamed PBT / carbon fiber composites. *Compos Part B* 2016; 98: 1–8.
- [166] Zhang H, Zhang G, Li J, et al. Composites : Part A Lightweight , multifunctional microcellular PMMA / Fe₃O₄ @ MWCNTs nanocomposite foams with efficient electromagnetic interference shielding. *Compos Part A* 2017; 100: 128–138.
- [167] Li Y, Shen B, Pei X, et al. Ultrathin carbon foams for effective electromagnetic interference shielding. *Carbon N Y* 2016; 100: 375–385.
- [168] Li Y, Shen B, Yi D, et al. The influence of gradient and sandwich configurations on the electromagnetic interference shielding performance of multilayered thermoplastic polyurethane / graphene composite foams. 2017; 138: 209–216.
- [169] Farhan S, Wang R, Li K. Electromagnetic interference shielding effectiveness of carbon foam containing in situ grown silicon carbide nanowires. *Ceram Int* 2016; 42:

- 11330–11340.
- [170] Nasr Esfahani A, Katbab AA, Taeb A, et al. Correlation between mechanical dissipation and improved X-band electromagnetic shielding capabilities of amine functionalized graphene/thermoplastic polyurethane composites. *Eur Polym J* 2017; 95: 520–538.
- [171] Stirna U, Cabulis U, Beverte I. Water-Blown Polyisocyanurate Foams from Vegetable oil polyols. *J Cell Plast* 2008; 44: 139–160.
- [172] Malik M, Kaur R. Synthesis of NIPU by the carbonation of canola oil using highly efficient 5, 10, 15-tris (pentafluorophenyl) corrolato-manganese (III) complex as novel catalyst. *Polym Adv Technol* 2018; 29: 1078–1085.
- [173] Malik M, Kaur R. Influence of aliphatic and aromatic isocyanates on the properties of poly (ether ester) polyol based PU adhesive system. *Polym Eng Sci* 2018; 58: 112–117.
- [174] Ibrahim S, Ahmad A, Mohamed NS. Synthesis and characterization of castor oil-based polyurethane for potential application as host in polymer electrolytes. *Bull Mater Sci* 2015; 38: 1155–1161.
- [175] Cao X, James Lee L, Widya T, et al. Polyurethane/clay nanocomposites foams: Processing, structure and properties. *Polymer (Guildf)* 2005; 46: 775–783.
- [176] Luyt AS, Molefi JA, Krump H. Thermal, mechanical and electrical properties of copper powder filled low-density and linear low-density polyethylene composites. *Polym Degrad Stab* 2006; 91: 1629–1636.
- [177] Gama N V., Soares B, Freire CSR, et al. Bio-based polyurethane foams toward applications beyond thermal insulation. *Mater Des* 2015; 76: 77–85.
- [178] <https://www.generalplastics.com/technical-papers/dielectric-materials-use-radomes>, <https://www.generalplastics.com/technical-papers/dielectric-materials-use-radomes> (2017, accessed 13 November 2017).

-
- [179] Pukánszky B. Mineral Filled Polymers. *Reference Module in Materials Science and Materials Engineering* 2016; <https://doi.org/10.1016/B978-0-12-803581-8.02598-4>.
- [180] Chen XY, Fan XY, Wang Z. Synergistic effect of carbon and phosphorus flame retardants in rigid polyurethane foams. *Fire Mater* 2018; 447–453.
- [181] Wang S, Du X, Jiang Y, et al. Journal of Colloid and Interface Science Synergetic enhancement of mechanical and fire-resistance performance of waterborne polyurethane by introducing two kinds of phosphorus – nitrogen flame retardant. *J Colloid Interface Sci* 2019; 537: 197–205.
- [182] Zhu H, Xu S. Synthesis and properties of rigid polyurethane foams synthesized from modified urea-formaldehyde resin. *Constr Build Mater* 2019; 202: 718–726.
- [183] Feldspar | Minerals Education Coalition, <https://mineralseducationcoalition.org/minerals-database/feldspar/> (2017, accessed 19 September 2017).
- [184] What is Kaolin Clay? Benefits, Powder, Skin, Side Effects, Properties of China /White Clay, <https://durablehealth.net/kaolin-clay/kaolin-clay-benefits-side-effects-properties/> (accessed 18 September 2017).
- [185] Pruettt RJ. Kaolin deposits and their uses: Northern Brazil and Georgia, USA. *Appl Clay Sci* 2016; 131: 3–13.
- [186] Ptáček P, Šoukal F, Opravil T, et al. The kinetic analysis of the thermal decomposition of kaolinite by DTG technique. *Powder Technol* 2011; 208: 20–25.
- [187] Zhong Y, Gao J, Chen P, et al. Recovery of Potassium from K - Feldspar by Thermal Decomposition with Flue Gas Desulfurization Gypsum and CaCO₃ : Analysis of Mechanism and Kinetics. *Energy and Fuels* 2016; 31: 699–707.
- [188] França de Sá S, Ferreira JL, Pombo Cardoso I, et al. Shedding new light on polyurethane degradation: Assessing foams condition in design objects. *Polym Degrad*

- Stab* 2017; 144: 354–365.
- [189] Kumar M, Kaur R. Glass fiber reinforced rigid polyurethane foam: synthesis and characterization. *e- Polym* 2017; 17: 517–521.
- [190] Debnath K, Singh I, Dvivedi A. Drilling Characteristics of Sisal Fiber-Reinforced Epoxy and Polypropylene Composites. *Mater Manuf Process* 2014; 29: 1401–1409.
- [191] Xing Y, Deng J, Zhang G, et al. Assessment in drilling of C / C-SiC composites using brazed diamond drills. *J Manuf Process* 2017; 26: 31–43.

RESEARCH PUBLICATIONS

INTERNATIONAL JOURNAL PUBLICATIONS

- **Anuja Agrawal**, Raminder Kaur, R. S. Walia, “PU Foam Derived from Renewable Sources: Perspective on Properties Enhancement: An Overview” **European Polymer Journal (SCI indexed)**, **95 (2017) 255-274, Elsevier (Impact Factor- 3.658)**
- **Anuja Agrawal**, Raminder Kaur, R. S. Walia, “Engineering Optimization of Process Parameters for Polymers: An Overview” **International Journal of Experimental Design and Process Optimisation**, **6 (2) (2019) 89-126, Inderscience.**
- **Anuja Agrawal**, Raminder Kaur, R. S. Walia, “Vegetable Oil Based Conducting Rigid PU Foam” **e-Polymers (SCI indexed)**, **19 (2019) 411-420, De-Gruyters, (Impact Factor- 1.491)**
- **Anuja Agrawal**, Raminder Kaur, R. S. Walia, “Flame Retardancy of Ceramic Based Rigid Polyurethane Foam Composites” **Journal of Applied Polymer Science (SCI indexed)**, **136 (48) (2019) 48250, Wiley, (Impact Factor- 2.188)**
- **Anuja Agrawal**, Raminder Kaur, R. S. Walia, “Investigation on Flammability of Rigid Polyurethane Foam-Mineral Fillers Composite” **Fire and Materials, (SCI indexed)**, **43 (8) (2019) 917-927, Wiley, (Impact Factor- 1.173)**
- **Anuja Agrawal**, Raminder Kaur, R. S. Walia, “Evaluation of Residual Compressive Strength for metallic filler reinforced Bio-Based RPUF Composite” **(under revision).**

PATENT FILED

- **Anuja Agrawal**, Raminder Kaur, R. S. Walia, “Bio-Based Rigid Polyurethane Foam Composition and Method Thereof, by **Delhi Technological University, Patent Application No: 201911027962.**

CONFERENCE PUBLICATIONS

- **Anuja Agrawal**, Raminder Kaur “Effect of CaCO₃ nano particles on the properties of bio- based Rigid PU Foam” presented in a **national conference** organized by Bhaskaracharya College of Applied Sciences, Delhi University, Delhi, Feb 2016.
- **Anuja Agrawal**, Raminder Kaur, R. S. Walia, “Thermal properties of castor oil based Rigid PU Foams: Effect of nano CaCO₃” 1st **International Conference** on New

Frontiers in Engineering, Science & Technology (NFEST-2018), New Delhi, India, January 8-12, 2018, ISBN: 978-93-86238-41-2, page 113-117

- **Anuja Agrawal**, Raminder Kaur “Mechanical Properties of Castor Oil Based RPUF: Effect of Low Cost Fillers” presented in an **international conference** organized by IIT, Delhi (23-25 Nov, 2017).
- **Anuja Agrawal**, Raminder Kaur, “Effect of Nano Filler on the Flammability of Bio-Based RPUF” presented in an **international conference** on Nano- structured materials & devices, organized by Society for technologically advanced materials of India (STAMI) & University of Delhi, (December 17-20, 2018), full paper published in **Integrated Ferroelectrics, An International Journal (SCI Indexed), Taylor & Francis (Impact Factor- 0.486)**.

APPENDIX-I

AP-1 Characterization of the Raw Materials

AP-1.1 Determination of the Acid Value

Approximately 5 gm of sample was dissolved in 50 ml of neutralized ethyl alcohol with slightly heating. The mixture was then cooled at room temperature, and was titrated against 0.1 N alcoholic KOH solution, using phenolphthalein as indicator. The Acid Value (mg KOH/g) can be given by using the equation:

$$\text{Acid Value} = (S - B) \times \frac{N}{W} \times 56.1$$

Where, S is the volume (mL) of the standard KOH solution consumed in sample titration, B is the volume (mL) of the standard KOH solution consumed in blank titration, W is the weight of Sample (g) and N is the normality of KOH.

AP-1.2 Determination of the Hydroxyl Value

Weigh 2 gm of sample in a conical flask and add 40 mL of acetylating solution (20 mL acetic anhydride in 80 mL of pyridine) into it. Boil for 1 hour on a water bath under total reflux condition, adjusting the level of the water to maintain it 2 to 3 cm above the level of the liquid in the flask. Cool down the contents of the flask at room temperature, by running water through the condenser. Titrate the contents of the flask against 0.1 N alcoholic KOH solution, using phenolphthalein as indicator. Similarly repeat the procedure for blank solution (without sample). The Hydroxyl Value (mg KOH/g) can be calculated using the equation:

$$\text{Hydroxyl Value} = (B - S) \times \frac{N}{W} \times 56.1$$

Where, B is the Volume of the standard KOH solution (mL) for blank solution, S is the Volume of the standard KOH solution (mL) for Sample titration, W is the weight of the sample (g) and N is the normality of KOH standard solution.

AP-1.3 Determination of the Percentage of NCO Content

Take approximately 2 g of MDI sample in a round neck flask and dissolve it into 20 mL of 2 N di-n-butyl amine solution. Heat the contents by means of water bath, under total reflux conditions, using air condenser for 30-40 minutes. Cool the contents to room temperature and mix 50 mL of methanol. Titrate it against 0.5 N HCl solution, using bromo-phenol blue as an indicator. The % NCO Content can be calculated using the equation:

$$\text{Percentage of NCO}(\%) = (B - S) \times \frac{N}{W} \times 4.2$$

Where, B is the volume of the standard HCl solution consumed in blank titration (in mL), S is the volume of the standard HCl solution consumed in sample titration (in mL), W is the weight of the sample (in g) and N is the Normality of standard HCl solution.

AP-2 Calculations of the Formulation for Polyurethane Foam Formation

Formulation of the polyurethane foam was calculated by using standard equations and performing experiments to optimize the properties of foams. Equations used are as follows:

$$\text{Equivalent weight of polyol} = \frac{56100}{\text{OH number}}$$

$$\text{Equivalent weight of Isocyanate} = \frac{4202}{\% \text{ NCO}}$$

$$\text{Parts Isocyanate} = \text{Equivalent Isocyanate} \times \text{Isocyanate equivalent weight}$$

$$\text{Equivalent Isocyanate} = \frac{\text{Equivalent B - side}(\text{polyol}) \times \text{NCO index}}{100}$$

CURRICULUM VITAE

ANUJA AGRAWAL

e-mail id- agrawala918@gmail.com



ACADEMIC QUALIFICATIONS:

S. No.	Degree	Division	University/ Institute	Year
1.	M.Tech. (Polymer Technology)	CGPA- 8.99 (Gold medalist)	Delhi Technological University	July 2015
2.	M.Sc. (Chemistry)	1 st (71.9%)	Agra University	1998
3.	B.Sc. (ZBC)	1 st (73.57%)	Agra University	1996
4.	Intermediate (12 th)	1 st (75.6%)	UP board, Allahabad	1993
5.	High school (10 th)	1 st (74.16%)	UP board, Allahabad	1991

NATIONAL LEVEL EXAMS QUALIFIED:

S.No.	Exam qualified	Position	Institution	Year
1.	GATE (XE- Polymer Science and Engineering, Thermodynamics)	AIR- 12 th SCORE- 774	-	2016
2.	GATE (Chemistry)	AIR- 532	-	2013
3.	GATE (Chemistry)	AIR- 451	-	2004
4.	CSIR-UGC NET	LECTURESHIP	CSIR-UGC	Dec 2003
5.	CSIR-UGC NET	LECTURESHIP	CSIR-UGC	Dec 2001
6.	CSIR-UGC NET	LECTURESHIP	CSIR-UGC	Jul 2001

M.Tech. PROJECTS:

[1] Major project- Some Studies on Antimicrobial Regenerated Cellulose Membranes using Lignocellulosic waste

[2] Minor project I- Kinetic Analysis of Drug Release from Composite Wound Dressing

[3] Minor project II- Study of Swelling Kinetics of Composite Wound Dressing

PERSONAL DETAILS:

Name: Anuja Agrawal
Husband's Name: Prof. Rajesh Kumar
Date of Birth: 16-10-1976